Synthesis and Application of Novel Polymeric N-halamine Antimicrobial Agents

by

Idris Cerkez

A dissertation submitted to the Graduate Faculty of
Auburn University
in partial fulfillment of the
requirements for the Degree of
Doctor of Philosophy

Auburn, Alabama
December 12, 2011

Keywords: N-halamines, antimicrobials, textiles, biocidal, coatings

Approved by

Royall M. Broughton, Chair, Professor of Polymer and Fiber Engineering
S. Davis Worley, Professor of Chemistry and Biochemistry
Peter Schwartz, Professor of Polymer and Fiber Engineering

Abstract

As one of the most effective biocides, N-halamine biocidal coatings for surfaces have gathered a great deal of interest in recent years. In this study, several novel N-halamine moieties were synthesized, characterized, and applied onto cotton fabric through various tethering groups and attachment techniques with the purpose of improving stabilities toward washing and ultraviolet light exposure (UVA). Five projects addressing different factors on stabilities were covered in this dissertation.

In the first project, an acyclic N-halamine precursor, 2-amino-2-methyl-1-propanol (AMP), was applied onto cotton using 1,2,3,4-butanetetracarboxylic acid (BTCA) as a crosslinking agent so as to impart durable press and antimicrobial functionalities simultaneously. BTCA content in the coating solution was altered to address the influence of crosslinking density on the stabilities.

In the second project, a novel epoxide containing N-halamine copolymer was synthesized, characterized, and applied onto cotton fabric. Antimicrobial efficacy, stability toward hydrolysis and UVA light exposure were evaluated along with comparison to previously synthesized epoxide-containing N-halamine monomer.

In the third project, cyclic N-halamine rings containing amine, amide, or imide functional groups were attached to the copolymer backbone synthesized in the second project with the purpose of addressing the influence of N-halamine chemical composition on biocidal efficacies and stabilities toward repeated laundering and UVA light exposure.

In the fourth project, a vinyl N-halamine monomer, hydantoin acrylamide, was copolymerized with a siloxane-, an epoxide- and a hydroxyl group-containing monomers. These novel copolymers were immobilized onto cotton fabric through hydrolysis of alkoxy groups and formation of silyl ether bonding, opening of the epoxide ring and subsequent reaction with hydroxyl groups on cellulose, and crosslinking between the hydroxyl groups on the copolymer and on cellulose, respectively. The effect of the aforementioned tethering groups on wash fastness, UVA light exposure, and antimicrobial efficiency was addressed.

In the last project, novel N-halamine polyelectrolytes were synthesized, characterized, and coated onto cotton fabric via a layer-by-layer assembly technique. Feasibility of electrostatic attraction utilization for N-halamine biocidal coatings was examined in terms of biocidal efficacy and stability to washing and sun light exposure.

Acknowledgments

The author would like to express his appreciation to his advisor, Prof. Royall M. Broughton, for his excellent guidance, endless support, and encouragement. The author expresses his sincere thanks to his co-advisor, Prof. S. D. Worley, for his guidance, support, and timely invaluable advice. The author is also grateful to his advisory committee member, Prof. Peter Schwartz, for his suggestions and discussions.

The author acknowledges Dr. Tung S. Huang for conducting antimicrobial tests and being the outside reader. The author's appreciation from the bottom of his heart goes to Dr. Hasan B. Kocer, for his teaching, guidance, and serving as if he was one of the advisory committee members. The author also expresses his gratitude to Prof. Yusuf Ulcay for his encouragement to do a Ph.D in the U.S. The author acknowledges to Turkish Ministry of National Education for provision of a Ph.D. scholarship. Thanks to the Department of Polymer and Fiber Engineering and Department of Chemistry and Biochemistry for providing the labs and equipments, and the U.S. Air Force and the U.S. Department of Commerce for aid in funding for his research.

The author appreciates his parents, Mustafa and Sukriye, his brother, Yunus, and his sister, Naime, for their endless support and love.

Table of Contents

List of Tables

List of Figures

CHAPTER 1

INTRODUCTION and LITERATURE REVIEW

1.1. Introduction

Even though there have been science and technology advances in the 21st century, human beings are powerless against a class of tiny creatures called microorganisms, which still threaten our lives. In fact, microorganisms have caused thousands of pandemic and epidemic diseases throughout history. The first epidemic documented in human history, the Plague of Athens, perished a quarter of Athenian population in 430 BC. The Plague of Justinian (541 AC), the first known pandemic, appeared in Egypt and rapidly spread throughout the Byzantine Empire. This devastating pandemic caused 10,000 people to die daily in Constantinople.[1] Several other bacterial or viral originated diseases such as the plague, smallpox, cholera, typhoid, typhus and influenza spread around the world and caused massive destructions. Due to mutation taking place in microorganisms' structure, some of the pandemics repeatedly occurred in 10-50 year intervals.[2] Most recently, the outbreak of Severe Acute Respiratory Syndrome (SARS) in 2003, H5N1 (Bird Flu) in 2004, and H1N1 (Swine flu) in 2009 increased awareness of the need for multidisciplinary approaches to prevent and control pandemic diseases.[3]

Microorganisms have been used as biological weapons by spreading infectious diseases through air or through contamination of drinking water or food. In fact, the use of biological warfare agents such as bacteria, viruses, and fungi dates back to prehistoric

times.[4,5] For instance, arrows dipped in manure, blood, or decomposed bodies were used by Scythian archers in 400 BC. In 1155 AD dead bodies were used to contaminate drinking water in the battle of Tortona. Bubonic plague-infected cadavers were catapulted over the walls of Caffa by Mongols in 1346; this is believed to be the cause of the plague pandemics which emerged later in Europe. Polish artillery general, Siemenowics, fired spheres filled with saliva from rabid dogs in 1650. As well in 1763, smallpox infected blankets were given to the Indians at Fort Pitt by a British officer which resulted in a massive decline in the Native American population. Similarly, Tunisians threw plague-infected clothing into La Calle in 1785. During the U.S. Civil War, Confederates contaminated Union troop's water sources by discarding dead animals into their wells and ponds. Most recently, in 2001 anthrax spore contaminated letters were distributed throughout the U.S. The aforementioned incidents are suggestive that genetically engineered pathogens might be used for destructive purposes in the future. Therefore, research on water disinfection and biological-protective clothing should be promoted as a preventative measure against acts of bioterrorism.

Prevention and reduction of healthcare-associated infections (HAIs), infections acquired during medical care or treatment, are crucial, because the infections cause billions of dollars of healthcare costs and millions of deaths each year around the world.In developed countries, 7 % of hospitalized patients are infected by HAIs; whereas, this number rises to 10 % in developing countries. The annual direct hospital cost of treating HAIs in the U.S. is estimated to range from 28.4 to 33.6 billion dollars.[6] In 2002, 1.7 million people in the U.S. were infected by HAIs leading to around 99,000 deaths.[7] *Clostridium difficile* along with antibiotic resistant bacteria such as Methicillin-resistant *Staphylococcus aureus* (MRSA), Vancomycin-resistant *Enterococci*, and *Escherichia coli* are the most dangerous bacteria

types responsible for most HAIs. Patients are exposed to these pathogens through airborne transmission or direct/indirect contact with contaminated surfaces. For instance, contamination of a central line might lead to a bloodstream infection, contamination of a catheter could cause a bladder or kidney infection (catheter-associated urinary tract infection), contamination of a ventilator might result in lung infections (ventilator-associated pneumonia), and contamination of surgical devices might lead to tissue infections (surgical site infections). According to recent surveillance data collected by the European Antimicrobial Resistance Surveillance Network, bloodstream HAIs caused by *E.Coli* and *S. aureus* increased 71 % and 34 % between 2002 and 2009 in Europe, respectively.[8] This alarming rate necessitates a state of the art, super effective, and long lasting sterilization method for medical environments. Antimicrobial treatment of medical devices, utensils, and textiles has the potential to reduce the mortality rate and the cost associated with HAIs.

Antimicrobial agents offer a promising solution to reduce the risk of future pandemics and epidemics; to prevent possible bioterrorism attacks; and to reduce the cost, morbidity, and mortality rate of HAIs. Therefore, there is a need to make robust, potent, durable, and stable antimicrobial coatings at a reasonable expense for various applications including textiles, medical devices, food packaging, filtration, diapers, and paints. Textiles materials, particularly natural fibers, are prone to microbial growth. Immobilization of antimicrobial agents onto textiles surfaces is an effective approach to prevent surface contamination and the transmission of airborne pathogens. Various antimicrobial agents have been developed in the art and immobilized onto medical textiles such as bed sheets, gowns, caps, masks, diapers, etc. N-halamines are one of the most effective biocidal agents used to inactivate a broad spectrum of microorganisms. Work in the Worley research

laboratories has developed numerous novel N-halamine biocides for various applications. However, recent studies by Ren et al.[9] and Kocer et al.[10] revealed that the stability and durability of N-halamine biocidal coatings toward repeated laundering and UVA light exposure need to be improved.

1.2. Objectives

The overall goal of this work is to develop novel N-halamine biocidal agents, immobilize these structures onto textile surfaces through various tethering groups, and the attachment chemistries with the purpose of improving the coatings' wash fastness and resistance to UVA light degradation. Specific objectives included:

- Development of inexpensive yet very efficient N-halamine biocidal coatings
- Analysis of crosslinking density effect on stability and durability
- Comparison of polymeric and monomeric N-halamine biocides
- Comparison of the chemical composition of N-halamine moieties
- Investigation of tethering groups' effect on stability and durability
- Immobilization of N-halamine biocides onto cotton surface through electrostatic attractions

1.3. Chapter Arrangement

This dissertation consists of seven chapters. Chapter 1 is the introduction of the topic, objectives and the literature review about common biocides, especifically N-halamines. Chapters 2 through 6 discuss the major part of each project in the fallowing order: utilization of polycarboxylic acids as tethering groups for N-halamines; comparison

of polymeric and monomeric N-halamine biocides; comparison of different N-halamine structures; evaluation of the effect of tethering groups; utilization of electrostatic attractions as an attachment technique. Each chapter has its own introduction, experimental, results and discussion, and conclusion sections. A general conclusion section is provided at the end of this text.

1.4. Literature Review

1.4.1. Structure of Bacterial Cells and the Mechanism of Antimicrobial Action

Since the microorganism class of interest in this work is bacteria, the cell structures of this kind of pathogen should be addressed before further discussing the inactivation mechanism of biocides. Bacteria are classified into two main groups based on their cell structure: Gram-negative and Gram-positive. The difference between these groups is the presence or absence of an outer cell membrane layer. As shown in Figure 1.1 below, Gram-negative bacteria have an extra membrane covering the cell wall which is a peptidoglycan layer. Acting as a barrier, this outer membrane consists of lipoproteins, lipopolysaccharides, and phospholipids making it more resistant to biocides than Gram-positive bacteria. On the other hand, Gram-positive bacteria are less prone to mechanical breakage, since their cell wall has a thicker peptidoglycan layer.

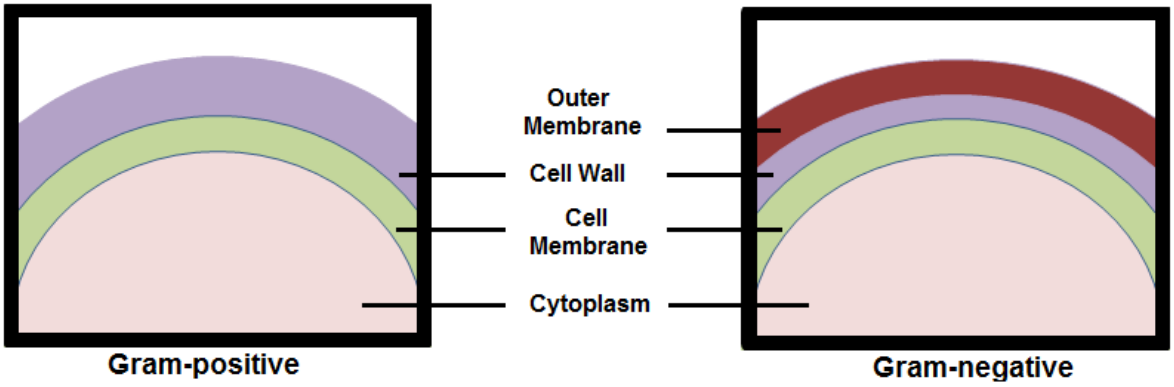

Figure 1. 1. Cell structures of Gram-positive and Gram-negative bacteria.

Antimicrobial activity is classified into two categories: bacteriostatic, where bacterial growth is prevented or inhibited and bactericidal, where an irreversible, lethal process takes place. In order for antimicrobial action to happen, a biocide needs to find and interact with a target site(s) on the bacteria. Interaction with bacteria can occur in three ways: with outer cell components, with the cell cytoplasmic membrane, and/or with cyptoplasmic constituents. Depending on the biocide and bacteria type, one or all three levels of these interactions could be possible. Initially, a biocide binds itself to the cell surface and alters the outer cell, so it can penetrate and reach target site(s). Since the cytoplasmic membrane provides the cell integrity, it is the target site for most of the biocides. Once it is disrupted by biocides, intracellular components including amino acids, nucleic acids, and proteins leak out, resulting in cell lysis. Some biocides react with cyptoplasmic constituents such as DNA, RNA, proteins, etc. and thus, inhibit cell growth.[11,12]

1.4.2. Common Biocidal Agents

According to their interaction with pathogens, biocides can be classified into two groups; oxidizing and non-oxidizing. Oxidizing biocides inactivate microorganisms by

causing an irreversible protein oxidization/hydrolysis leading to rapid cell death. Halogens, hydroxyl radicals, chloramines, and peroxides are considered as oxidizing biocidal agents. Contrastingly, non-oxidizing biocides alter the cell wall permeability, interfering with the microorganism's biological activity. Aldehydes, quaternary ammonium compounds, quaternary phosphonium compounds, and phenolics are some examples of non-oxidizing biocides.[13] In general; oxidizing biocides operate as faster disinfecting agents than do nonoxidizing biocides.

The most common biocides are biguanides, quaternary ammonium salts, peroxides, alcohols, heavy metals and halogens. Alcohols such as ethyl alcohol and isopropyl alcohol are effective biocides. They function mainly to dissolve the cell wall resulting in cell integrity damage. Moreover, these biocides form hydrogen bonding with proteins and enzymes, causing denaturing of bacteria which leads to inactivation of catalytic functions.[14] Even though alcohols act rapidly, use of them as biocides is limited, because they are very volatile, and a high concentration (60-85%) is needed for effective biocidal activity. Alternatively, their volatile nature makes them a good candidate for skin antiseptics, since they do not leave any residue.

Biguanides contain a positive charge and a lipophilic function. Initially, a biguanide binds itself to the bacteria cell wall through ionic interactions between the positive charge of the biguanide molecule and the negatively charged phosphate head groups of the phospholipids. Then the bacterial cell membrane is disrupted by sinking the biguanide nonpolar groups through the cell wall's hydrophobic domains. Poly(aminopropyl biguanide) (PAPB) and chlorhexidine (CHX) shown in Figure 1.2 are two of the most widely used biguanides. Their wide range of applications include swimming pool sanitizers, cosmetics,

leather preservatives, contact lens disinfectants, cleansers in agriculture and food handling, treatments of hatching eggs, fibers and textiles, and technical fluids like cutting oils and glues.[15] On the other hand, after several years of usage, microorganisms become resistant to biguanides.[14]

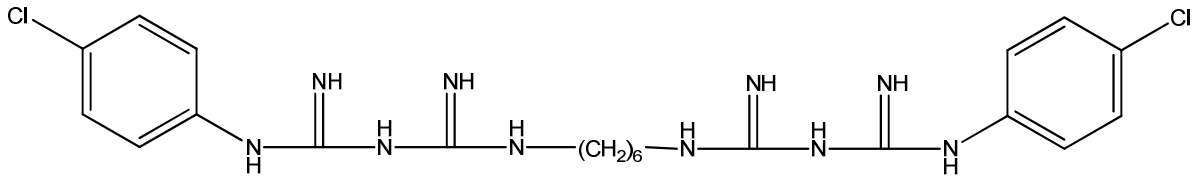

CHX

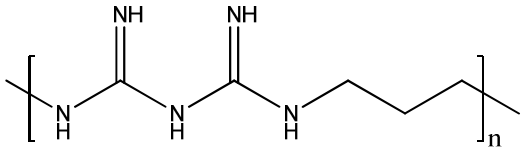

PAPB

Figure 1. 2. Structure of biguanides.

Quaternary ammonium salts (Quats) such as cetylpyridinium chloride and benzalkonium chloride have similar bacteria inactivation mechanisms. They are absorbed onto the cell wall through an ionic attraction; then, they penetrate the cell wall and disrupt the cytoplasmic membrane which results in cell lysis. They contain at least one long hydrocarbon chain which facilities the penetration process (Figure 1.3). This lipophilic chain usually consists of 8-19 alkyl groups with a maximal biocidal activity at around 14 alkyl groups. Even though quats are effective biocides to Gram-positive bacteria, they are not very effective against to Gram-negative bacteria, so the use of these biocides is limited.[14,16]

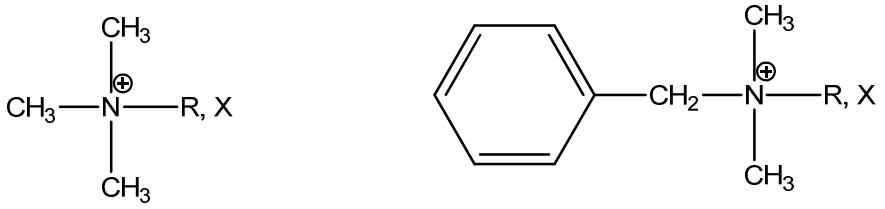

R = C8-C19 alkyl group
X = Cl, Br

Figure 1. 3. Structure of quaternary ammonium salts.

Heavy metals such as silver, copper, mercury, zinc, arsenic, and antimony and their salts are another class of antimicrobial agents. Among these, silver has been widely used. They primarily interact with thiol groups in enzymes, proteins, and other cellular components. It is also proposed that heavy metal salts act by binding to key functional groups of fungal enzymes through an ion exchange process.[17] Even though heavy metals are inexpensive biocides, high toxicity and low inactivation rate limit their use.

Aldehydes, such as glutaraldehyde and formaldehyde, prevent biofilm formation by binding to surfaces. They crosslink various proteins which try to from surface biofilms. Inter and intra crosslinking of various bacteria aminoacids lead to a loss of structure or function. For instance, glutaraldehyde binds with the bacteria cell wall and disrupts functions such as enzyme inhibition, viral infectivity, and transport disruption.[18] Despite the fact that aldehydes are very effective to a broad spectrum of bacteria, being volatile and toxic to human life limit their application areas.

Peroxides are green materials, since they degrade to water and oxygen. They are effective biocides against fungi, bacteria and spores. Their mechanism of action involves the oxidation of thiol groups which disrupts proteins and enzymes. Common applications for peroxides include wound and surface cleaners, sewages odor control, and swimming pool

disinfection. On the other hand, peroxides are volatile and toxic which limit their wider applications.[19]

Halogen based biocides such as Cl_2, Br_2, I_2, HOCl, Cl_2O and NaOCl are very effective disinfectants used to inactivate a broad spectrum of microorganisms including bacteria, spores, and viruses. Their inactivation mechanism involves the oxidation of proteins in the protoplasm leading to irreversible destruction of enzymatic activities. Chlorine and bromine are the most common halogen-based biocides used to disinfect swimming pools, spas and whirlpools. Chlorine dissolves in water to form hypochlorous acid which then dissociates to form hypochlorite depending on pH. When the pH is around 7.5, hypchlorous acid predominates; when the pH value is above 7.5, hypochlorous acid exists in the hypochlorite form. Hypochlorous acid is a much more powerful biocidal agent than is hypochlorite. The amount of Cl_2, HOCl and OCl is defined as "free chlorine".

$$Cl_2 + H_2O \rightleftharpoons HOCl + H^+ + Cl^-$$

$$HOCl \rightleftharpoons OCl^- + H^+$$

Halogens are inexpensive and so easy to apply that even household bleach contains 5-6 % sodium hypchlorite in it. However, they are instable, corrosive, and toxic which limits their wider applications.[14,19]

1.4.3. N-halamines

Even though halogens are very effective biocides, they are instable and leach "free chlorine" into water. Halogens can be stabilized by N-halamine compounds. N-halamines are defined as organic or inorganic compounds containing one or more nitrogen-halogen covalent bond(s). Chlorine, bromine or iodine could serve as the halogen for the compound,

but in general only chlorine and bromine stored N-halamines are of commercial interest, since they are relatively stable. What makes N-halamines unique is their low hydrolysis constant leading to only a small amount of free chlorine leaching into water, as well as their increased stability, rechargeability, and effectiveness against a broad spectrum of microorganisms in relatively short contact times. The inactivation mechanism involves the transfer of the oxidative halogen to the microorganisms' cell membrane causing oxidation of thiol groups and cell disruption.[12] Once all the halogen is consumed, they can be simply recharged upon exposure to a halogen source such as household bleach. N-halamines can be shown as the general formula below where R and R' groups might be an organic group, inorganic group, hydrogen, or halogens.

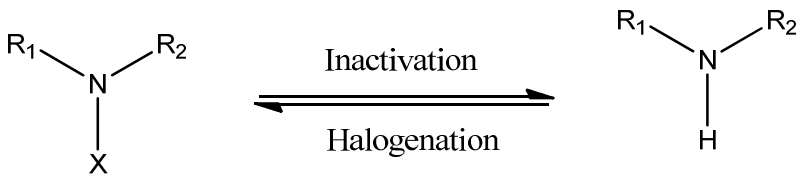

R1, R2 = Organic group, Inorganic group, H, Cl, Br
X = Cl, Br

Figure 1. 4. Rechargeable structure of N-halamines.

Inorganic N-halamines are generally used for water disinfection, since they are inexpensive and do not react appreciably with organic materials to form toxic trihalomethanes. Nevertheless, they are sensitive to water temperature and pH, toxic to some plants and animals, and exhibit relatively weaker biocidal activity.[20] Structure of some inorganic N-halamines are shown in Figure 1.5 below.

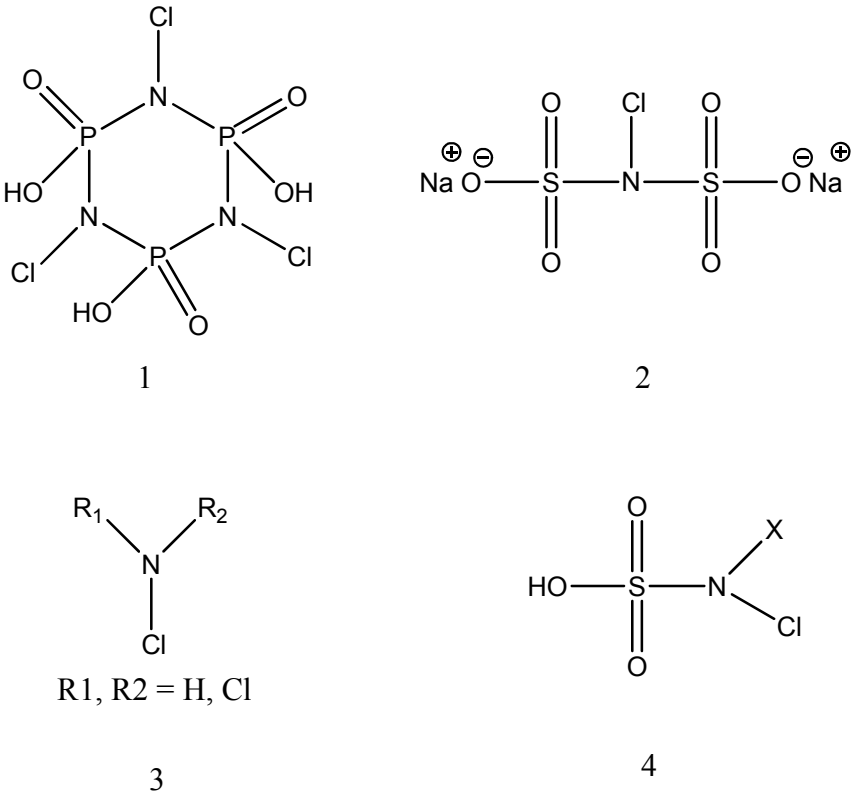

Figure 1. 5. Structure of some inorganic N-halamines.

1. Trichoroimidometaphosphate, **2**. Sodium N-chloroimidometaphosphate, **3**. Chloroamines, **4**-N-chlorosulfamic acids or N,N-dichlorosulfamic acid

Organic N-halamines are divided into three groups; amine, amide, and imide halamine bonds. The stability and biocidal efficacy of organic N-halamines are dependent upon chemical structure. Stability toward dissociation of the nitrogen-halogen bond decreases from amine to imide structure (Figure 1.6). Therefore, imide N-halamies are the most prone while amine N-halamines are the least prone to release "free halogen" into water. The difference between the dissociation constant comes from their chemical structure. Presence of two electron donating groups (alkyl groups) adjacent to nitrogen stabilizes the N-X bond. Conversely, the two electron withdrawing groups adjacent to nitrogen make the

N-X bond less polar and destabilizes it. Amide type N-halamines have both electron donating and withdrawing groups, so their stability is between imides and amines. From the biocidal efficacy point of view, N-halamines containing imide functionality exhibit faster biocidal action than do those containing amines, since increasing dissociation constant increases the rapidness of biocidal efficacy. Thus, the order of halogen stability is amine>amide>imide, but the order of inactivation rate is the reverse.[21,22]. Therefore, amide containing N-halamine structures are preferable for optimum biocidal efficacy and stability.

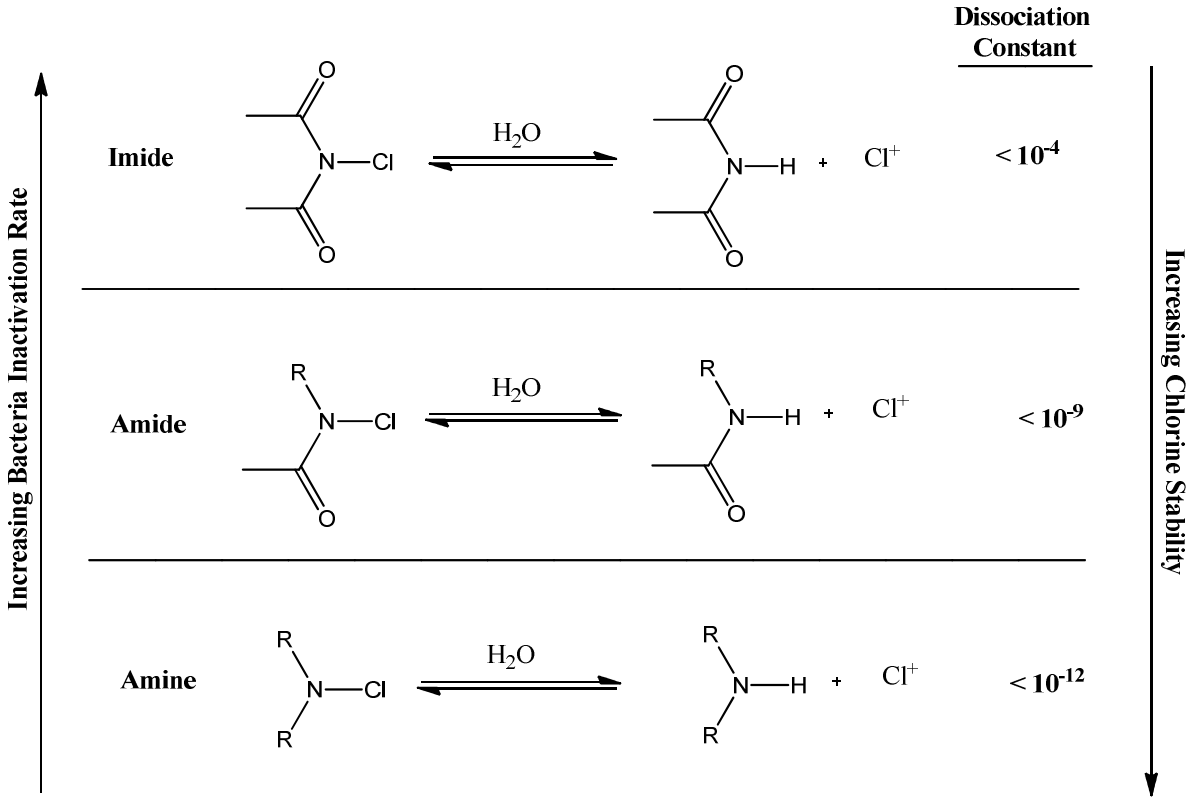

Figure 1. 6. Structures of organic N-halamines.[22]

Cyclic N-halamine compounds containing no α hydrogen adjacent to the nitrogen of the N-X bond are more stable than their acyclic counterparts. The presence of an α hydrogen

in the structure causes dehydrohalogenation. This reaction is accelerated by UV or heat exposure. Once dehydrohalgenation occurs, the N-halamines lose their rechargeability due to formation of a C=N bond (Figure 1.7).

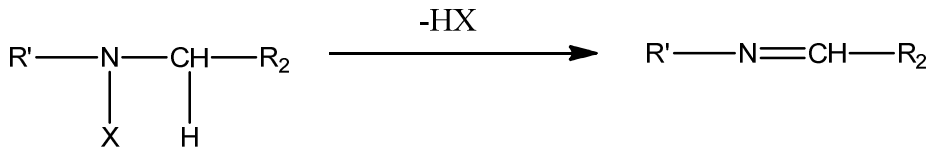

Figure 1. 7. Alpha dehydrohalogenation.

Work in Worley's laboratories at Auburn University has focused on synthesis and application of novel N-halamine-containing compounds and materials since the 1980s. Cyclic N-halamines such as 3-halo-4,4-dimethyl-2-oxazolidinones, 1,3-dihalotetramethyl-2-imidazolidinones, and 1,3-dihalo-2,2,5,5-tetramethylimidazolindin-4-ones were synthesized primarily for water disinfection. Structures of several other cyclic N-halamines are shown in Figure 1.8 below.

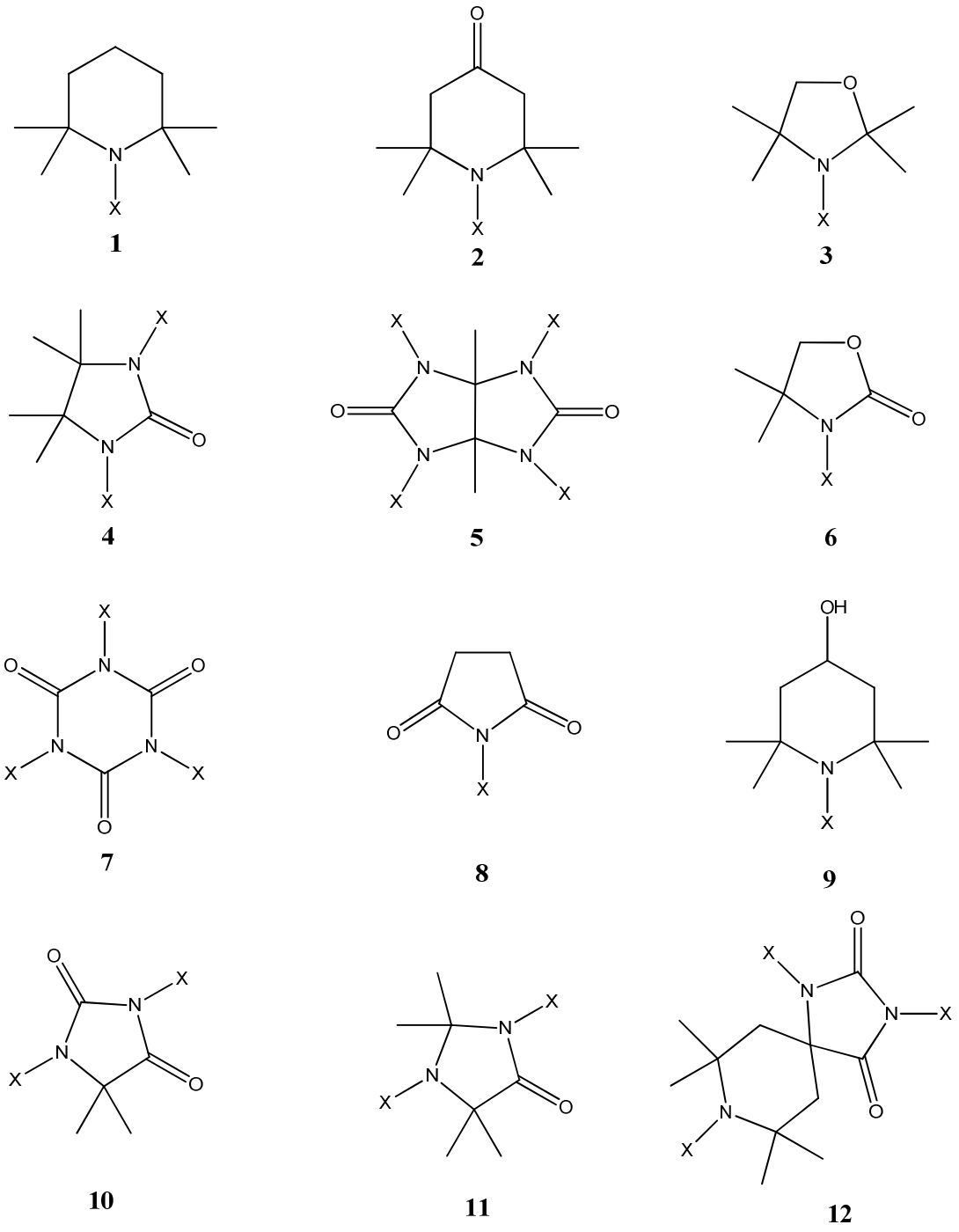

Figure 1. 8. Structures of cyclic N-halamines.

For X = H ; **1**: 2,2,6,6-tetramethylpiperidine, **2**: 2,2,6,6-tetramethylpiperidin-4-one, **3**: 2,2,4,4-tetramethyloxazolidine,**4:**4,4,5,5-tetramethylimidazolidin-2-one,

5: 3a,6a-dimethyltetrahydroimidazo[4,5-d]imidazole-2,5(1H,3H)-dione,**6**:4,4-dimethyloxazolidin-2-one, **7**: ,3,5-triazinane-2,4,6-trione (cyanuric acid), **8**: pyrrolidine-2,5-dione (succinimide), **9:**2,2,6,6-tetramethylpiperidin-4-ol, **10:** 5,5-dimethylimidazolidine 2,4-dione (or 5,5-dimethylhydantoin), **11:** 2,2,5,5-tetramethylimidazolidin-4-one, **12**: 7,7,9,9-tetramethyl-1,3,8-triazaspiro[4.5]decane-2,4-dione.

1.4.4. N-halamine Based Antimicrobial Polymers

There are basically three approaches to incorporate N-halamamine compounds into polymeric materials so as to render them biocidal:

1. N-halamine monomers can be copolymerized with other monomers or polymers
2. N-halamine compounds can be coated or grafted onto polymer surfaces
3. N-halamine compounds can be incorporated to the host polymer as an additive during polymer processing

Several polymeric materials, including cellulose, polyester, nylon, polyurethane, polyacrylonitrile, polyvinylacetate, and polymethylmethacrylate were rendered biocidal in Worley's laboratories by utilization of one of the aforementioned approaches. These approaches are explained below.

1. Sun[23] was the first to incorporate N-halamine structures to a polymer backbone. He synthesized poly(4-vinylacetophenone) from polystyrene by utilization of a Friedel-Crafts acylation and then formed a hydantoin ring around the ketone moiety by the Bucherer-Berg reaction. The homopolymer is insoluble in water and upon chlorination or bromination acts as a contact biocide. Chen in Worley's group further enhanced the

utilization of this novel monomer by preparing biocidal polymeric beads. Crosslinked Poly 1 beads inactivated Gram-negative and Gram-positive bacteria, fungi, and rotaviruses in seconds of contact time.[24,25]

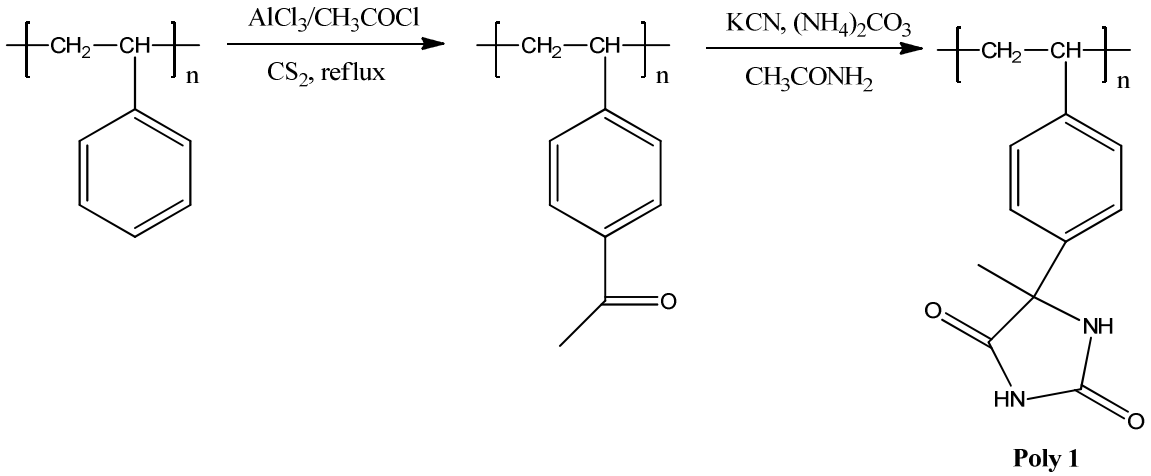

Figure 1. 9. Synthesis of poly(5-methyl-5-(4'-vinylphenyl)-hydantoin).[23]

Sun[26] synthesized another novel N-halamine monomer, 3-allyl-5,5-dimethylhydantoin, and copolymerized it with vinylacetate, methylmethacrylate, and acrylonitrile. The resultant copolymers exhibited potent antimicrobial properties to a broad spectrum of microorganisms.

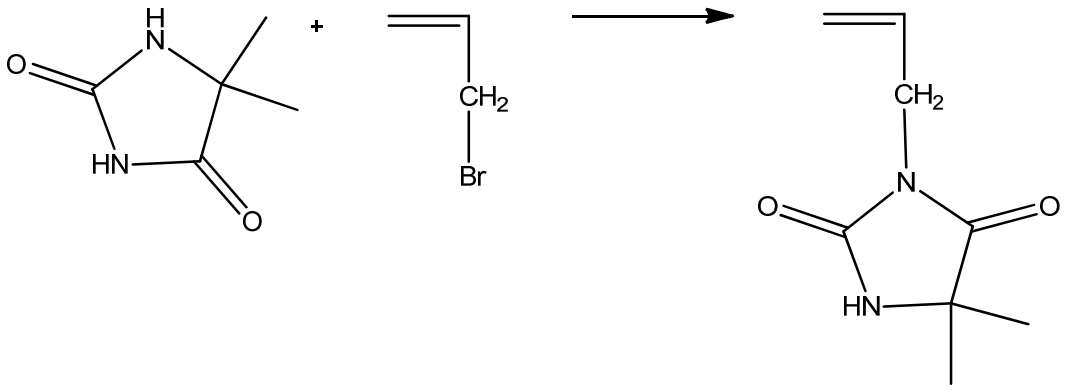

Figure 1. 10. Synthesis of 3-allyl-5,5-dimethylhydantoin.[26]

Due to to the "autoinhibition" effect of the allylic structure, high moleculer weight could not be achieved with 3-allyl-5,5-dimethylhydantoin. Therefore, Sun[27] synthesized a new vinyl N-halamine monomer precursor, 3-(4'-vinylbenzyl)-5,5-dimethylhydantoin, which has higher reactivity and compatibility with various commercial monomers, as opposed to previously synthesized allylic monomers. Potent antimicrobial activity was obtained with the chlorinated homopolymers, as well as, copolymers with various monomers.

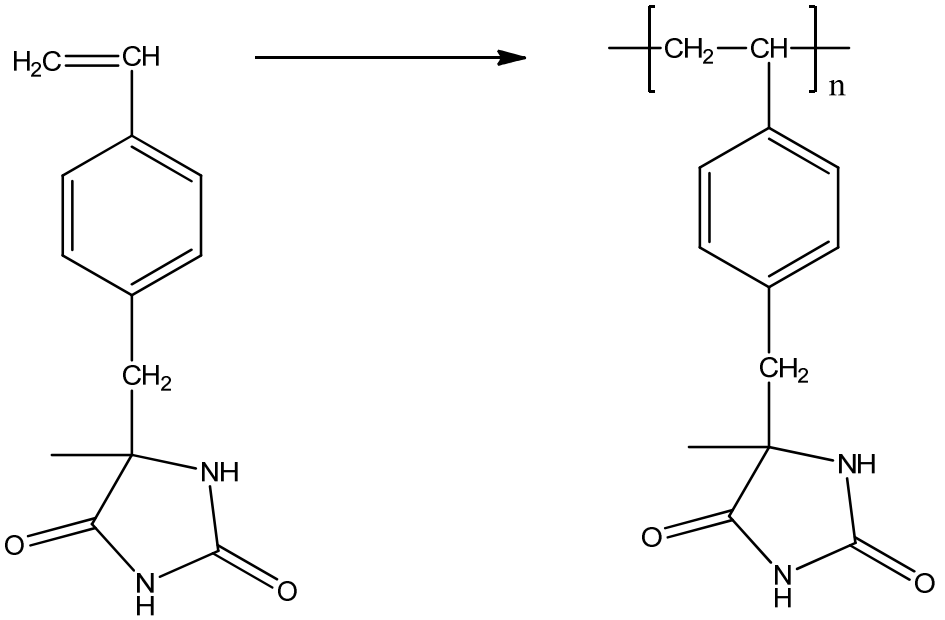

Figure 1. 11. Structure of 3-(4'-vinylbenzyl)-5,5-dimethylhydantoin monomer and homopolymer.[27]

Eknoian[28] and Li[29] synthesized various acrylic type N-halamine monomers and copolymers with various commercial monomers. Antimicrobial tests revealed that these novel monomers and copolymers were very effective and have potential to be used as surface active biocidal agents.

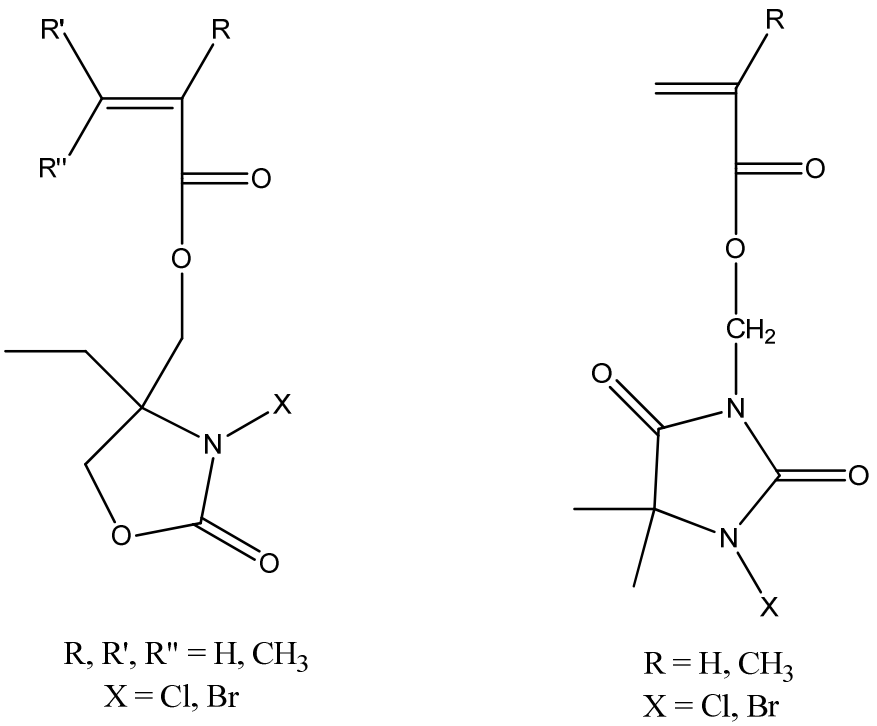

Figure 1. 12. Structure of acrylic N-halamine monomers.

Most recently, Kocer[30] synthesized a novel hydantoin-containing acrylamide monomer having 31 wt % halogen loading capability. The monomer was synthesized by forming a hydantoin ring from the ketone moiety of a commercial monomer, N-(1,1-dimethyl-3-oxobutyl) acrylamide. He copolymerized the monomer with a siloxane containing monomer using different feed ratios. Immobilization of the chlorinated copolymers onto cotton fabric resulted in 8 log reductions of Gram-negative and Gram-positive bacteria within 5 min of contact time.

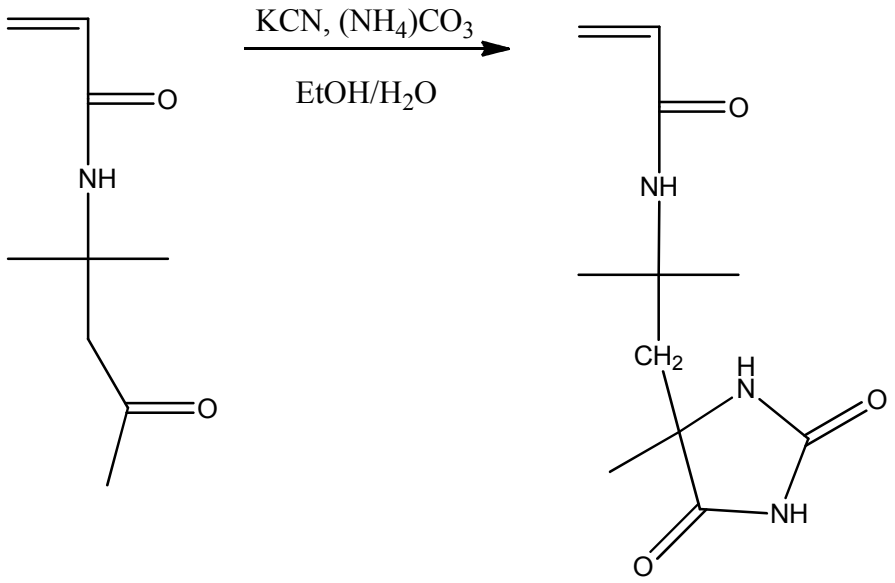

Figure 1. 13. Structure of hydantoin acrylamide monomer.[30]

2. Several N-halamine precursors have been covalently coated onto polymer surfaces via tethering groups. Siloxanes, epoxides, and polycarboxylic acid based coupling agents have been used to immobilize N-halamine compounds as surface active biocidal agents.

Alkoxy siloxanes were utilized to bond cyclic N-halamines onto surfaces including cellulose[31], polyester[32], silica gel,[33] and paint.[16] Worley et al.[34] was the first to describe the synthesis of BA1 (Figure 1.14) which is a commercial product on the market now. It is produced by a fairly simple procedure through reacting the potassium or sodium salt of hydantoin with 3-chloropropyltriethoxysilane. Rechargeable, stable, and very effective antimicrobial coatings were employed by utilization of different siloxane coupling agents with various N-halamine precursors.

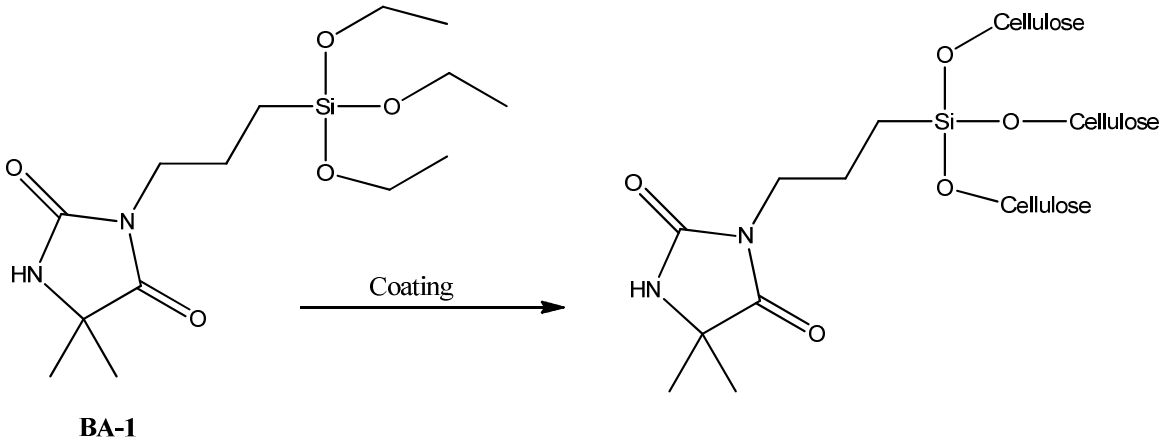

BA-1

Figure 1. 14. Immobilization of hydantoin siloxane onto cellulose.

Epoxides have also been used to tether N-halamine compounds onto polymer surfaces. Liang et al.[35] synthesized a series of novel N-halamine epoxide precursors. Among these, 3-glycidyl-5,5-dimethylhydantoin (Figure 1.15) was of commercial interest, since it is water soluble and provides durable, very effective antimicrobial coatings on cotton fabric.

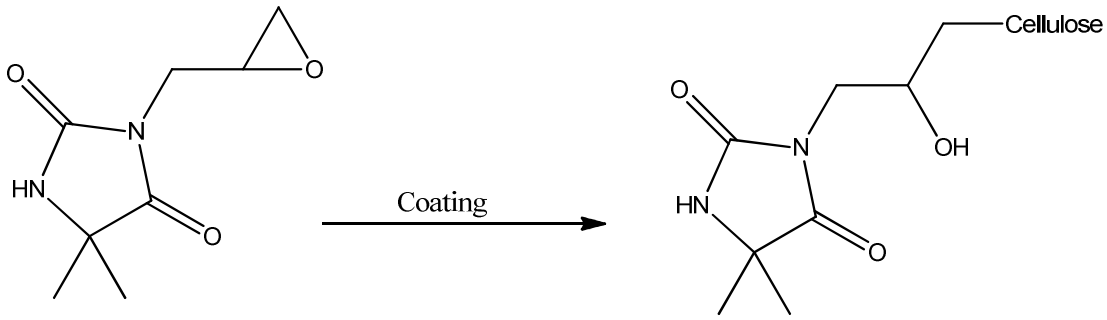

Figure 1. 15. Immobilization of hydantoin epoxide onto cellulose.

Polycarboxylic acid based crosslinking agents were also utilized to immobilize N-halamine structure on materials. Lee at al.[36] was the first to describe a way of making biocidal coatings on cotton fabric using 1,2,3,4-butanetetracarboxylic acid (BTCA) as a

crosslinking agent. Recently, Ren et al.[37,38] synthesized N-halamine compounds having diol groups, and applied them on cotton fabric using BTCA as a coupling agent. The treated fabrics exhibited not only antimicrobial functionality, but also improvement in wrinkle recovery angle.

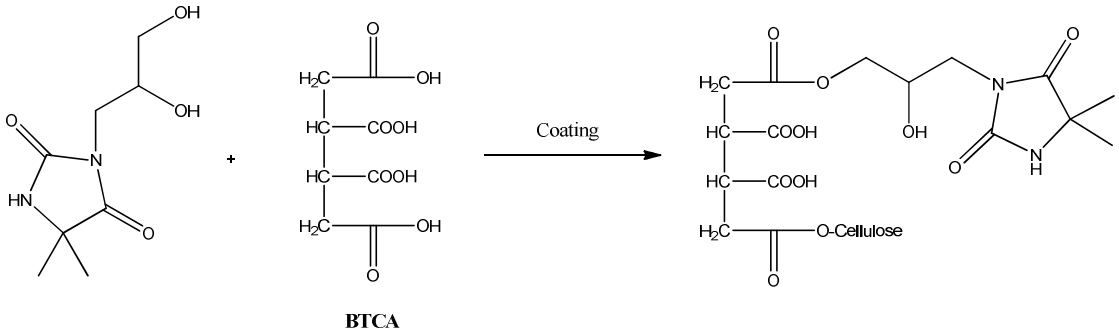

Figure 1. 16. Immobilization of hydantoin diol onto cellulose with BTCA .

Grafting was another technique employed to functionalize surfaces. Lin et al.[39] described a way of making N-halamine based biocidal polyester. First, the surface of polyester fabric was modified by a controlled hydrolysis of ester groups using ammonium hydroxide, so that amide groups could be formed. Then, 3-hydroxylmethyl-5, 5-dimethylhydantoin was covalently bonded to amide ended groups. An effective biocidal coating against a broad spectrum of bacteria was obtained without sacrificing too much of the fabric's strength.

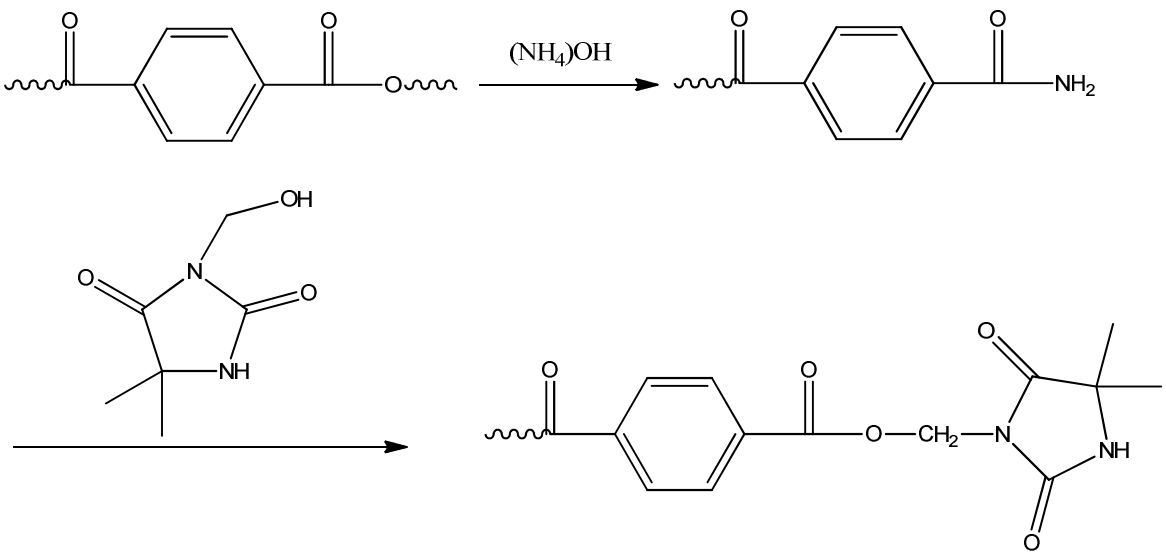

Figure 1. 17. Grafting N-halamine precursor onto polyester.[39]

Lin et al.[40] also reported an N-halamine based antimicrobial treatment of nylon fabrics. Heterocyclic N-halamine precursors were covalently bonded to the nylon surface using formaldehyde as a crosslinking agent. Initially, nylon fabrics were treated with formaldehyde solution in order to form hydroxylmethyl functional groups on the surface. Then, N-halamine compounds having hydroxyl groups were grafted by reacting with hydroxymethyl groups. Halogenated swatches exhibited around 7 log reduction of both Gram-negative and Gram-positive bacteria within 10 min of contact time.

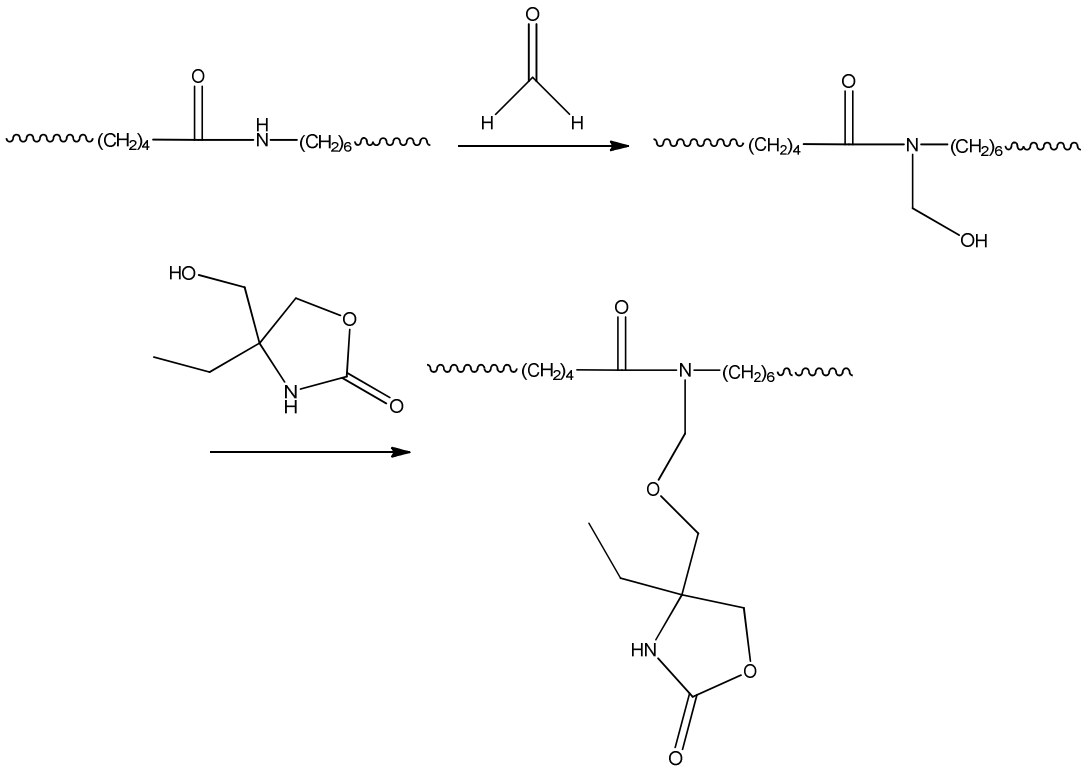

Figure 1. 18. Grafting N-halamine precursors onto nylon.[40]

Liu and Sun[41] grafted acyclic N-halamine precursors such as methacrylamide and acrylamide on cotton fabric by free radical polymerizations. Use of radical initiators resulted in hydrogen atom abstraction leading to the formation of macromolecular radicals which then react with the vinyl bonds of the N-halamine precursors. Even though this imparts an effective biocidal coating, implementation of this method on a commercial scale is difficult, since acyclic precursors are prone to hydrolysis, and the grafting yield is low.

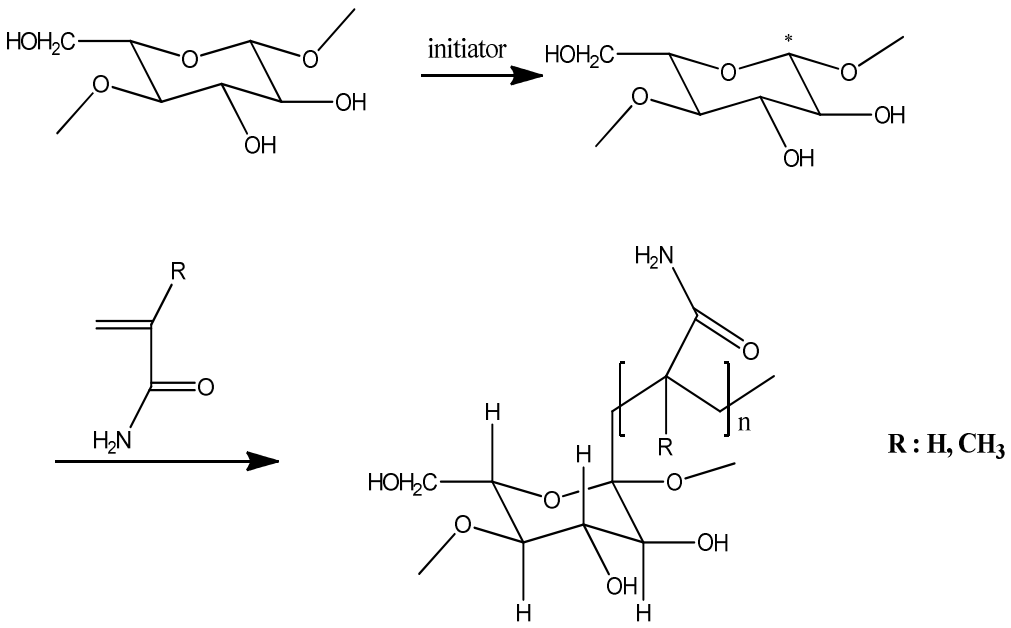

Figure 1. 19. Radical graft polymerization of acylic N-halamine precursors.[41]

3. Mixing N-halamine precursors with a host polymer during processing is another commonly applied technique used to obtain fibers or polymers having antimicrobial functionality. For instance, Lee et al.[42] dissolved *m*-aramid and cellulose in a common solvent, 1-butyl-3-methylimidazolium chloride, and they employed a dry-jet-wet spinning to form composite fibers. Similarly, Badrossamay and Sun[43] incorporated several N-halamine precursors onto a polypropylene surface via a melt graft polymerization technique. The halogenated fibers exhibited potent antimicrobial functionality against Gram-negative bacteria.

1.4.5. References

(1) Hays, J. N. *Epidemics and pandemics: their impacts on human history*; Abc-clio: Santa Barbara **2005**.

(2) Potter, C. W. *Journal of applied microbiology* **2001**, *91*, 572-579.

(3) Binder, S.; Levitt, A. M.; Sacks, J. J.; Hughes, J. M. *Science* **1999**, *284*, 1311.

(4) Szinicz, L. *Toxicology* **2005**, *214*, 167-181.

(5) Smart, J. K. *Medical Aspects of Chemical and Biological Warfare. Washington, DC: Office of the Surgeon General* **1997**, 9-86.

(6) Scott, R. D. *The direct medical costs of healthcare-associated infections in US hospitals and the benefits of prevention*; Division of Healthcare Quality Promotion National Center for Preparedness, Detection, and Control of Infectious Diseases, Centers for Disease Control and Prevention: Atlanta, GA, 2009.

(7) Klevens, R. M.; Edwards, J. R.; Richards, C. L.; Horan, T. C.; Gaynes, R. P.; Pollock, D. A.; Cardo, D. M. *Public Health Reports* **2007**, *122*, 160.

(8) Gagliotti, C.; Balode, A.; Baquero, F.; Degener, J.; Grundmann, H.; Gur, D.; Jarlier, V.; Kahlmeter, G.; Monen, J.; Monnet, D. *Euro surveillance* **2011**, *16*.

(9) Ren, X.; Kou, L.; Liang, J.; Worley, S. D.; Tzou, Y. M.; Huang, T. S. *Cellulose* **2008**, *15*, 593-598.

(10) Kocer, H. B.; Akdag, A.; Worley, S. D.; Acevedo, O.; Broughton, R. M.; Wu, Y. *ACS Applied Materials & Interfaces* **2010**, *2*, 2456-2464.

(11) Maillard, J. Y. *Journal of applied microbiology* **2002**, *92*, 16S-27S.

(12) Denyer, S. P. *International biodeterioration & biodegradation* **1995**, *36*, 227-245.

(13) Kelland, M. A. *Production chemicals for the oil and gas industry*; CRC: Boca Raton, 2009.

(14) Wu, R. PhD. Dissertation, Auburn University, 2004.

(15) de Paula, G. F.; Netto, G. I.; Mattoso, L. H. C. *Polymers*, *3*, 928-941.

(16) Kou, L.; Liang, J.; Ren, X.; Kocer, H. B.; Worley, S. D.; Tzou, Y. M.; Huang, T. S. *Industrial & Engineering Chemistry Research* **2009**, *48*, 6521-6526.

(17) McDonnell, G.; Russell, A. *Clinical microbiology reviews* **1999**, *12*, 147-179.

(18) Manivannan, G. *Disinfection and decontamination: Principles, applications and related issues*; CRC: Boca Raton, 2007.

(19) Kocer, H. B. Ph.D. Dissertation, Auburn University, 2009.

(20) Zhu, C. Master Thesis, Auburn University, 2008.

(21) Akdag, A.; Okur, S.; McKee, M. L.; Worley, S. D. *Journal of Chemical Theory and Computation* **2006**, *2*, 879-884.

(22) Qian, L.; Sun, G. *Journal of applied polymer science* **2003**, *89*, 2418-2425.

(23) Sun, G.; Wheatley, W. B.; Worley, S. D. *Industrial & Engineering Chemistry Research* **1994**, *33*, 168-170.

(24) Chen, Y.; Worley, S. D.; Kim, J.; Wei, C. I.; Chen, T. Y.; Santiago, J. I.; Williams, J. F.; Sun, G. *Industrial & Engineering Chemistry Research* **2003**, *42*, 280-284.

(25) Chen, Y.; Worley, S. D.; Kim, J.; Wei, C. I.; Chen, T. Y.; Suess, J.; Kawai, H.; Williams, J. F. *Industrial & Engineering Chemistry Research* **2003**, *42*, 5715-5720.

(26) Sun, Y.; Sun, G. *Journal of applied polymer science* **2001**, *80*, 2460-2467.

(27) Sun, Y.; Sun, G. *Journal of Polymer Science Part A: Polymer Chemistry* **2001**, *39*, 3348-3355.

(28) Eknoian, M. W.; Worley, S. D.; Bickert, J.; Williams, J. F. *Polymer* **1999**, *40*, 1367-1371.

(29) Li, Y.; Worley, S. D. *Journal of bioactive and compatible polymers* **2001**, *16*, 493.

(30) Kocer, H. B.; Worley, S. D.; Broughton, R. M.; Huang, T. S. *Reactive and Functional Polymers* **2011**, *71*, 561-568.

(31) Worley, S. D.; Chen, Y.; Wang, J. W.; Wu, R.; Cho, U.; Broughton, R. M.; Kim, J.; Wei, C. I.; Williams, J. F.; Chen, J. *Surface Coatings International Part B: Coatings Transactions* **2005**, *88*, 93-99.

(32) Ren, X.; Kocer, H. B.; Kou, L.; Worley, S. D.; Broughton, R. M.; Tzou, Y. M.; Huang, T. S. *Journal of applied polymer science* **2008**, *109*, 2756-2761.

(33) Liang, J.; Barnes, K.; Akdag, A.; Worley, S. D.; Lee, J.; Broughton, R. M.; Huang, T. S. *Industrial & Engineering Chemistry Research* **2007**, *46*, 1861-1866.

(34) Worley, S. D.; Chen, Y.; Wang, J.; Wu, R.; Li, Y.; US Patent App. 20,040/127,667: **2003**.

(35) Liang, J.; Chen, Y.; Ren, X.; Wu, R.; Barnes, K.; Worley, S. D.; Broughton, R. M.; Cho, U.; Kocer, H.; Huang, T. S. *Industrial & Engineering Chemistry Research* **2007**, *46*, 6425-6429.

(36) Lee, J.; Broughton, R. M.; Akdag, A.; Worley, S. D.; Huang, T. S. *Textile Research Journal* **2007**, *77*, 604-611.

(37) Ren, X.; Kocer, H. B.; Worley, S. D.; Broughton, R. M.; Huang, T. S. *Carbohydrate Polymers* **2009**, *75*, 683-687.

(38) Ren, X.; Akdag, A.; Kocer, H. B.; Worley, S. D.; Broughton, R. M.; Huang, T. S. *Carbohydrate Polymers* **2009**, *78*, 220-226.

(39) Lin, J.; Winkelmann, C.; Worley, S. D.; Kim, J.; Wei, C. *Journal of applied polymer science* **2002**, *85*, 177-182.

(40) Lin, J.; Winkelman, C.; Worley, S. D.; Broughton, R. M.; Williams, J. F. *Journal of applied polymer science* **2001**, *81*, 943-947.

(41) Liu, S.; Sun, G. *Industrial & Engineering Chemistry Research* **2006**, *45*, 6477-6482.

(42) Lee, J.; Broughton, R. M.; Worley, S. D.; Huang, T. S. *Journal of Engineered Fibers and Fabrics* **2007**, *2*, 25-32.

(43) Badrossamay, M. R.; Sun, G. *Journal of Biomedical Materials Research Part B: Applied Biomaterials* **2009**, *89*, 93-101.

CHAPTER 2

MULTIFUNCTIONAL COTTON FABRIC: ANTIMICROBIAL AND DURABLE PRESS

2.1. Introduction

Healthcare-associated infection is one of the world's most devastating problems causing millions of deaths and billions of dollars of healthcare cost each year. The annual direct hospital cost of treating healthcare-associated infections in the United States is estimated to be in the range of 28.4 to 33.6 billion dollars.[1] In 2002, 1.7 million people in the United States were infected by healthcare-associated infections leading to around 99,000 deaths.[2] Textile materials, particularly natural fibers, are very susceptible to microbial growth. Therefore, antimicrobial treatment of medical textiles such as gowns, bed sheets, uniforms, aprons, masks, etc, is essential to reduce the risk of spreading pathogenic microorganisms.

Numerous biocidal materials including quaternary ammonium salts,[3-6] *N*-halamines,[7-12] metal ions,[13,14] biguanides,[15,16] phosphonium compounds[17,18] and several others have been studied as a means to prevent transmission of microbial infections. Among those, *N*-halamines are one of the most effective classes of biocidal compounds applied to inactivate a broad spectrum of microorganisms including Gram-negative and Gram-positive bacteria, fungi, viruses, and yeasts in relatively brief contact times.[12] The inactivation mechanism involves transfer of the oxidative halogen to the microbial cell membrane.[19] Once all of the halogen on the surface is consumed, it can be regenerated simply by exposure to a halogen

source such as household bleach (Fig. 2.1). Three decades of *N*-halamine work in these laboratories began with water disinfection in the 1980s.[12] Later polymeric *N*-halamines were introduced to aqueous media disinfection.[20,21] Then the work was extended to antimicrobial treatments of materials such as cellulose,[10, 22, 23] nylon,[24] polyester,[25] polyurethane,[26,27] and polyacrylonitrile.[28] Extensive work has been done on antimicrobial coatings of cellulose, because it is widely used in the medical textile industry. Various *N*-halamine compounds have been immobilized onto cotton fabric through tethering groups,[29,30] grafting,[31,32] or electrostatic attractions.[33]

Polycarboxylic acid derivatives have been widely investigated as durable press finishing agents, since they do not release formaldehyde as does conventional dimethyloldihydroxyethylene urea.[34] Several studies pertaining to polycarboxylic acid treatment of cotton fabric have been done as a means to optimize durable press finishing and to minimize mechanical loss of cotton fabric caused by the treatment process.[35-38]

There is a need to make multifunctional coatings on textile surfaces so as to provide health safety and improved life quality. This study aims to impart biocidal and durable press functionalities to cotton fabric by a simple pad-dry-cure procedure. It had been reported earlier that cyclic *N*-halamines could be coated onto cotton using durable press finishing treatments with polycarboxylic acids.[39,40] In this study an acyclic *N*-halamine precursor, 2-amino-2-methyl-1-propanol (AMP), was applied onto cotton fabric using 1,2,3,4-butanetetracarboxylic acid (BTCA) as a crosslinking agent with the purpose of providing an inexpensive way of establishing antimicrobial and durable press functionalities. The coating was rendered biocidal upon dilute household bleach treatment and was used to inactivate Gram-negative and Gram-positive bacteria. Wrinkle recovery angle measurements were

performed to evaluate durable press efficacy. In addition, mechanical testing, washing stabilities, and UVA and storage stability evaluations have been conducted.

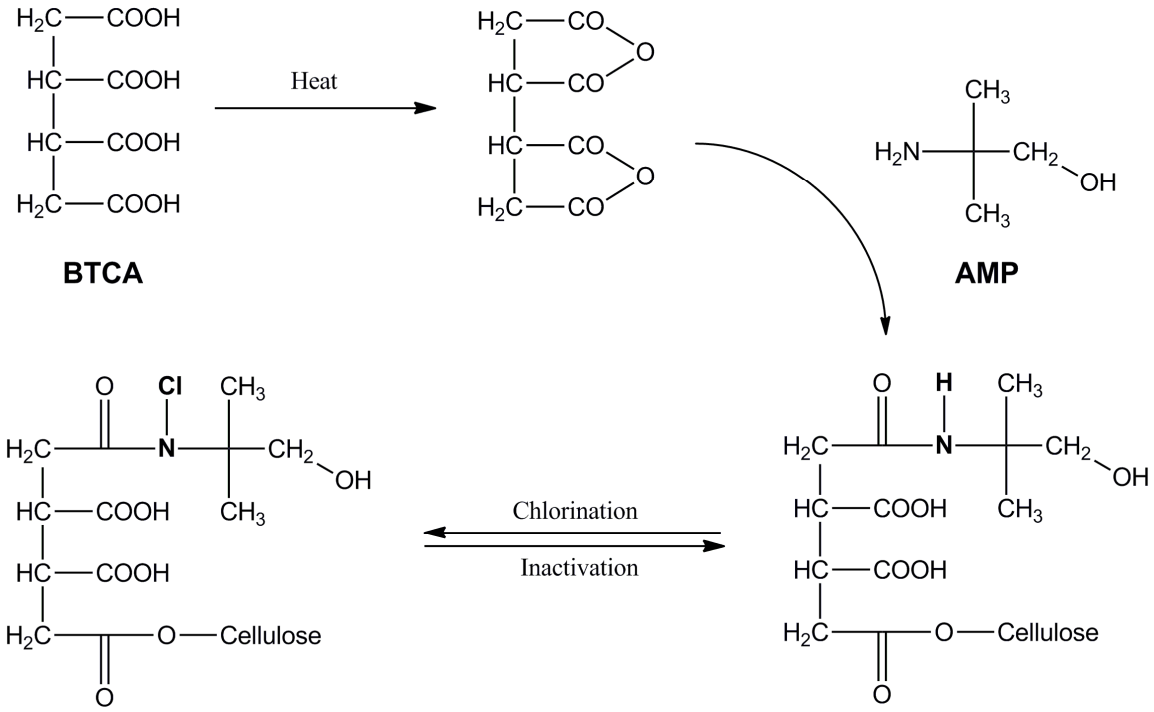

Figure 2.1. Attachment of 2-amino-2-methyl-1-propanol to Cellulose and Conversion to an N-halamine.

2.2. Experimental

2.2.1. Materials

All starting chemicals and solvents were purchased from Aldrich Chemical Company (Milwaukee, WI) or TCI America (Boston, MA), and used as is unless otherwise noted. Desized, scoured, and bleached (100%) cotton (Style 400 Cotton Print Cloth) was obtained from Testfabrics. Inc. (West Pittson, PA). Clorox® brand (Clorox, Inc., Oakland, CA) household bleach was used for chlorination. Bacteria cultures of *Staphylococcus aureus* ATCC 6538 and *Escherichia coli* O157:H7 ATCC 43895 were purchased from

American Type Culture Collection (Rockville, MD), and Trypticase soy agar was obtained from Difco Laboratories (Detroit, MI).

2.2.2. Instrumentation

^{13}C NMR spectra recorded with 1024 scans were obtained using a Bruker 400 MHz spectrometer. ATR-IR data recorded with 64 scans at 4 cm^{-1} resolution were obtained with a Nicolet 6700 FT-IR spectrometer with an ATR (Attenuated Total Reflectance) accessory on a diamond crystal. An Instron Model 1122 Textile Tester was used for mechanical testing. A TA instrument Q500 was used to obtain the thermal gravimetric analysis (TGA) data collected at a heating rate of 10 ^{o}C/min under nitrogen atmosphere.

2.2.3. Coating and Chlorination Procedure

BTCA and AMP were dissolved in water at specified concentrations. Cotton swatches were soaked in the coating solution for 15 min, and then uniformly padded through a laboratory wringer (Birch Brothers Southern, Waxhaw, NC). The immersed swatches were dried at 130 °C for 10 min, followed by curing at 175 °C for 5 min. Finally, the swatches were washed vigorously with 0.5 wt % detergent water for 15 min, followed by rinsing with distilled water.

The coated samples swatches were chlorinated with 10 wt % aqueous solution of household bleach (0.6 % wt Cl^{+}) at pH 7 for 1 h, followed by rinsing with distilled water. The cotton swatches were dried at 45 °C for 1 h to remove any occluded free chlorine from the surfaces. An iodometric/thiosulfate titration[30] was used to determine oxidative Cl^{+}%

content on the swatches. The weight percentage of chlorine was calculated according to equation 1.

$$Cl^{+}\% = \left(\frac{35.45 * N * V}{2 * W} \right) * 100 \quad (1)$$

In this equation $Cl^{+}\%$ is the weight percent of oxidative chlorine on the samples, N and V are the normality (equiv/L) and volume (L) of the $Na_2S_2O_3$ (titrant), respectively, and W is the weight of the cotton sample in g.

2.2.4. Synthesis of 2,3-bis(2-((1-hydroxy-2-methylpropan-2-yl)amino)-2-oxoethyl)succinic acid

In a round bottom flask, 20 mmol of AMP and 10 mmol of BTCA were dissolved in 25 ml of anhydrous N, N-dimethylacetamide (DMAc). The temperature was gradually increased to 155 °C within 15 min, and the solution was stirred at that temperature for 5 min. Then the solution was cooled to room temperature, and 50 ml of chloroform were added. A white solid product precipitated which was recovered by filtration. ^{13}C NMR (D_2O, 400 MHz) δ 23.98, 38.77, 47.94, 57.41, 68.87, 180.42, 181.66.

2.2.5. Stability Testing

American Association of Textile Chemists and Colorists (AATCC) test method 61-1996 and a laboratory model Lauder-Ometer were used to evaluate the durability of the coatings and the stability of chlorine on the swatches toward laundering. In order to evaluate the stability of bound chlorine toward washing, one set of the samples was chlorinated before washing. To address the durability of unchlorinated and chlorinated coatings as a

function of washing cycles, a second set of the samples was chlorinated both before and after the washing cycles, and a third set was chlorinated only after the washing cycles, respectively.

An accelerated weathering tester (The Q-panel Company, Cleveland, OH, USA) was used to evaluate UVA light stability of the bound chlorine and the coatings on the cotton fabric. Chlorinated and unchlorinated cotton swatches were exposed to UVA light (Type A, 315-400 nm) for times in the range of 1-72 h. One set of the chlorinated samples was titrated after a specified time of UVA exposure in order to assess the chlorine stability, and the other set was rechlorinated and then titrated so as to address rechargeability. Unchlorinated samples were chlorinated and then titrated to evaluate the durability of the coating itself.

2.2.6. Wrinkle Recovery Angle Measurement and Mechanical Testing

Wrinkle recovery angle measurements were performed using AATCC test method 66-1998, Option 2. In this method, 40x15 mm swatches were folded, and 500 ± 5 g of weight was applied onto the swatches for 5 min, after which time the weight was removed. The recovery angles were measured in both warp (lengthwise yarns) and weft (widthwise yarns) directions, and the sum of these angles was reported as the wrinkle recovery angle (WRA).

ASTM D-5035-95 and ASTM D-2261-96 were employed for tensile and tear strength determinations, respectively. All of the samples were conditioned at standard lab conditions (65% RH and 21 °C) for 1 day prior to testing. 12 in/min crosshead speed was applied to the swatches, and 4 replicates were produced for each sample with their averages reported herein.

2.2.7. Biocidal Efficacy Testing

A modified AATCC "sandwich test" was conducted for evaluation of biocidal efficacies of the coatings. In this method, chlorinated and unchlorinated (control sample) swatches were challenged with *S. aureus* (ATCC 6538) and *E. coli* O157:H7 (ATCC 43895). Suspensions of known bacteria population (colony forming units, CFU) were prepared by suspending the bacteria in pH 7 phosphate buffer solution (100 μM). Then 25 μL of this suspension were placed to the center of a 2.54 cm square swatch, and a second identical swatch was placed on top of it. In order to make an adequate contact with the bacteria, a sterile weight was placed on the "sandwich". Three different contact times were employed: 5, 10, and 30 min. After the specified contact times, the samples were quenched with 0.02 N sodium thiosulfate solution by vortexing for 2 min so as to neutralize any oxidative chlorine left on the sample. Serial dilutions were made using pH 7, 100 μM phosphate buffer and plated on Trypticase soy agar plates. The plates were incubated at 37 °C for 24 h and then counted for viable CFU of bacteria for the biocidal efficacy analysis.

2.3. Results and Discussion

2.3.1. Characterization of the Coatings

BTCA and AMP were dissolved in water and applied onto cotton fabric according to the procedure described above. When heat was applied, BTCA formed cyclic anhydride structures[35] which then reacted with the NH_2 group of AMP and the OH groups of cellulose (Fig. 1). The coating on the cotton fabric was characterized by ATR-IR spectroscopy (Fig. 2.2). As can be seen, when only 3.5 wt % BTCA was coated onto cotton (B), the carbonyl stretching mode was obtained at 1722 cm^{-1}.[38,39] On the other hand, when AMP and BTCA were coated together (C), a new band at 1696 cm^{-1} appeared indicating amide formation

between BTCA and AMP. This vibrational band shifted to a slightly higher wavenumber upon chlorination (D) signifying the disruption of N-H···O=C hydrogen bonding as conversion of N-H to N-Cl occurred.[40] Furthermore, upon chlorination some acid groups of BTCA were converted into the carboxylate anion which exhibited a vibrational band at 1573 cm^{-1}.[36]

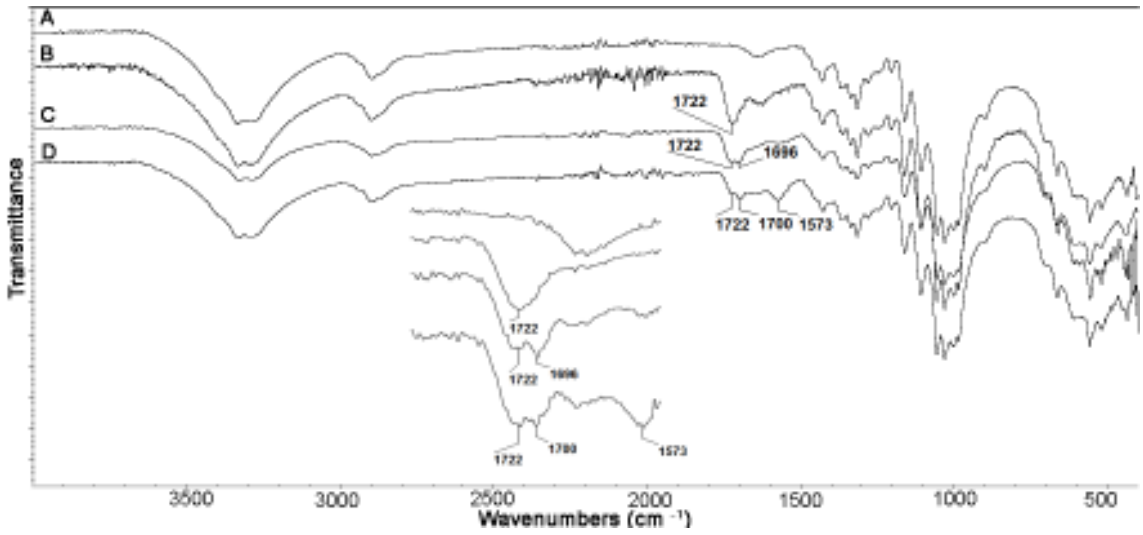

Figure 2.2. ATR-IR Characterization of the coating on cotton fabric. A:Cotton fabric, B: BTCA coated cotton fabric (3.5 wt %), C: BTCA (3.5 wt %) and AMP (1.5 wt %) Coated Cotton Fabric, D: BTCA (3.5 wt %) and AMP (1.5 wt %) chlorinated -coated cotton fabric.

Anhydrides are known to preferentially react with amine groups as opposed to hydroxyls.[41] Thus, when BTCA formed the anhydride, it then reacted with the amine group rather than the hydroxyl group of AMP, since amines are stronger nucleophiles than are alcohols.[39] In order to address the reaction pathway, AMP and BTCA were reacted in DMAc as described in the experimental section and then characterized by ATR-IR and NMR spectroscopies. The ATR-IR spectra of AMP, BTCA and their product are shown in Fig. 2.3. In these spectra, 1592 (A) and 1692 cm^{-1} (B) correspond to the amine bending mode of AMP and the carbonyl stretching mode of BTCA, respectively.[36,42] When AMP and

BTCA were reacted (C), the amine bending mode disappeared, and a new band around 1643 cm^{-1} corresponding to the amide stretching mode appeared.[43] On the other hand, the band corresponding to the carbonyl stretching mode of BTCA shifted slightly to a higher wavenumber. The C-O stretching mode of the primary alcohol moiety present in AMP was observed at 1050 cm^{-1}. NMR spectra of the product also supported the formation of an amide bond rather than ester bonding of AMP and BTCA. As can be seen in the ^{13}C NMR spectra (Fig. SP.2.3, Supplementary Data), upon reaction the signal for the tertiary carbon atom of AMP shifted downfield (from 52 ppm to 57 ppm) due to reduced electron density, whereas the methylene group signal of AMP shifted upfield (from 73 ppm to 68 ppm) further signifying that the reaction took place through the amine group.

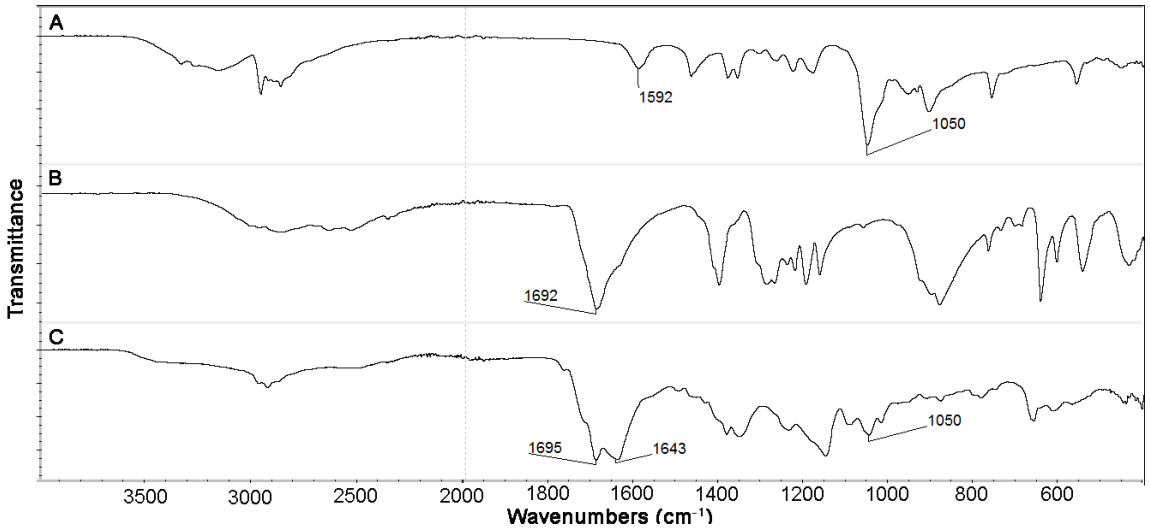

Figure 2.3. ATR-IR Spectra of AMP (A), BTCA (B), 2,3-bis(2-((1-hydroxy-2-methylpropan-2-yl)amino)-2-oxoethyl)succinic acid (C).

TGA data of untreated and treated cotton fabrics are shown in Fig.2.4. As expected, AMP/BTCA treatment lowered the thermal decomposition temperature (from 348 °C to 339 °C) and increased the char amount (from 7 % to 12 %), since crosslinking imparts higher

thermal stability.[34] When the coated samples were chlorinated, the thermal decomposition temperature decreased even more (to 330 °C) due to the chlorination process weakening the fabric. Furthermore, the chlorinated samples exhibited higher % residue (18%) than the unchlorinated samples as observed in a previous *N*-halamine study.[44]

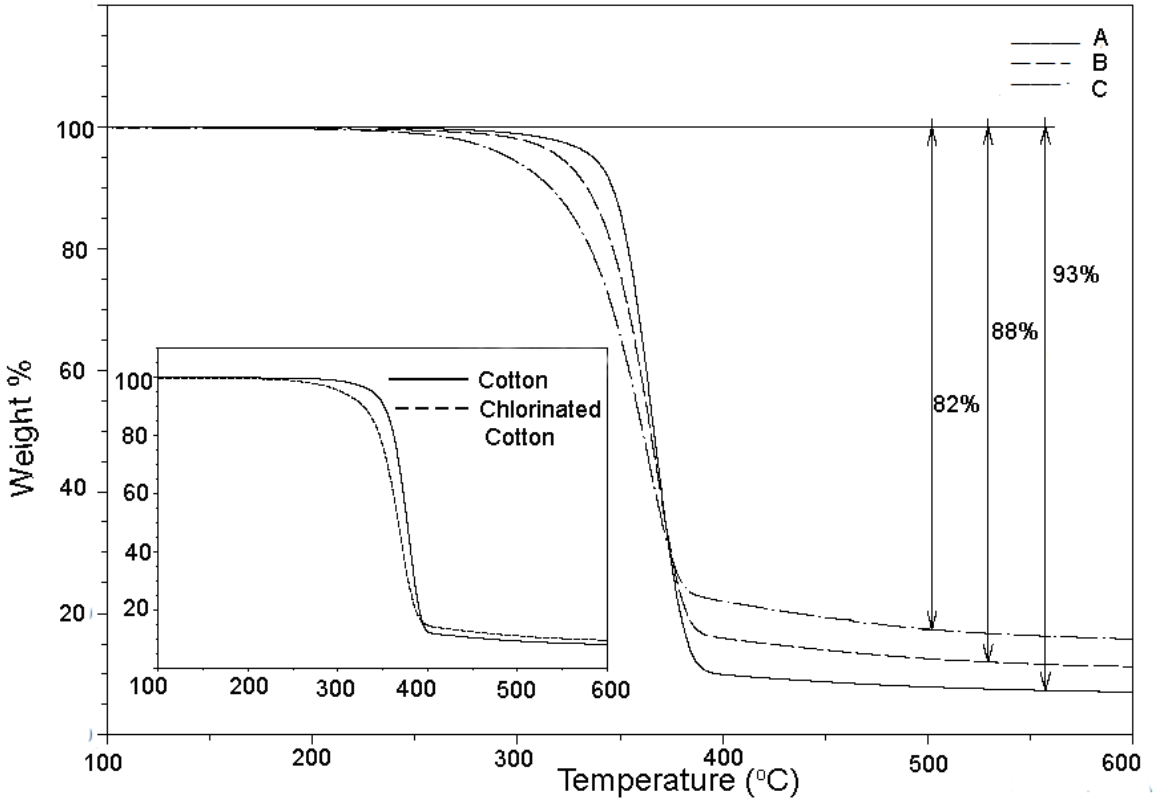

Figure 2.4. TGA of Cotton Fabric (A), 5 wt % AMP / BTCA coated cotton fabric (B) and 5 wt % AMP / BTCA chlorinated – coated cotton fabric (C).

2.3.2. Washing Stability

Stability and durability of the coatings toward repeated laundering have been determined by measuring the remaining chlorine content of the swatches as shown in Table 2.1. In this table, the X column represents the swatches chlorinated only before the washing tests, the Y column shows the swatches chlorinated both before and after the washing tests,

and the Z column demonstrates the swatches chlorinated only after the washing tests. Two different sets of experiments have been performed in order to observe the effect of BTCA content on washing stability and durability. In the first experiment 5 wt % (1.5 % AMP + 3.5 % BTCA) coated swatches and in the second experiment 7.5 wt % (1.5 % AMP + 6 % BTCA) coated samples were evaluated. In general, coating of AMP together with BTCA exhibited promising stability toward repeated laundering (Table 2.1-X), such that more than 50 % of the initial chlorine remained even after 50 washing cycles. ATR-IR analysis of the swatches exposed to 50 laundering cycles supported the existence of the coating (Fig. SP.2.4, Supplementary Data). Although AMP is an acyclic *N*-halamine precursor, the stabilities of the coatings were even better than some of the previously reported cyclic *N*-halamines attached onto cotton fabric using different tethering groups.[23, 29, 30, 45, 46] A possible reason for this superior stability might be the existence of crosslinked structures both within and on the surfaces of the cotton fiber, protecting the coatings from excessive mechanical effects of the washing cycles. When the swatches shown in the X column were rechlorinated (Y column), the remaining chlorine contents increased substantially, showing that the chlorine loss with increasing washing cycles in column X was due mostly to N-Cl bond dissociation rather than the coating being hydrolyzed away from the surface. In both cases, durability in the Y column was preferable to that in the Z column, since prechlorination rendered the surface more hydrophobic, which then reduced the hydrolysis effects reported earlier in some other studies.[25,47] When the BTCA content in the coating solution was increased, the durability of the coating improved significantly as expected, since increased crosslinking on the surface shielded the *N*-halamine moiety from washing

mechanical effects. This shielding effect was also observed during titration, as the oxidative chlorine reacted more slowly when the BTCA content was higher.

Table 2.1. Stability and durability toward washings of the coatings on the cotton fabric (Cl^+ % remaining).

Number of Machine Washes[a]	5 wt % Coated (1.5 % AMP+3.5 % BTCA)			7.5 wt % Coated (1.5 % AMP+6 % BTCA)		
	X	Y	Z	X	Y	Z
0	0.32			0.33		
5	0.23	0.32	0.28	0.27	0.31	0.32
10	0.20	0.31	0.26	0.26	0.32	0.30
25	0.18	0.29	0.24	0.18	0.32	0.30
50	0.17	0.26	0.23	0.18	0.32	0.29

[a]: A washing cycle is equivalent to five normal machine washings in AATCC Test Method 61, X: Chlorinated before washing, Y: Chlorinated before washing and rechlorinated after washing, Z: Unchlorinated before washing, but chlorinated after washing.

2.3.3. UVA Light Stability

Stability of the coatings toward UVA light exposure is illustrated in Table 2.2. The BTCA amount in the coating solution was varied so as to observe the effect of crosslinking density.

Table 2.2. Stability toward UVA light exposure of the coatings on the cotton fabric (Cl^+ % remaining).

Exposure time (h)	5 wt % Coated (1.5 % AMP+3.5 % BTCA)		7.5 wt % Coated (1.5 % AMP+6 % BTCA)	
	Chlorinated	Unchlorinated	Chlorinated	Unchlorinated
0	0.29		0.26	
1	0.08		0.13	
2	0.07		0.10	
3	0.05		0.09	
6	0.02		0.05	
12	0.01		0.03	
24	0		0.02	
Rechlorination	0.15	0.29	0.18	0.27
48	0		0.01	
Rechlorination	0.10	0.19	0.15	0.23

For the chlorinated (5 wt % coated swatches) exposed to UVA light, all of the oxidative chlorine was lost within 24 h of exposure. When 24 h and 48 h exposed samples were rechlorinated, around 50 % and 30 % of the initial chlorine loading was restored, respectively, revealing that the chlorine lost was due to both N-Cl bond dissociation and a decomposition taking place in the structure. On the other hand, no decomposition was observed for the unchlorinated samples chlorinated at the end of 24 h UVA exposure, whereas 35 % decomposition was detected when they were chlorinated at the end of 48 h UVA exposure. This observation led to the conclusion that unlike previously studied *N*-halamine coatings,[48] a slight photodecomposition of the coating took place under UVA light exposure even without the coating being chlorinated. This decomposition was also detected by ATR-IR analysis of the UV irradiated samples (Fig. SP.2.5, Supplementary Data) and the mechanism for this photodecomposition is under study. Increased BTCA amount (7.5 wt % coated) resulted in a slower chlorine loss and a lesser magnitude of photodecomposition, but in general the same trend as in the 5 wt % coated swatches was observed.

2.3.4. Storage Stability

Storage stability of the coatings in sealed conditions was evaluated by measuring the remaining chlorine contents of the bleached swatches over a 60 d period (Table 2.3). Two sets of 5 wt % coated swatches were stored in a conditioning room (21 °C, 65% relative humidity); one set was placed under lab light on a bench, and the other was stored in a dark environment. Swatches stored in darkness retained around 70 % and 50 % of the initial chlorine loading at the end of 30 and 60 d, respectively; whereas, the swatches stored under lab lighting lost almost all of the chlorine within 30 d. However, upon rechlorination, 90 % of the initial chlorine was restored revealing that the loss was primarily due to dissociation of the N-Cl bond rather than polymer decomposition. Overall, the storage stability in this work was comparable to cyclic *N*-halamine coatings studied previously.[49]

Table 2.3. Storage stability of 5 wt % (1.5 % AMP + 3.5 % BTCA) coated cotton fabric (Cl^+ % remaining).

Number of days	Lab Light Storage	Dark Storage
0	0.34	0.34
5	0.19	0.29
10	0.13	0.28
14	0.09	0.26
20	0.05	0.25
25	0.03	0.24
30	0.02	0.24
Rechlorination	0.30	nd[a]
60	0.04	0.16
Rechlorination	0.24	0.33

[a] nd: Not determined

2.3.5. Wrinkle Recovery Measurement and Mechanical Testing

Sufficient chlorine loading of about 0.30 wt % for an effective biocidal efficacy[30] could be reached with the presence of 1.5 wt % AMP in the coating solution. Therefore, the BTCA concentration in the coating solution varied from 1.5 to 9 wt % with constant 1.5 wt % AMP in the coating solution, and wrinkle recovery angles of the coated swatches were measured. As can be seen in Fig. 2.5, increasing the BTCA concentration in the coating solution increased the wrinkle recovery angle exponentially, as reported previously.[38,50]

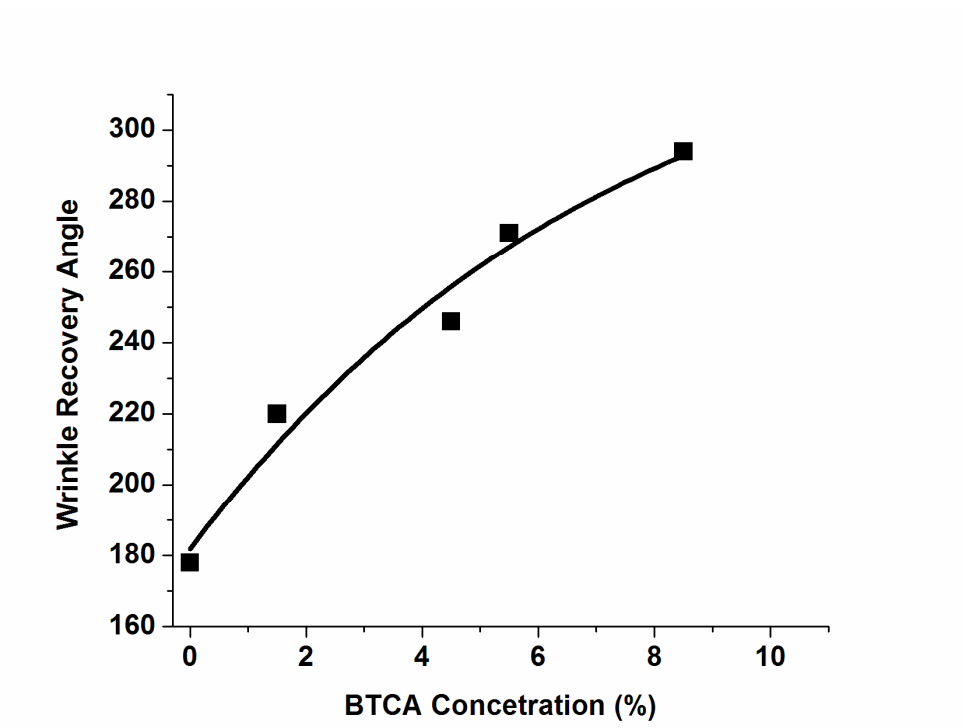

Figure 2.5. Effect of BTCA concentration on wrinkle recovery angle.

Mechanical test and wrinkle recovery angle measurement results are summarized in Table 2.4. Both the tensile and the tear load decreased dramatically when the cotton fabric was treated with only 6 wt % BTCA. This loss was due to intramolecular crosslinking in the

fibers (reversible loss) and depolymerization of the cellulose macromolecules by the acidity of the treatment solution[37] (pH=1.9) which has been observed in several other studies.[34,36,50] Interestingly, adding AMP (1.5 wt %) to the coating solution improved the strength retention tremendously. This was probably due to reduced acidity of the coating solution in the presence of AMP (pH 3.2) and the less amount of crosslinking as evidenced by lower wrinkle recovery angle (WRA). When the AMP/BTCA treated fabric was exposed to bleach, strength retention was further enhanced, because NaOH present in the bleaching solution destroyed some of the ester linkages between cellulose and BTCA leading to reduced intramolecular crosslinking. However, this increase was small revealing that the strength loss at that curing condition was due mostly to the acidity of the treatment solution.

Table 2.4. Mechanical testing and WRA measurement results of 7.5 wt % coated (1.5 % AMP + 6 % BTCA) cotton fabrics.

	Tensile Breaking Load (N)		**Average Tear Load (N)**		**WRA**
	Weft[d]	Warp[e]	Weft	Warp	(c+f)[f]
Untreated	173	279	5.25	6.26	198
BTCA Coated[a]	54	152	0.82	1.88	296
BTCA+AMP Coat.[b]	74	216	1.07	2.70	280
BTCA+AMP Coat.-Cl[c]	83.5	225	1.35	3.14	273

[a]: Treated with only 6 % wt BTCA. [b]:Treated with 7.5 % wt AMP/BTCA (1.5 % AMP+6 % BTCA). [c]:Treated with 7.5 % wt AMP/BTCA (1.5 % AMP+6 % BTCA) and then chlorinated. [d]:Widthwise. [e]:Lengthwise. [f]:Sum of the wrinkle recovery angle in weft and warp direction.

2.3.6. Biocidal Efficacy Test

The unchlorinated-treated and chlorinated-treated cotton swatches (1.5 wt % AMP + 3.5 wt % BTCA) were challenged with *E. coli* O157:H7 and *S. aureus* at concentrations of around 10^6 CFU, and the results are summarized in Table 2.5. The chlorinated swatches inactivated all of the Gram-negative and Gram-positive bacteria within 5 min of contact time. The unchlorinated control swatches did not exhibit any significant biocidal efficacy with 0.17 log *E. coli* O157:H7 and 0.52 log *S. aureus* reductions within 30 min of contact time. This limited degree of reduction is due to the adhesion of the bacteria to the fabric surfaces.[46] Previous studies in these laboratories showed that comparable biocidal efficacies are obtained when the chlorine loading is around 0.30 wt %.[51] Since 7.5 % wt coated swatches provided around the same chlorine loadings, we expect to have equally effective biocidal efficacy when the BTCA concentration is higher.

Table 2.5. Biocidal test results 5 wt % (1.5 % AMP + 3.5 % BTCA) coated cotton fabrics.

		E. coli O157:H7 [a]		***S. aureus*** [b]	
	Contact time (min)	**%**	**Log Reduction**	**%**	**Log Reduction**
Control	30	31.7	0.17	69.7	0.52
Chlorinated Cl^+ % 0.32	5	100	6.72	100	6.25
	10	100	6.72	100	6.25
	30	100	6.72	100	6.25

[a]: The inoculums concentration was 6.72 log. [b]: The inoculums concentration was 6.25 log

2.4. Conclusions

2-amino-2-methyl-1-propanol has been coated onto cotton fabric using 1,2,3,4-butanetetracarboxylic acid as a crosslinking agent. BTCA acted not only as a crosslinking

agent between the fabric and AMP, but also it improved the wrinkle recovery angle of to the cotton fabric. The coating was rendered biocidal upon bleach exposure; it exhibited highly efficient antimicrobial functionality against *E. coli* O157:H7 and *S. aureus*, providing complete kill within 5 min of contact time. Only 1.5 wt % AMP was sufficient for this effective biocidal efficacy. The coating was also very stable and durable toward repeated laundering. Even though a photolytic decomposition was observed upon exposure to UVA light, the coating exhibited sufficient storage stability for industrial uses. Coating of cotton fabric with AMP/BTCA has industrial potential, since very effective antimicrobial and durable press functionalities could be imparted by coating an inexpensive *N*-halamine precursor via a fairly simple procedure.

2.5. References

(1) Scott, R. D. The direct medical costs of healthcare-associated infections in US hospitals and the benefits of prevention; Division of Healthcare Quality Promotion National Center for Preparedness, Detection, and Control of Infectious Diseases Coordinating Center for Infectious Diseases Centers for Disease Control and Prevention: Atlanta, **2009**.

(2) Klevens, R. M.; Edwards, J. R.; Richards, C. L.; Horan, T. C.; Gaynes, R. P.; Pollock, D. A.; Cardo, D. M. *Public Health Reports* **2007**, *122*, 160.

(3) Eren, T.; Som, A.; Rennie, J. R.; Nelson, C. F.; Urgina, Y.; Nüsslein, K.; Coughlin, E. B.; Tew, G. N. *Macromolecular Chemistry and Physics* **2008**, *209*, 516.

(4) Lewis, K.; Klibanov, *A. M. Trends in Biotechnology* **2005**, *23*, 343.

(5) Sauvet, G.; Fortuniak, W.; Kazmierski, K.; Chojnowski, J. *Journal of Polymer Science Part A: Polymer Chemistry* **2003**, *41*, 2939.

(6) Tiller, J. C.; Liao, C. J.; Lewis, K.; Klibanov, A. M. *Proceedings of the National Academy of Sciences of the United States of America* **2001**, *98*, 5981.

(7) Chen, Z.; Sun, Y. *Industrial & Engineering Chemistry Research* **2006**, *45*, 2634.

(8) Goddard, J. M.; Hotchkiss, J. H. *Journal of Food Protection* **2008**, *71*, 2042.

(9) Kenawy, E. R.; Worley, S. D.; Broughton, R. M. *Biomacromolecules* **2007**, *8*, 1359.

(10) Qian, L.; Sun, G. *Journal of Applied Polymer Science* **2004**, *91*, 2588.

(11) Makal, U.; Wood, L.; Ohman, D. E.; Wynne, K. J. *Biomaterials* **2006**, *27*, 1316.

(12) Worley, S. D.; Williams, D. E. *Critical Reviews in Environmental Science and Technology* **1988**, *18*, 133.

(13) Rai, M.; Yadav, A.; Gade, A. *Biotechnology Advances* **2009**, 27, 76.

(14) Son, W. K.; Youk, J. H.; Park, W. H. *Carbohydrate Polymers* **2006**, *65*, 430.

(15) Huang, W.; Leonas, K. K. *Textile Research Journal* **2000**, *70*, 774.

(16) Ikeda, T.; Yamaguchi, H.; Tazuke, S. Antimicrobial Agents and Chemotherapy **1984**, *26*, 139.

(17) Kanazawa, A.; Ikeda, T.; Endo, T. *Journal of Polymer Science Part A: Polymer Chemistry* **1993**, *31*, 3003.

(18) Kenawy, E. R.; Abdel Hay, F. I.; El Shanshoury, A. E. R. R.; El Newehy, M. H. *Journal of Polymer Science Part A: Polymer Chemistry* **2002**, *40*, 2384.

(19) Denyer, S. P.; Stewart, G. *International Biodeterioration & Biodegradation* **1998**, *41*, 261.

(20) Sun, G.; Wheatley, W. B.; Worley, S. D. *Industrial & Engineering Chemistry Research* **1994**, *33*, 168.

(21) Worley, S. D.; Sun, G. *Trends in Polymer Science* **1996**, 4, 364.

(22) Chen, Z.; Luo, J.; Sun, Y. *Biomaterials* **2007**, *28*, 1597.

(23) Liang, J.; Barnes, K.; Akdag, A.; Worley, S. D.; Lee, J.; Broughton, R. M.; Huang, T. S. *Industrial & Engineering Chemistry Research* **2007a**, *46*, 1861.

(24) Lin, J.; Winkelman, C.; Worley, S. D.; Broughton, R. M.; Williams, J. F. *Journal of Applied Polymer Science* **2001**, *81*, 943.

(25) Ren, X.; Kocer, H. B.; Kou, L.; Worley, S. D.; Broughton, R. M.; Tzou, Y. M.; Huang, T. S. *Journal of Applied Polymer Science* **2008a**, *109*, 2756.

(26) Luo, J.; Chen, Z.; Sun, Y. *Journal of Biomedical Materials Research Part A* **2006**, *77A*, 823.

(27) Worley, S. D.; Li, F.; Wu, R.; Kim, J.; Wei, C. I.; Williams, J. F.; Owens, J. R.; Wander, J. D.; Bargmeyer, A. M.; Shirtliff, M. E. *Surface Coatings International Part B: Coatings Transactions* **2003**, *86*, 273.

(28) Ren, X.; Akdag, A.; Zhu, C.; Kou, L.; Worley, S. D.; Huang, T. S. *Journal of Biomedical Materials Research Part A* **2009**, *91*, 385.

(29) Kocer, H. B.; Worley, S. D.; Broughton, R. M.; Huang, T. S. *Reactive and Functional Polymers* **2011**, *71*, 561.

(30) Liang, J.; Chen, Y.; Ren, X.; Wu, R.; Barnes, K.; Worley, S. D.; Broughton, R. M.; Cho, U.; Kocer, H.; Huang, T. S. *Industrial & Engineering Chemistry Research* **2007b**, *46*, 6425.

(31) Liu, S.; Sun, G. *Journal of Applied Polymer Science* **2008**, *108*, 3480.

(32) Sun, Y.; Sun, G. *Journal of Applied Polymer Science* **2003**, *88*, 1032.

(33) Cerkez, I.; Kocer, H. B.; Worley, S. D.; Broughton, R. M.; Huang, T. S. *Langmuir* **2011**, *27*, 4091.

(34) Jang, J.; Yoon, K. C.; Ko, S. W. *Fibers and Polymers* **2001**, *2*, 184.

(35) Gillingham, E. L.; Lewis, D. M.; Voncina, B. *Textile Research Journal* **1999**, *69*, 949.

(36) Sricharussin, W.; Ryo-Aree, W.; Intasen, W.; Poungraksakirt, S. *Textile Research Journal* **2004**, *74*, 475.

(37) Xu, W. *Textile Research Journal* **2000**, *70*, 957.

(38) Xu, W.; Li, Y. *Textile Research Journal* **2000**, *70*, 588.

(39) Lee, J.; Broughton, R. M.; Akdag, A.; Worley, S. D.; Huang, T. S. *Textile Research Journal* **2007**, *77*, 604.

(40) Ren, X.; Kocer, H. B.; Worley, S. D.; Broughton, R. M.; Huang, T. S. *Carbohydrate Polymers* **2009**, *75*, 683.

(41) Naik, S.; Bhattacharjya, G.; Talukdar, B.; Patel, B. K. *European Journal of Organic Chemistry* **2004**, *2004*, 1254.

(42) Rhee, S. H.; Lee, S. J.; Tanaka, J. *Journal of Biomaterials Science* **2006**, Polymer Edition, *17*, 357.

(43) Wicks Jr, Z. W.; Chen, G. F. *The Journal of Organic Chemistry* **1979**, *44*, 1244.

(44) Chen, Y.; Wang, L.; Yu, H.; Shi, Q.; Dong, X. *Journal of Materials Science* **2007**, *42*, 4018.

(45) Kou, L.; Liang, J.; Ren, X.; Kocer, H. B.; Worley, S. D.; Tzou, Y. M.; Huang, T. S. *Industrial & Engineering Chemistry Research* **2009**, *48*, 6521.

(46) Ren, X.; Kou, L.; Kocer, H. B.; Zhu, C.; Worley, S. D.; Broughton, R. M.; Huang, T. *S. Colloids and Surfaces A: Physicochemical and Engineering Aspects* **2008b**, *317*, 711.

(47) Worley, S. D.; Chen, Y.; Wang, J. W.; Wu, R.; Cho, U.; Broughton, R. M.; Kim, J.; Wei, C. I.; Williams, J. F.; Chen, *J. Surface Coatings International Part B: Coatings Transactions* **2005**, *88*, 93.

(48) Kocer, H. B.; Akdag, A.; Worley, S. D.; Acevedo, O.; Broughton, R. M.; Wu, Y. *ACS Applied Materials & Interfaces* **2010**, *2*, 2456.

(49) Ren, X.; Kou, L.; Liang, J.; Worley, S. D.; Tzou, Y. M.; Huang, T. S. *Cellulose* **2008**, *15*, 593.

(50) El-Tahlawy, K. F.; El-Bendary, M. A.; Elhendawy, A. G.; Hudson, S. M. *Carbohydrate Polymers* **2005**, *60*, 421.

(51) Kocer, H. B.; Akdag, A.; Ren, X.; Broughton, R. M.; Worley, S. D.; Huang, T. S. *Industrial & Engineering Chemistry Research* **2008**, *47*, 7558.

2.6. Supporting Information

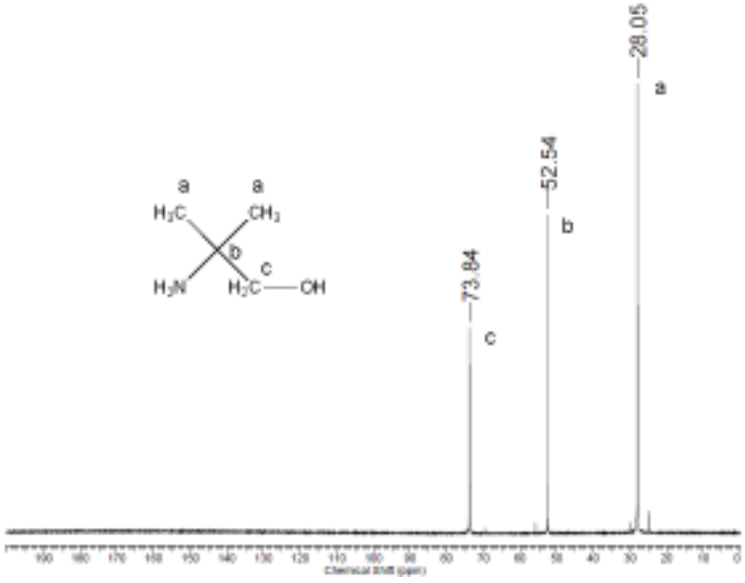

Figure SP.2.1. ^{13}C NMR Spectra of 2-amino-2-methly-1-propanol.

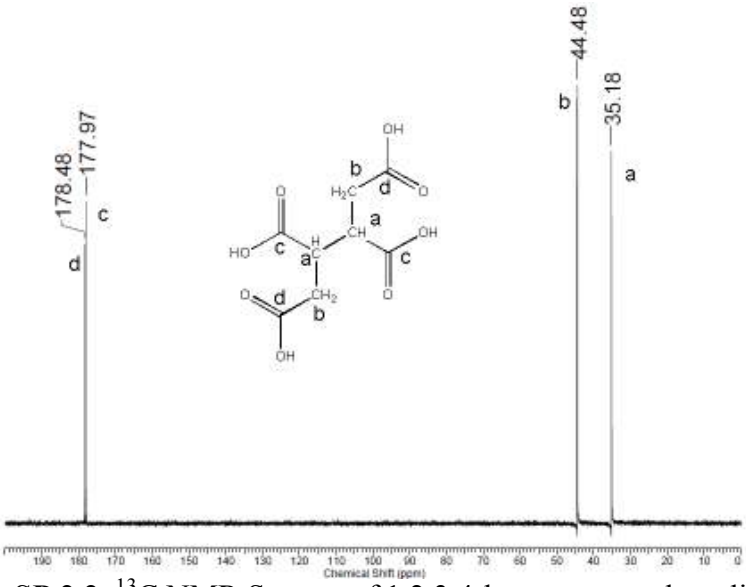

Figure SP.2.2. ^{13}C NMR Spectra of 1,2,3,4-butanetetracarboxylic acid.

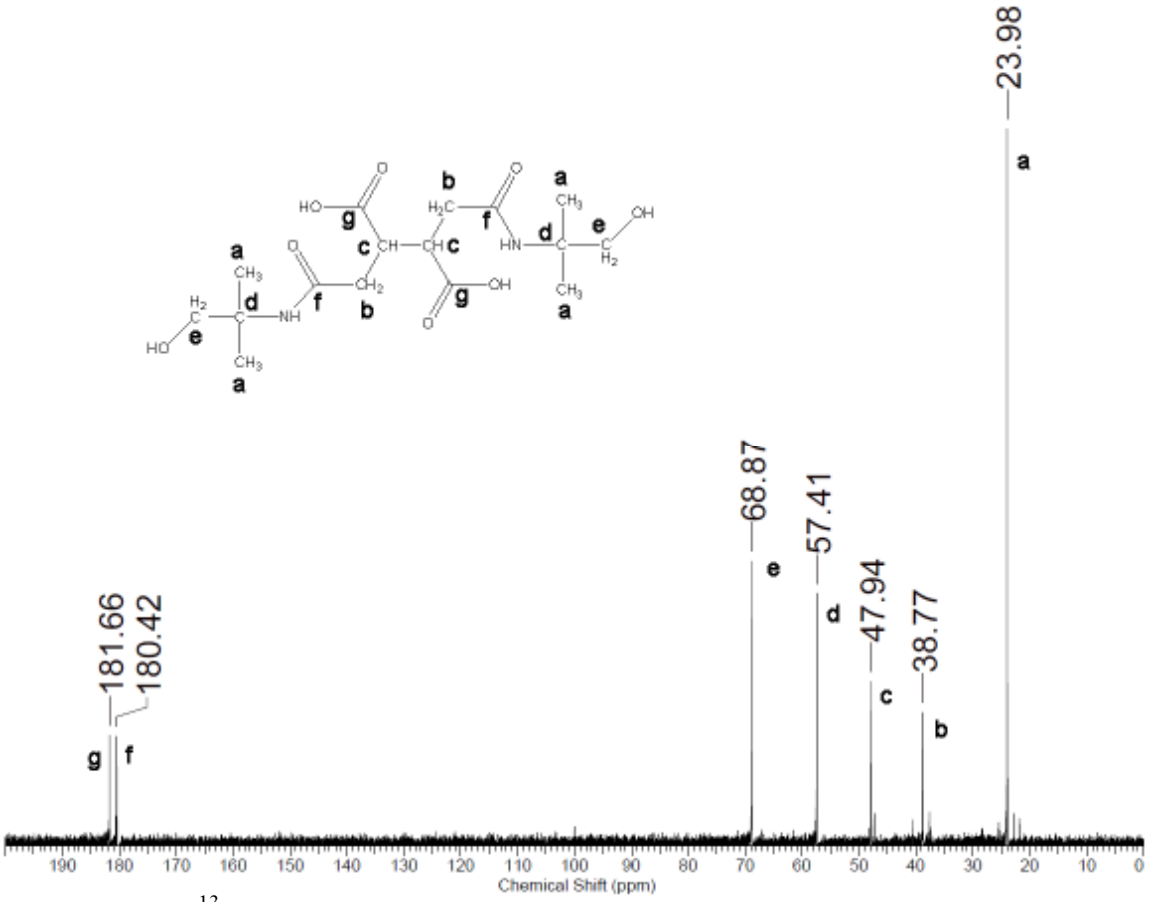

Figure SP.2.3. ^{13}C NMR Spectra of 2,3-bis(2-((1-hydroxy-2-methylpropan-2-yl)amino)-2-oxoethyl)succinic acid.

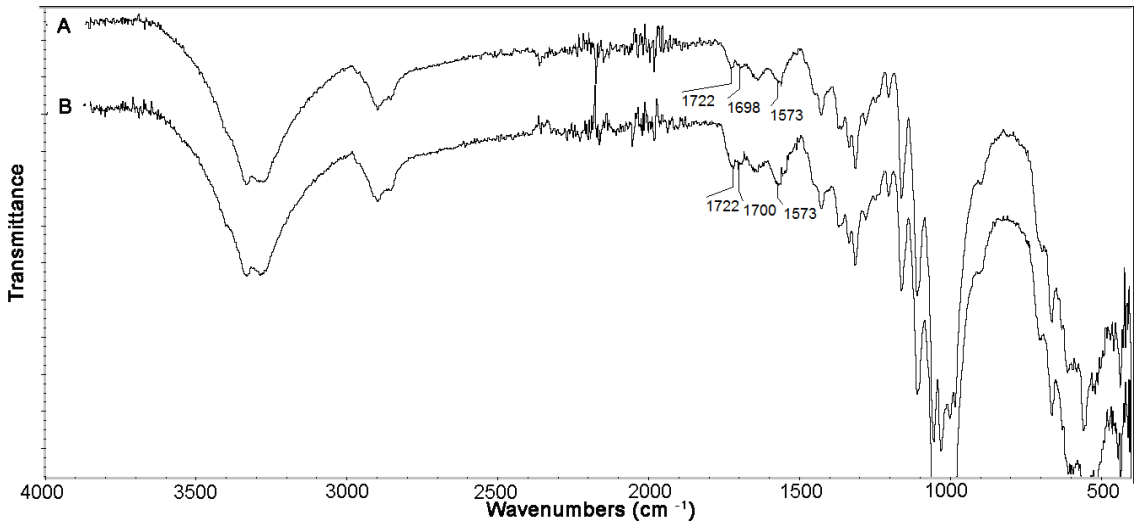

Figure SP.2.4. ATR-IR Spectra of AMP/BTCA treated (3.5 %) cotton fabric after 50 washing cycles (A), rechlorinated AMP/BTCA treated cotton fabric after 50 washing cycles (B).

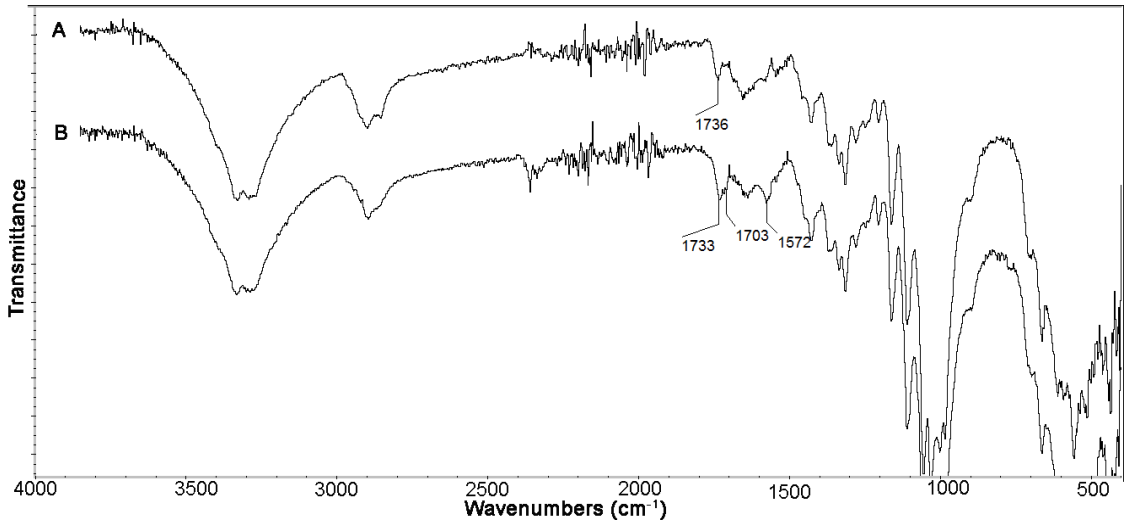

Figure SP.2.5. ATR-IR Spectra of AMP/BTCA treated (3.5 %) cotton fabric after 1 d of UVA light exposure (A), Rechlorinated AMP/BTCA treated cotton fabric after 1 d of UVA light exposure (B).

CHAPTER 3

POLMERIC ANTIMICROBIAL N-HALAMINE EPOXIDES

3.1. Introduction

Extensive work on *N*-halamine antimicrobial compounds has been reported from these laboratories for three decades (1-3). The work began with disinfection in aqueous solution (1) and was then extended to antimicrobial polymers for use in potable water disinfection (2) and antimicrobial textiles (3). N-halamine materials have been also investigated extensively in other laboratories (4-9). Quaternary ammonium salts (10-13), metal ions (14-16), and light-activated coatings (17,18) are also being evaluated as antimicrobial agents in infection control. Among these antimicrobial materials, N-halamine compounds are advantageous due to their long-term stabilities, non-toxicities to humans, biocidal functions against a broad range of microorganisms, and regenerable properties upon exposure to household bleach.

Antimicrobial N-halamine moieties have been attached to surfaces such as cellulose fibers by several grafting (4), tethering (19,20), and co-polymerization (21, 22) methods. One of the more successful methods (20) has been to bond the N-halamine precursors (eg. hydantoin derivatives) to epoxides which can then tether to a surface such as cellulose fiber through covalent ether linkages (see Figure 1). The effort in this regard was the reaction of the sodium salt of 5,5-dimethylhydantoin with epichlorohydrin, followed by curing onto cellulose fibers; chlorination with dilute household bleach then produced antimicrobial

fibers which were capable of producing 6-log inactivations of *Staphylococcus aureus* and *Escherichia coli* O157:H7 within 10 min of contact time and withstanding 50 machine washes without losing their biocidal efficacies (20). Although other monomeric epoxide derivatives have been subsequently developed and applied onto various surfaces such as polyester (23), one of the drawbacks of epoxide **GH** (Figure 3.1) was the inability to obtain loadings of Cl^+ greater than 0.15 wt% on cotton without employing tedious chromatographic techniques for purification of **GH**. Generally a Cl^+ loading of 0.3 to 0.4 wt% is preferred for best antimicrobial performance.

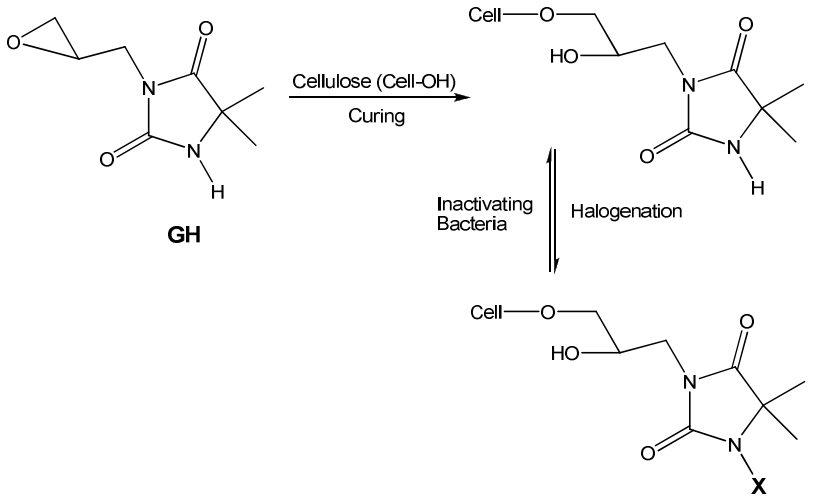

Figure 3. 1. Preparation of GH-based antimicrobial cellulose (X = Cl, Br).

Since epoxide linkages provide superior physical properties such as washing stability for the monomeric **GH's** (20), an investigation of polymeric N-halamine epoxides was undertaken in hopes of enhancing chlorine loadings on cellulose fibers so as to improve antimicrobial efficacies. In this study, we synthesized a new copolymer by the free radical polymerization of two commercially available monomers 3-chloro-2-hydroxypropylmethacrylate (**CM**) and glycidyl methacrylate (**GM**) as shown in Figure 3.2. The copolymer was successfully coated onto cotton fabric and then treated with 5,5-

dimethylhydantoin potassium salt to produce N-halamine precursor moieties on the surface. The monomeric hydantoin epoxide **GH** was also prepared for comparison of the stabilities, UV resistances, and antibacterial activities of the epoxide derivatives.

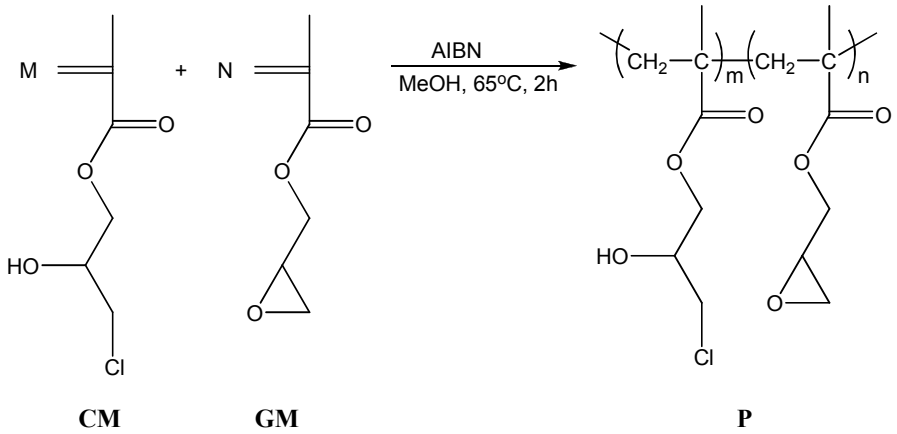

CM **GM** **P**

Figure 3. 2. Structure of the synthesized copolymer.

3.2. Experimental

3.2.1. Materials

Chemicals were purchased from Sigma-Aldrich (Saint Louis, MO) and used without further purification unless otherwise stated.

3.2.2. Instrumentation

NMR spectra were obtained using a Bruker 400 MHz spectrometer; ^{1}H and ^{13}C spectra were recorded with 16 and 1024 scans, respectively. FTIR data were obtained with a Nicolet 6700 FT-IR spectrometer with an ATR (Attenuated Total Reflectance) accessory, recorded with 64 scans at 2 cm^{-1} resolution.

3.2.3. Preparation of 3-glycidyl-5, 5-dimethylhydantoin (GH, henceforth referred to as monomer M)

3-glycidyl-5,5-dimethylhydantoin was prepared according to a procedure outlined previously (20). Briefly, the sodium salt of 5,5-dimethyl hydantoin was prepared by reacting 5,5-dimethylhydantoin with an equimolar quantity of NaOH in water at ambient temperature for 10 min. Then preparation of M was accomplished by subsequent addition of epichlorohydrin and stirring for 10 h. Following the reaction, water was removed by vacuum evaporation, and the product was dissolved in acetone. Then the byproduct sodium chloride was removed by filtration, and the acetone was removed by evaporation to obtain the product. The structure was confirmed by NMR and FTIR analysis (20).

3.2.4. Synthesis of the Copolymer (P).

The copolymer of 3-chloro-2-hydroxypropylmethacrylate (**CM**) and glycidyl methacrylate (**GM**) was synthesized by free radical polymerization. In a 100,mL round bottom flask, 4.47g (25 mmol) of **GM**, 3.55g (25 mmol) **CM**, and 0.08 g AIBN (2,2′-Azobis(2-methylpropionitrile)) were dissolved in 20 mL of methanol. Nitrogen was bubbled through the solution for 15 min to remove any dissolved oxygen. The mixture was stirred at 65 ^{o}C for 2 h. The copolymer was precipitated during cooling of the mixture. The gum-like, non-stick copolymer was separated from the mixture and washed with methanol several times to remove unreacted monomers. The methanol was evaporated under reduced pressure at room temperature, and the copolymer was recovered as pellets with a yield of 78 %. The intrinsic viscosity of the copolymer was 0.79 dL/g (in dimethylsulfoxide, 25 ^{o}C).

3.2.5. Coating and Chlorination Procedures

M and **P** were first dissolved in acetone, and the mixture was stirred for 15 min to produce a uniform solution. Cotton swatches (Style 400 Bleached 100% Cotton Print Cloth from Testfabrics, Inc., West Pittston, PA) in the size of 300 cm^2 were soaked in the coating solution (25 g) for 15 min, then uniformly padded through a laboratory wringer (Birch Brothers Southern, Waxhaw, NC), and then cured at 165^oC for 1 h. After curing, the swatches were soaked in a 0.5 % detergent solution for 15 min, rinsed several times with water, and conditioned in a standard environment (21^oC, 65 % RH). The weight gains on the fabrics after the coating procedure are summarized in Table 3.1. For the monomeric coating, the weight gain on the fabric did not increase by increasing coating solution concentration. This was a result of every monomeric epoxide moiety requiring one hydroxyl group on the cellulose surface to bind. However, for the polymeric epoxide the weight gain, and therefore the chlorine loading, increases by increasing coating solution concentration because epoxide groups can be attached as large macromolecules containing multiple hydantoin moieties onto to the cellulose surface.

Table 3. 1. Coating onto cotton at different concentrations of the coating solutions.

Compound	Concentration of the coating solution (wt%)	Weight gain of the fabric (wt%)	Cl^+% loading
M	1.5	1.48	0.16
	5	1.16	0.14
	10	1.33	0.15
P	1.5	1.48	0.16
	5	5.19	0.55

The copolymer-coated fabrics were then immersed into 0.5 M 5,5-dimethylhydantoin potassium salt solution in EtOH for 5 min while under reflux (see Figure 3.3). The fabric became stiffer and slightly yellow during the immersing treatment due to KCl salt formation on the fabric surface; however, immediately after rinsing with tap water the fabric became softer and white.

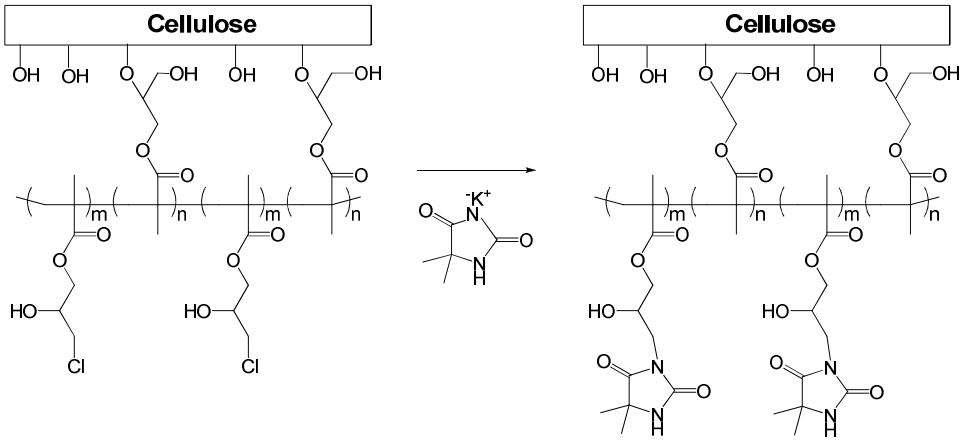

Figure 3. 3. Hydantoin treatment of the copolymer coated cotton fabric.

The treated fabrics were chlorinated by soaking in a 1% aqueous solution of household bleach (6% sodium hypochlorite) at pH 7 (adjusted with 6 N HCl) for 60 min. After rinsing with tap and distilled water, the swatches were then dried at 45 ^{o}C for 1 h to remove any occluded chlorine from the material. The chlorine concentrations loaded onto the coated samples were determined by a iodometric/thiosulfate titration procedure. The weight percent Cl^{+} on the samples was calculated by the following formula;

$$Cl^{+}\,\% = [(N \times V \times 35.45) / (2 \times W)] \times 100 \quad \ldots\ldots (1)$$

where Cl^+ % is the weight percent of oxidative chlorine on the samples, N and V are the normality (equiv/L) and volume (L) of the titrant sodium thiosulfate, respectively, and W is the weight of the sample in g.

3.2.6. Stability Testing

The stability and rechargeability of chlorine on the samples were evaluated by using a standard washing test according to AATCC Test Method 61. The cotton samples were washed for the equivalents of 5, 10, 25, and 50 machine washes in a Launder-Ometer. The Cl^+ % loadings on the samples before and after the washings were determined by the titration procedure mentioned above.

UVA light stability of the bound chlorine and the coatings on cotton fabric samples were determined using an Accelerated Weathering Tester (The Q-panel Company, Cleveland, OH, USA). The samples were placed in the UV (Type A, 315-400 nm) chamber for contact times ranging up to 24 h. After specific times of exposure to UVA irradiation, the samples were removed from the UV chamber and titrated, or rechlorinated and titrated. The temperature was 37.6^{o}C, and the relative humidity was 17 % during the UVA light irradiation.

3.2.7. Biocidal Efficacy Testing

A ‘‘sandwich test’’ was used to evaluate the biocidal efficacies. Both chlorinated and unchlorinated coated cotton samples were challenged with *S. aureus* (ATCC 6538) and *E. coli* O157:H7 (ATCC 43895) bacterial suspensions in pH 7 phosphate buffer solution (100 mM). Suspensions (25 μl) of the bacterial solution were added to the center of a 2.54

cm square fabric swatch, and a second identical swatch was placed on top of the first swatch. A sterile weight was used to ensure sufficient contact of the swatches with the inocula. The contact times for the bacteria with the swatches were 5, 10, and 20 min. At those contact times the fabric swatches were quenched with 0.02 N sodium thiosulfate solution to remove any oxidative chlorine which could cause extended disinfection. Serial dilutions of the solutions contacting the surfaces were plated on Trypticase agar, incubated for 24 h at 37^{o}C, and colony counts were made to determine the presence or absence of viable bacteria. Unchlorinated control samples were treated in the same manner.

3.3. Results and Discussion

3.3.1. Synthesis and Characterization of the Copolymer

GM was copolymerized with **CM** in equimolar amounts, and the resulting copolymer consisted of almost equimolar comonomer units. The amount of the **CM** in the copolymer composition contributes to the halogen loading capability (antimicrobial property); whereas the tethering epoxide monomer (**GM**) contributes to the adhesion property of the copolymer. NMR and FTIR analyses were used to confirm the structure of the synthesized copolymer. A ^{1}H NMR spectrum of the copolymer is shown in Figure 3; the primary evidence for the polymer formation is the disappearance of the vinyl proton signals between 5.5 and 6.5 ppm. The signals at 2.66 ppm and 2.81 ppm can be assigned to the protons of the epoxide group (24), indicating tethering functionality remains after polymerization. The resonance signal of the methyl groups split into three peaks at 0.79, 0.96, and 1.18 ppm which are assigned to syndiotactic, heterotactic, and isotactic structures,

respectively (24). The signal at 0.79 ppm with the highest intensity indicates that the copolymer is predominantly syndiotactic.

The average composition of the monomers in the copolymer was determined from the corresponding ^{1}H NMR spectrum shown in Figure 3.4. Assignments of the signals for the copolymer were based upon comparison with the corresponding signals in the NMR of the two monomers (see Supporting Information Section). The mole fraction of **CM** in the copolymer was calculated by comparing the signal area of an epoxide methylene proton (Fig. 3, c, 2.66 ppm) of **GM** to the methine proton signal area (Fig. 3.4, i, 4.28 ppm) of **CM**. Consequently, the reactivity ratio of **GM** was slightly higher than **CM**, resulting in a slightly lower **CM** amount (m/(m+n) = 0.47) in the copolymer as compared to its feed ratio (M/(M+N) = 0.50).

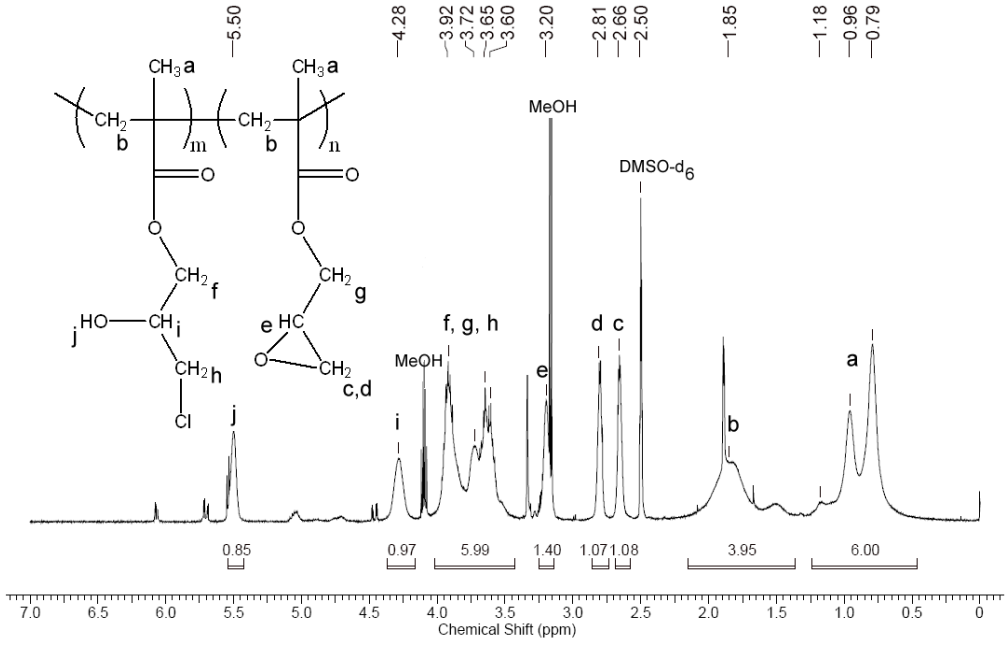

Figure 3. 4. ^{1}H NMR spectra of the synthesized copolymer (solvent: DMSO-d6).

The FTIR spectrum of the synthesized copolymer in Figure 3.5(P) was also suggestive of the copolymer formation by disappearance of the vinyl bond stretching vibration at around 1640 cm^{-1}. The bands at 1723 and 1148 cm^{-1} correspond to ester group vibrational modes, while the bands at 903 and 745 cm^{-1} can be assigned to epoxide (24) and CH_2-Cl group (25) vibrations, respectively.

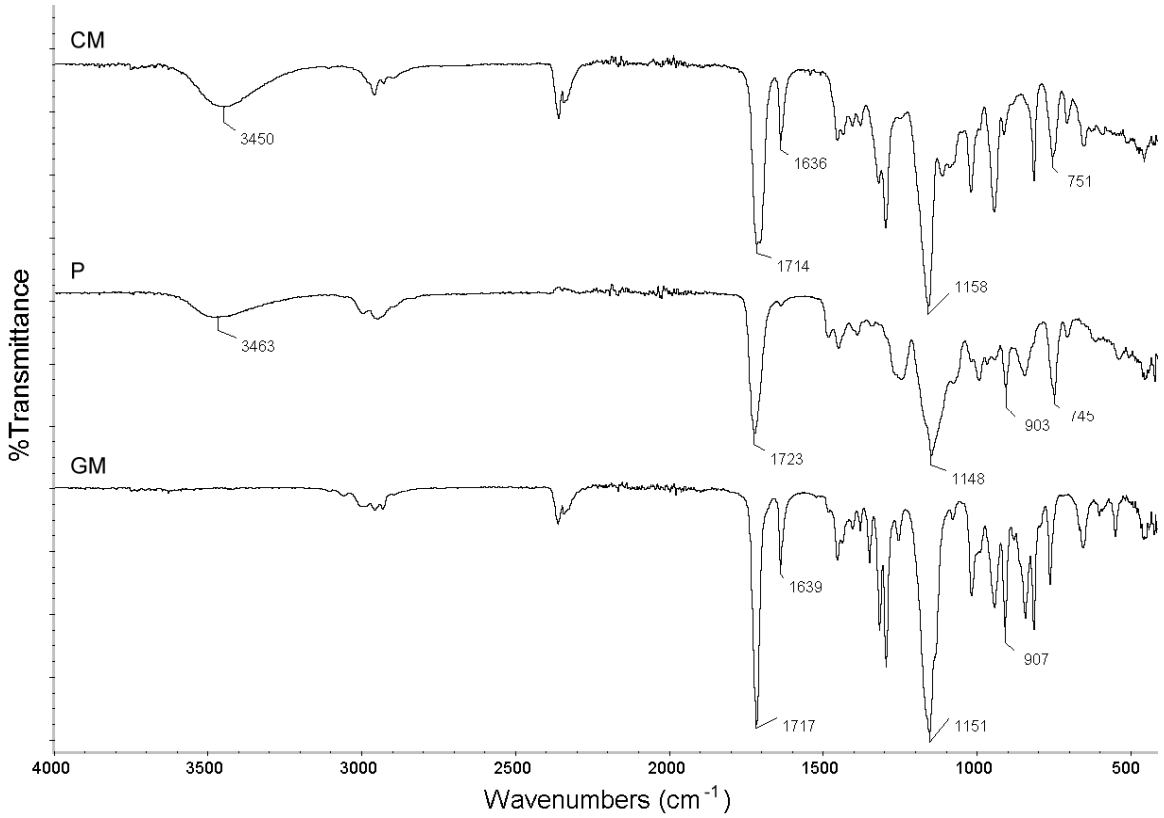

Figure 3. 5. FTIR spectra of the synthesized copolymer and the two monomers.

Figure 3.6 shows the FTIR spectra of cotton fabric and the additional processes to produce a biocidal cotton fabric. There is an additional band for the copolymer-coated fabric (B) at 1727 cm^{-1} which is assigned to ester group vibrations of the copolymer. After the treatment with 5,5-dimethlhydantoin potassium salt (C), two additional bands appeared

at 1701 and 1766 cm^{-1} which can be assigned to the carbonyl groups of the amide structure on the hydantoin moiety. These bands shifted to 1719 and 1787 cm^{-1} (respectively) after chlorination (D), indicating disruption of N-H · · ·O=C hydrogen bonding as conversion of N-H to N-Cl occurred.

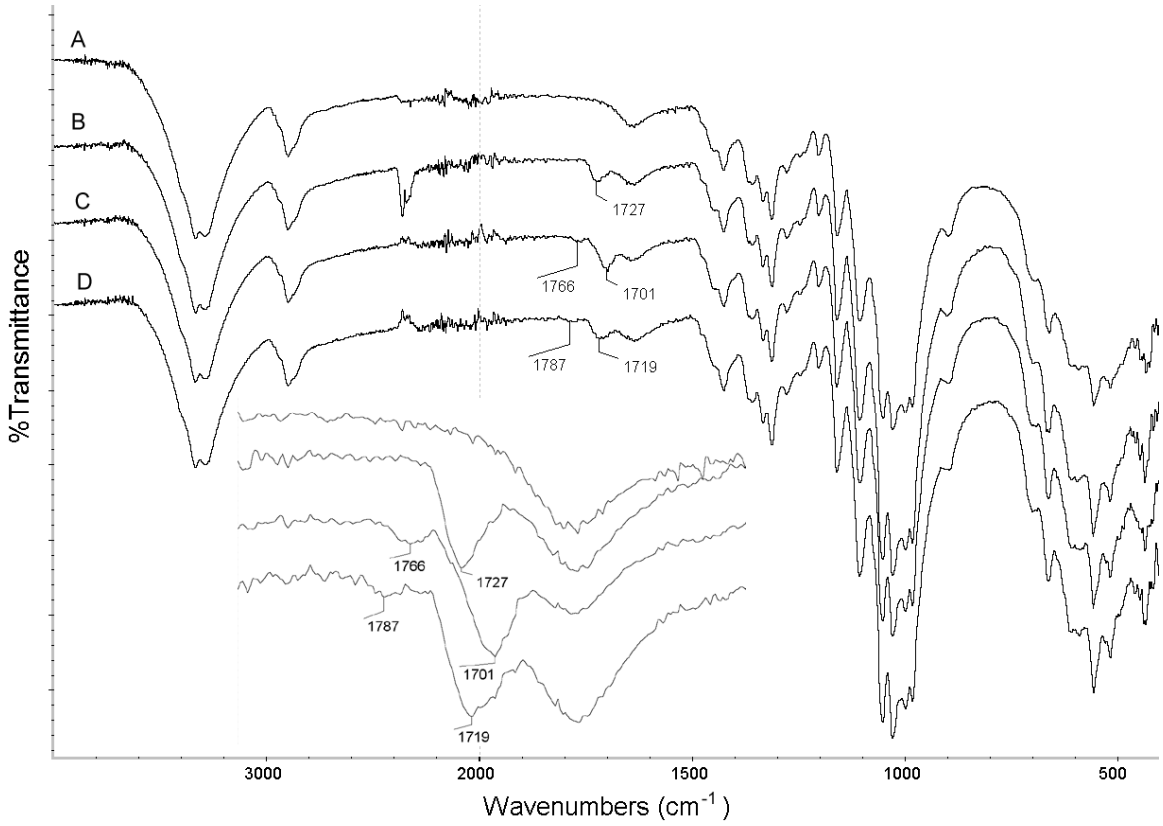

Figure 3. 6. FTIR spectra of (A) cotton, (B) copolymer-coated, (C) hydantoin treated copolymer-coated, and (D) chlorinated hydantoin treated copolymer-coated fabrics.

3.3.2. Stability toward Washing and Ultraviolet Light Irradiation

The stabilities toward machine washing of coated fabric swatches are presented in Table 2. Three types of washing experiments were performed - prechlorinated coatings at the concentration levels indicated at 0 machine washes Table 3.2C, prechlorinated and rechlorinated after a given number of machine washes (R), and unchlorinated until after a

given number of machine washes (U). The initial chlorine loadings of the coated fabrics (0 machine washes) were 0.13 and 0.15 for the monomer (**M**) and the copolymer (**P**) coated fabrics, respectively. Several observations can be made pertaining to the data in Table 2. First, **M** lost all of the bound chlorine within 25 cycles, while almost half of the initial chlorine still remained on **P** coated fabric even after 50 cycles (Table 3.2C). This could be due to more hydrophobic character of the polymeric coating as compared to the monomeric coating. Moreover, these rates of loss are not a result of the dissociation of tethering groups (epoxide) from cotton because rechlorination of the coated fabrics provided chlorine loadings at approximately their initial values (Table 3.2R). The unchlorinated coatings (U) were also very resistant toward washing cycles.

Table 3. 2. Stability toward washing of coatings on the cotton (Cl^+ % remaining).

MW[a]	M			P		
	C	R	U	C	R	U
0	0.13			0.15		
5	0.01	0.11	0.12	0.14	0.15	0.15
10	0.01	0.11	0.11	0.12	0.15	0.15
25	0	0.11	0.11	0.11	0.14	0.14
50	0	0.11	0.11	0.08	0.13	0.15

[a] MW: Machine washes, [b] C: Chlorinated before washing, R: Chlorinated before washing and rechlorinated after washing, U: Unchlorinated before washing, but chlorinated after washing, [c] The error in the measured Cl^+ weight percentage values was ±0.01.

Table 3.3 illustrates the stabilities of the coatings (**M** and **P**) and chlorinated coatings (**M-Cl** and **P-Cl**) on cotton toward UVA light degradation following a series of rechlorinations after successive exposures; the data for **M** and **P** represent chlorination after UVA exposure of the unchlorinated samples at the indicated UVA contact times. Several

conclusions can be drawn from these data. First, both coatings lost oxidative chlorine upon exposure to UVA photons slowly within 24 h, and the UVA exposed samples were almost completely rechlorinated after 24 h (R_1). However, following UVA exposure cycles, and rechlorinations (R_2 to R_5), a progressive decline in chlorine loading occurred upon rechlorination which was more dramatic for the polymeric coating. This could be due to the more UV sensitive ester structures in the polymeric epoxide coating. On the other hand, unchlorinated coatings on cotton exhibited no significant decomposition in the presence of the UVA irradiation over the entire 120 h of exposure. The stabilities were quite remarkable given that a six hour exposure in the UV chamber was equivalent to the same time in direct midday summer sunlight.

Table 3. 3. Effect of UVA irradiation on the coatings (Cl^+ % remaining).

Time (h)	M-Cl	M	P-Cl	P
0	0.14		0.15	
0.5	0.13		0.15	
1.5	0.10		0.14	
6	0.08		0.09	
24	0.03		0.04	
24R_1	0.13	0.14	0.13	0.15
48	0.01		0.02	
48R_2	0.11	0.15	0.13	0.14
72	0.01		0.01	
72R_3	0.11	0.14	0.11	0.15
96	0.01		0.01	
96R_4	0.10	0.14	0.07	0.14
120	0.01		0.01	
120R_5	0.08	0.14	0.03	0.14

* R_1 to R_5 indicate rechlorination of samples after UVA exposure for the specified time intervals.

3.3.3. Antimicrobial Efficacies

The treated cotton swatches were challenged with *S. aureus* and *E. coli* O157:H7 at concentrations of about 10^7 CFU (colony-forming units), as summarized in Table 3.4. The biocidal efficacy of the monomeric coating **M** as compared to the polymeric coating **P** with similar chlorine loading onto cotton fabric was evaluated. In addition, a cotton fabric containing a higher amount of the polymer on the surface (**PH**), providing a higher chlorine loading, was also tested. Unchlorinated control samples (**M**, **P**, and **PH**) provided only about 0.50 log reductions, due to the adhesion of bacteria to the cotton swatches, within 20 min contact time intervals. All of the chlorinated coated samples inactivated all *S. aureus* with log reduction of ~6.3 in a contact time of 5 min, in the repeated experiments. On the other hand, a longer period of contact time 10 min was required to inactivate all Gram-negative bacteria (*E. coli*) for **M-Cl** and **P-Cl** for a chlorine loading of ca. 0.15 % onto cotton. Moreover, the cotton fabric coated with a higher amount of the polymer (**PH**), providing a higher chlorine loading (0.55 %), inactivated all *E. coli* within 5 min of contact time. As expected, the higher amount of the chlorine loading on the cotton fabric resulted in a faster inactivation rate.

Table 3. 4. Biocidal Tests.

Sample Cl^+%	Contact time (min)	Exp1 Log reduction		Exp2 Log reduction	
		S. aureus	***E. coli***	***S. aureus***	***E. coli***
M	20	0.25	0.42	0.37	0.05
P	20	0.19	0.28	0.36	0.04
PH	20	0.14	0.52	0.56	0.02
M-Cl	5	6.25	4.60	6.73	6.75
0.14	10	6.25	6.72	6.73	6.75
	20	6.25	6.72	6.73	6.75
P-Cl	5	6.25	4.42	6.73	6.75
0.15	10	6.25	6.72	6.73	6.75
	20	6.25	6.72	6.73	6.75
PH-Cl	5	6.25	6.72	6.73	6.75
0.55	10	6.25	6.72	6.73	6.75
	20	6.25	6.72	6.73	6.75

Exp 1: The inoculum concentrations were 6.25, and 6.72 logs for *S. aureus* and *E. coli*, respectively. Exp 2: The inoculum concentrations were 6.73, and 6.75 logs for *S. aureus* and *E. coli*, respectively.

3.4. Conclusions

It can be concluded from this work that N-halamine-functionalized epoxides, when tethered to cellulose fibers, provide a very effective antimicrobial property, with disinfection capability within a few minutes of contact time. Also, when included in a copolymer which may have multiple attachment points to the cellulose, the N-halamine groups are more stable toward a laundering process and are capable of loading a higher amount of oxidative chlorine, rendering them more effective in antimicrobial activity. Both monomeric and polymeric N-halamine epoxides bound to cellulose lose chlorine over an extended period of time when exposed to UVA irradiation, but they can be rechlorinated after the exposure. The copolymer synthesized in this study possesses considerable potential for use in the health care industry for fabrics or other surfaces containing functional groups that can be reacted with the epoxide moieties.

3.5. References

(1) Worley, S.D.; Williams, D.E. Halamine Water Disinfectants. *CRC Crit. Rev. Environ. Control* **1988**, *18*, 133-175.

(2) For example see: Sun, G.; Wheatley, W.B.; Worley, S.D. A New Cyclic N-halamine Biocidal Polymer. *Ind. Eng. Chem. Res.* **1994**, *33*, 168-170.

(3) For example see: Worley, S.D.; Chen, Y.; Wang, J.W.; Wu, R.; Cho, U.; Broughton, R.M.; Kim, J.; Wei, C.I.; Williams, J.F.; Chen, J.; Li, Y. Novel N-Halamine Siloxane Monomers and Polymers for Preparing Biocidal Coatings. *Surf. Coat. Int. Part B: Coat. Trans.* **2005**, *88*, 93–100.

(4) Liu, S.; Sun, G. New Refreshable N-Halamine Polymeric Biocides: N-Chlorination of Acyclic Amide Grafted Cellulose. *Ind. Eng. Chem. Res.* **2009**, *48(2)*, 613-618.

(5) Chen, Z.; Sun, Y.Y. N-Halamine-based Antimicrobial Additives for Polymers: Preparation, Characterization, and Antimicrobial Activity. *Ind. Eng. Chem. Res.* **2006**, *45*, 2634-2640.

(6) Makal, U.; Wood, L.; Ohman, D.E.; Wynne, K.J. Polyurethane Biocidal Polymeric Surface Modifiers. *Biomaterials* **2006**, *27*, 1316-1326.

(7) Kenawy, E.R.; Worley, S.D.; Broughton, R.M. The Chemistry and Applications of Antimicrobial Polymers: A state-of-the-art review. *Biomacromolecules* **2007**, *8(5)*, 1359-1384.

(8) Coulliette, A.D.; Peterson, L.A.; Mosberg, J.A.; Rose, J.B. Evaluation of A New Disinfection Approach: Efficacy of Chlorine and Bromine Halogenated Contact

Disinfection for Reduction of Viruses and Microcystin Toxin. *Am. J. Trop. Med. Hyg.* **2010**, *82(2)*, 279-88.

(9) Goddard, J.M.; Hotchkiss, J.H. Rechargeable Antimicrobial Surface Mmodification of Polyethylene. *J. Food Protection* **2008**, *71(10)*, 2042-2047.

(10) Sauvet, G.; Fortuniak, W.; Kazmierski, K.; Chojnowski, J. Amphiphilic Block and Statistical Siloxane Copolymers with Antimicrobial Activity. *J. Polym. Sci. A: Polym. Chem.* **2003**, *41*, 2939-2948.

(11) Klibanov, A.M. Permanently Microbicidal Materials Coatings. *J. Mater. Chem.* **2007**, *17*, 2479-2482.

(12) Waschinski, C.J.; Zimmermann, J.; Salz, U.; Hutzler, R.; Sadowski, G.; Tiller, J.C. Design of Contact-Active Antimicrobial Acrylate-Based Materials Using Biocidal macromers. *Adv. Mater.* **2008**, *20*, 104-108.

(13) Eren, T.; Som, A; Rennie, J.R.; Nelson, J.F.; Urgina, Y.; Nusslein, K.; Coughlin, E.B.; Tew, G.N. Antibacterial and Hemolytic Activities of Quaternary Pyridinium Functionalized Polynorbornenes. *Macromol. Chem. Phys.* **2008**, *209*, 516-524.

(14) Nagar, R. Structural and Microbial Studies of Some Transition Metal Complexes. *J. Inorg. Biochem.* **1989**, *37*, 193-200.

(15) Takano, S.; Tamegai, H.; Itoh, T.; Ogata, S.; Fujimori, H.; Ogawa, S.; Iida, T.; Wakatsuki, Y. ROMP Polymer-based Antimicrobial Films Repeatedly Chargeable with Silver Ions. *React. Funct. Polym.* **2011**, *71(2)*, 195-203.

(16) Perelshtein, I.; Applerot, G.; Perkas, N.; Wehrschetz-Sigl, E.; Hasmann, A.; Guebitz, G.M.; Gedanken, A. Antibacterial Properties of an In Situ Generated and

Simultaneously Deposited Nanocrystalline ZnO on Fabrics. *ACS Appl. Mater. Interfaces* **2009**, *1(2)*, 361–366.

(17) Wilson, M. Light-Activated Antimicrobial Coating for the Continuous Disinfection of Surfaces. *Infect. Control Hosp. Epidemiol.* **2003**, *24*, 782-784.

(18) Ohko, Y.; Utsumi, Y.; Niwa, C.; Tatsuma, T.; Kobayakawa, K.; Satoh, Y.; Kubota, Y.; Fujishima, A.. Self-sterilizing and Self-cleaning of Silicone Catheters Coated with TiO_2 Photocatalyst Thin Films: Preclinical Work. *J. Biomed. Mat. Res.* **2000**, *58*, 97-101.

(19) Kocer, H.B.; Worley, S.D.; Broughton, R.M.; Huang, T.S. A Novel N-Halamine Acrylamide Monomer and Its Copolymers for Antimicrobial Coatings. *React. Funct. Polym.* **2011**, *71*, 561-568.

(20) Liang, J.; Chen, Y.; Ren, X.; Wu, R.; Barnes, K.; Worley, S.D.; Broughton, R.M.; Cho, U.; Kocer, H.B.; Huang, T.S. Fabric Treated with Antimicrobial N-Halamine Epoxides. *Ind. Eng. Chem. Res.* **2007**, *46*, 6425-6429.

(21) Ren, X.; Kou, L.; Kocer, H.B.; Zhu, C.; Worley, S.D.; Broughton, R.M.; Huang, T.S. Antimicrobial Coating of An N-Halamine Biocidal Monomer on Cotton Fibers via Admicellar Polymerization. *Colloids and Surfaces A: Physicochem. Eng. Aspects.* **2008**, *317*, 711-716.

(22) Cerkez, I.; Kocer, H.B.; Worley, S.D.; Broughton, R.M.; Huang, T.S. N-Halamine Biocidal Coatings via a Layer-by-Layer Assembly Technique. *Langmuir* **2011**, *27(7)*, 4091-4097.

(23) Liang, J.; Wu, R.; Wang, J.W.; Barnes, K.; Worley, S.D.; Cho, U.; Lee, J.; Broughton, R.M.; Huang, T.S. N-Halamine Biocidal Coatings. *J Ind. Microbiol Biotechnol.* **2007**, *34*, 157-163.

(24) Espinosa, M.H.; Toro, P.J.O.; Silva, D.Z. Microstructural Analysis of Poly(glycidyl methacrylate) by ^{1}H and ^{13}C NMR Spectroscopy. *Polymer* **2001**, *42*, 3393-3397.

(25) Lee, M.J.; Hur, S.W.; Durig, J.R. Conformational Stability, Vibrational Assignments, and Normal Coordinate Analysis from FT-IR Spectra of Xenon Solutions and ab initio Calculations of Epichlorohydrin. *J. Mol. Struct.* **1998**, *444*, 99-113.

3.6. Supporting Information

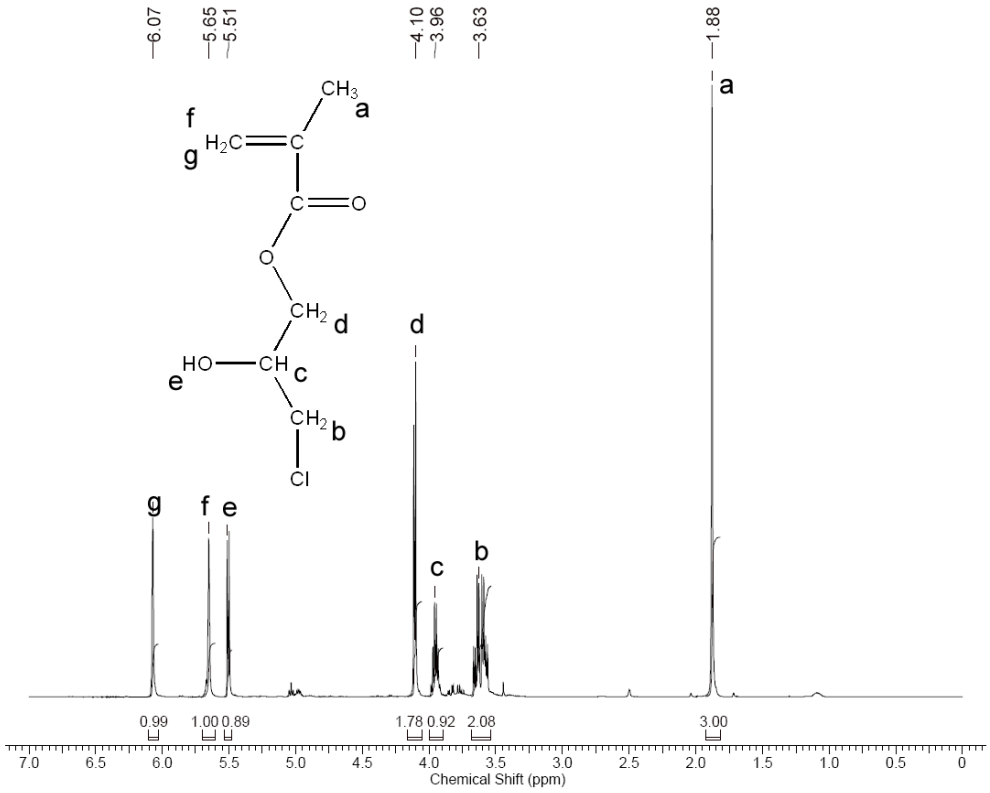

Figure SP.3. 1. ^{1}H-NMR spectra of 3-chloro-2-hydroxypropyl methacrylate (solvent: DMSO-d6).

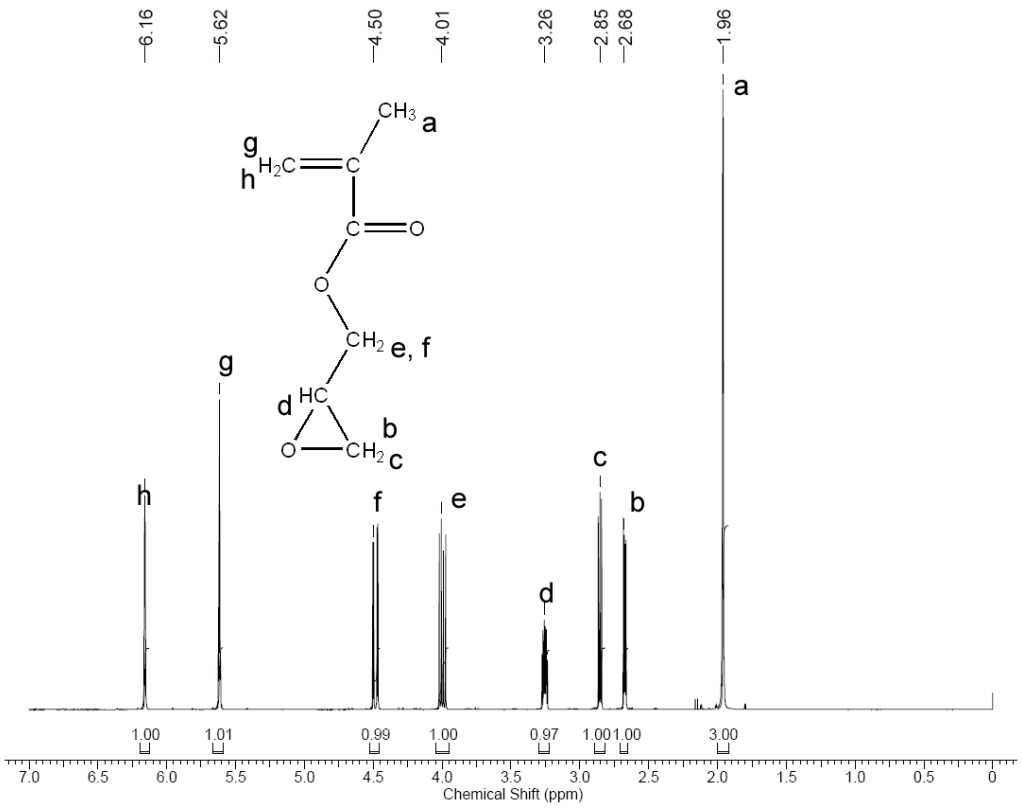

Figure SP.3. 2. ^{1}H-NMR spectra of glycidyl methacrylate (solvent: DMSO-d6).

CHAPTER 4

EPOXIDE TETHERING OF POLYMERIC N-HALAMINE MOIETIES

4.1. Introduction

With a growing concern about multidrug resistance microorganisms such as Methicillin-resistant *Staphylococcus aureus* and Vancomysin-resistant *Enterococcus*, antimicrobial treatment of materials has gained great importance. The increasing number of healthcare-associated infections requires the prevention of biofilm formation on surfaces to reduce the risk of spreading pathogenic microorganisms.[1] Therefore, quaternary ammonium salts,[2-4] metals ions,[5] N-halamines,[6-8] and a variety of materials have been used as biocidal coatings.

N-halamine compounds are one of the most effective biocidal agents used to inactive a broad spectrum of microorganism including bacteria, viruses, fungi, and yeasts. In general, N-halamines might contain amine, amide, or imide functionality as the active site. The stabilities of these different functionalities to hydrolysis increase from imide to amide to amine due to increased stability of the nitrogen-halogen bond caused by presence of electron-donating substituents adjacent to nitrogen atom.[9] The mechanism of action for the N-halamines is through a direct contact in which the oxidative halogen is transferred to the biological cell membrane leading to oxidation of thiol groups which results destruction of the cell structure.[10] Therefore, the disinfection rate of N-halamines increases from amine to imide as evidenced by the dissociation constants.[11] N-halamines are unique in that once the

oxidative halogen is consumed, it can be simply recharged upon exposure to a halogen source such as household bleach (Figure 4.1).

Research and development work in these laboratories has produced various novel N-halamine moieties which have been incorporated onto many surfaces including cellulose,[12] polyester,[13] nylon,[14] polyurethane,[15] and acrylonitrile.[16] Electrostatic attractions,[17] grafting,[18] or coupling agents such as alkoxy silanes[19] and epoxides[20] were employed to functionalize material surfaces. In a recent study,[21] we reported the attachment of a new epoxide-containing copolymer, poly(3-chloro-2-hydroxypropylmethacrylate-co-glycidyl methacrylate) (P), onto cotton fabric which was treated with the potassium salt of 5,5-dimethylhydantoin (DMH-K) to produce an N-halamine precursor on the surface (Figure 4.1). The coating was rendered biocidal upon exposure to dilute household bleach, and it exhibited remarkable biocidal efficacies and washing stabilities.

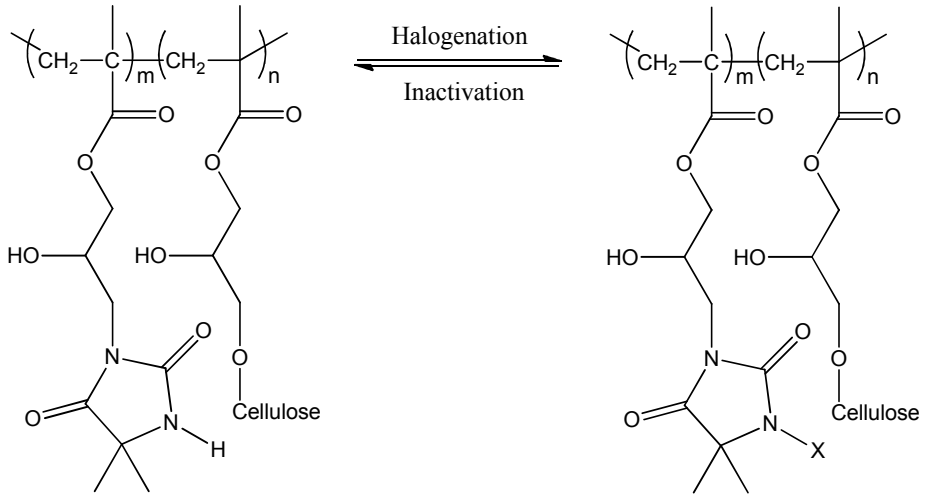

Figure 4. 1. Regenerability of N-halamines (X = Cl, Br).

Since the previously synthesized P-coated cotton fabric exhibited promising stabilities, the work has been extended to other N-halamine structures having different functional groups. In this study, 7,7,9,9-tetramethyl-1,3,8 triazaspiro[4.5]decane-2,4-dione

potassium salt (TTDD-K), 2,2,5,5-tetramethylimidazolidinone sodium salt (TMIO-Na), and DMH-K were attached to the backbone of polymer P on cotton fabric with the purpose of addressing the stabilities and biocidal efficacies of these aforementioned structures (Figure 4.2).

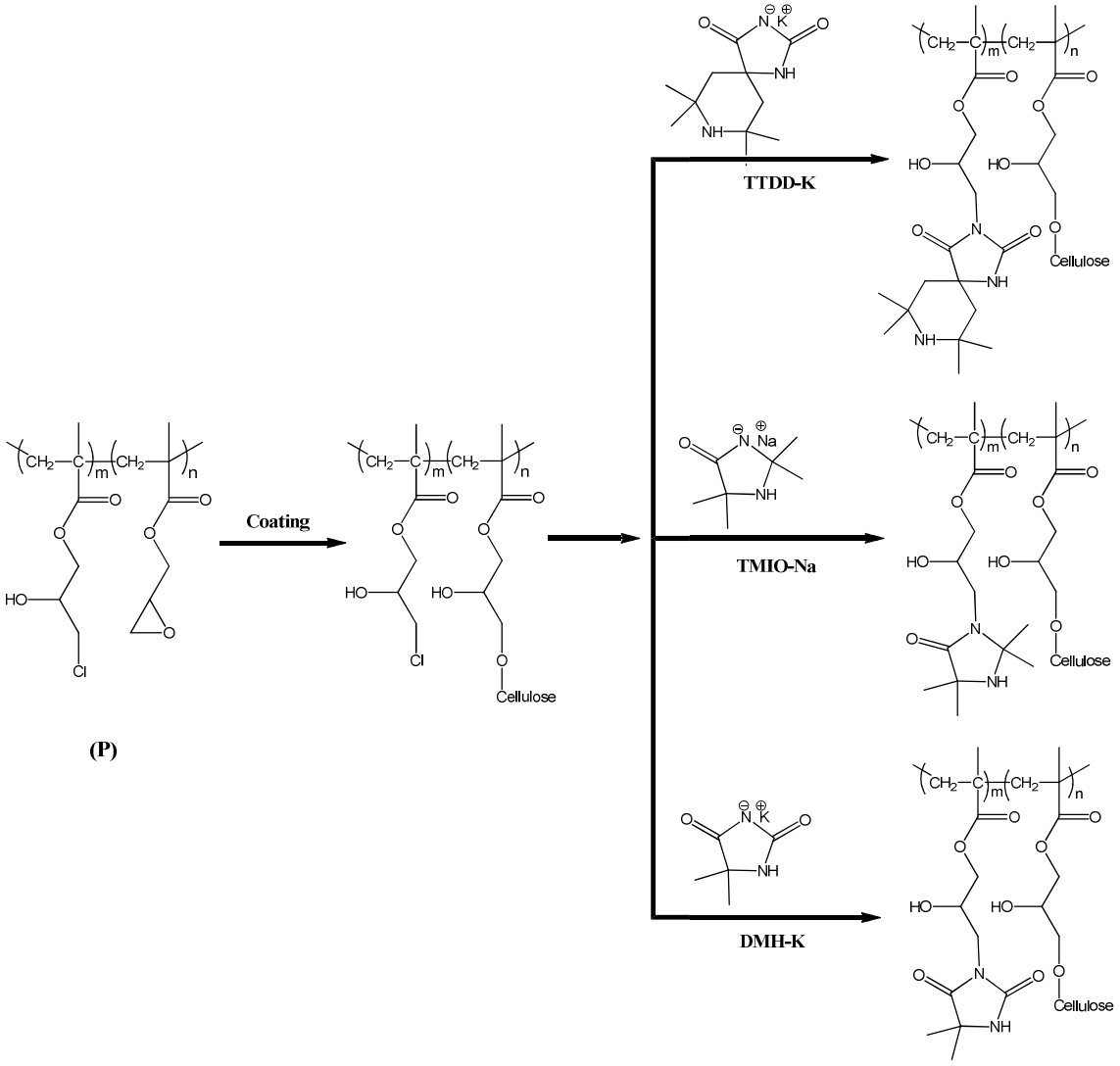

Figure 4. 2. Attachment of N-halamine moieties (X = Cl, Br).

4.2. Experimental

4.2.1. Materials and Instrumentation

All starting chemicals were purchased from Aldrich Chemical Company (Milwaukee, WI) or TCI America (Boston, MA), and used as is unless otherwise noted. Desized, scoured, and bleached (100%) cotton (Style 400 Cotton Print Cloth) was obtained from Testfabrics. Inc. (West Pittson, PA). Clorox® brand (Clorox, Inc., Oakland, CA) household bleach was used for chlorination. Bacteria cultures of *Staphylococcus aureus* ATCC 6538 and *Escherichia coli* O157:H7 ATCC 43895 were purchased from American Type Culture Collection (Rockville, MD), and Trypticase soy agar was obtained from Difco Laboratories (Detroit, MI).

NMR spectra recorded with 16 (^{1}H) and 1024 (^{13}C) scans were obtained using a Bruker 400 MHz spectrometer. ATR-IR data recorded with 64 scans at 4 cm^{-1} resolution were obtained with a Nicolet 6700 FT-IR spectrometer with an ATR (Attenuated Total Reflectance) accessory utilizing a diamond crystal. UV/vis spectra were collected with a Shimadzu UV/Vis Spectrophotometer (Shimadzu Scientific Instruments Inc., Durham, NC).

4.2.2. Synthesis

The copolymer P was synthesized by following the previous procedure[21] and characterized by NMR spectra as shown in the supporting information section (Figure SP 4.1).

The potassium salt of DMH (Figure 4.2) was produced by dissolving an equal molar amount (50 mmol) of DMH and KOH in 200 ml EtOH. After the solution was refluxed for 10 min, EtOH was removed by evaporation, and a white solid was obtained. ^{1}H NMR

(DMSO-d_6, 400 MHz) 1.07 (s, 6H), 6.41 (s, 1H), ^{13}C NMR (DMSO-d_6, 400 MHz) δ 25.55, 59.34, 172.60, 193.20.

The potassium salt of TTDD (Figure 4.2) was produced by dissolving an equal molar amount (50 mmol) of TTDD and KOH in 200 ml of EtOH. The solution was refluxed for 10 min, and then the product was recovered as white crystals by evaporation of the solvent. ^{1}H NMR (D_2O, 400 MHz) 1.10 (s, 6H), 1.23 (s, 6H), 1.54 (s, 4H); ^{13}C NMR (D_2O, 400 MHz) δ 27.23, 33.78, 42.58, 48.65, 64.32, 173.90, 196.49.

In order to produce the sodium salt of TMIO (Figure 4.2), 25 mmol TMIO were dissolved in anhydrous dimethylformamide. To this solution, an equal molar amount of NaH was added while the solution was being held in an ice bath. The solution was stirred at room temperature for 5 h. Then the solvent was removed by reduced pressure, and a white solid product was obtained. ^{1}H NMR (D_2O, 400 MHz) 1.19 (s, 6H), 1.28 (s, 6H). ^{13}C NMR (D_2O, 400 MHz) δ 26.00, 29.56, 60.44, 72.26, 181.37.

4.2.3. Coating and Chlorination Procedure

The synthesized copolymer P was dissolved in acetone at a specified concentration, and the cotton fabric was soaked in that coating solution for 10 min. The fabrics were then padded onto a laboratory wringer (Birch Brothers Southern, Waxhaw, NC), and cured at 165 °C for 1h. After the curing process, the swatches were washed with 0.5 % detergent water for 10 min. Finally, the copolymer-coated cotton fabrics were soaked into 0.5 M DMH-K, TTDD-K, or TMIO-Na solutions in EtOH, EtOH, and DMF at 80 °C for 15 min, respectively. A final washing step with 0.5 % detergent water solution for 10 min was conducted to remove any unattached salts, followed by several water rinses.

The coated swatches were halogenated with 10 wt % aqueous solution of household bleach at pH 7 for 1 h, followed by rinsing with distilled water. Then the fabrics were dried at 45 °C for 1 h to remove occluded chlorine from the surfaces. An iodometric/thiosulfate titration was used to determine oxidative Cl^+% content on the swatches. The weight percentage of chlorine was calculated according to equation 1.

$$Cl^+\% = \left(\frac{35.45 * N * V}{2 * W} \right) * 100 \quad (1)$$

In this equation Cl^+% is the weight percent of oxidative chlorine on the samples, N and V are the normality (equiv/L) and volume (L) of the $Na_2S_2O_3$ (titrant), respectively, and W is the weight of the cotton sample in g.

4.2.4. Stability Testing

UVA light (type A, 315-400 nm) stability of the coatings was evaluated using an accelerated weathering tester (The Q-panel Company, Cleveland, OH, USA). Briefly, the chlorinated and unchlorinated swatches were stored under the tester for a certain exposure time, and then chlorine loadings remaining and restored upon rechlorination after the exposure were determined by the analytical titration method mentioned above.

Wash fastness was evaluated using American Association of Textile Chemists and Colorists (AATCC) test method 61-1996 and a laboratory model Lauder-Ometer. In brief, 2.54x5.08 cm^2 swatches were agitated with stainless steel balls in a rotating canister (42 rpm) filled with 150 mL of 0.15 wt % AATCC detergent water solution at 49 °C. Three different sets of experiments were conducted: the remaining chlorine loadings were measured after the washing test to address the halogen stability (X column, Table 4.1), the

swatches were recharged to evaluate how much of the coating was washed away from the surface (Y column, Table 4.1), and the unchlorinated swatches were chlorinated after the washing test (Z column, Table 4.1).

4.2.5. Antimicrobial Efficacy Testing

The cotton swatches (both chlorinated and unchlorinated) were challenged with *S. aureus* (ATCC 6538) and *E. coli* O157:H7 (ATCC 43895) for 2 to 10 min contact times. A "sandwich test" was conducted for antimicrobial assessment of the coated fabrics. Briefly, a bacterial suspension was prepared in 100 μM phosphate buffer (pH 7), and then 25 μL of the prepared suspension was placed in between two swatches (2.54 cm^2). A sterile weight was placed on top of the swatches to ensure sufficient contact with the bacteria. After specified contact times, oxidative chlorine were neutralized by quenching the swatches with 5.0 mL of 0.02 N sodium thiosulfate solution through vortexing for 2 min. Serial dilutions were prepared using 100 μM phosphate buffer solution (pH 7) and plated on Trypticase soy agar plates which were incubated at 37 °C for 24 h. Finally, the viable bacteria were enumerated for antimicrobial assessment.

4.3. Results and Discussion

4.3.1. Characterization of the Coatings

The coatings and subsequent treatments were characterized by ATR-IR spectroscopy. After the cotton fabric was coated with the copolymer P, an additional band at 1728 cm^{-1} formed as an indication of the copolymer immobilization on the surface (Figure 4.3). This band corresponds to the ester carbonyl stretching mode present in the copolymer

structure, and it is consistent with the observation of previous study.[21] ATR-IR characterization of the cotton fabrics after the N-halamine treatments are shown in Figure 4.4. When the coated cotton fabric was treated with DMH-K, the amide and imide carbonyl stretching modes of the hydantoin ring appeared at 1701 and 1764 cm^{-1}, respectively (Figure 4.4-A). Similarly, the amide and the imide carbonyl stretching modes of the TTDD-K treated fabric were obtained at 1712 and 1774 cm^{-1} (Figure 4.4-B). The vibrational band for the amide carbonyl stretching of the TMIO ring was observed at 1735 cm^{-1} (Figure 4.4-C).

Upon exposure to bleach, both the imide and amide carbonyl stretching modes of the hydantoin and TTDD rings shifted to higher wavenumbers (Figure SP.4.8). This type of shifting has also been observed in some of the previous N-halamine coatings and is primarily due to reduced hydrogen bonding after the chlorination process.[12] On the other, hand no shifting was observed for the TMIO treated fabrics upon bleach treatment

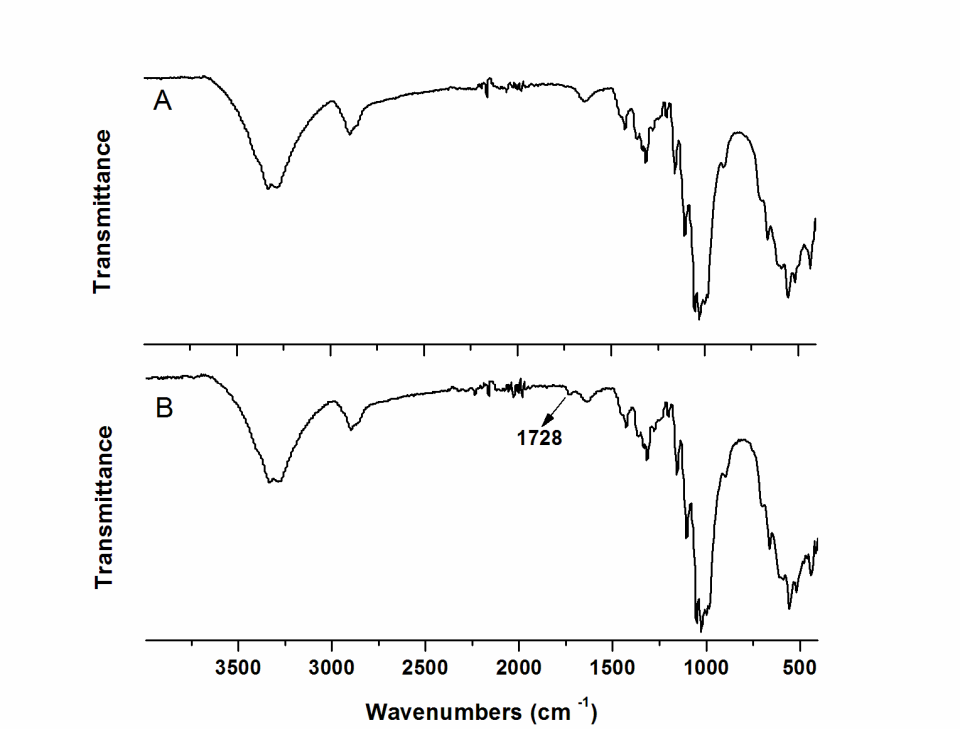

Figure 4. 3. ATR-IR characterization of the copolymer P coated cotton fabric. A: Cotton fabric. B: Copolymer P coated cotton fabric.

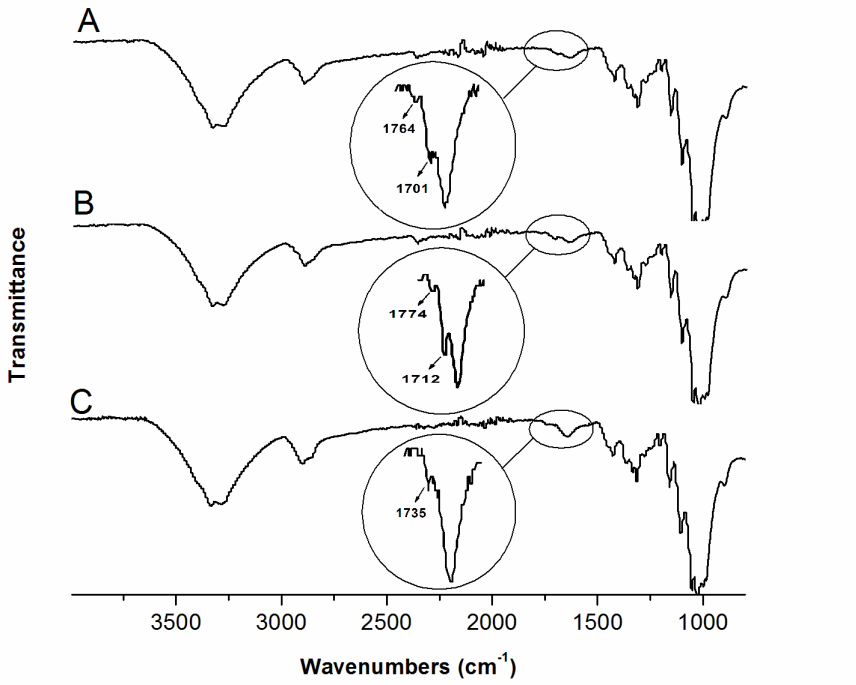

Figure 4. 4. ATR-IR characterization of N-halamine treatments (before chlorination). A: DMH-K treated cotton fabric. B: TTDD-K treated cotton fabric. C: TMIO-Na treated cotton fabric.

4.3.2. Washing Stabilities

The cotton fabrics coated with 3 wt % of the copolymer P were treated with the heterocyclic N-halamines and then subjected to repeated laundering. As can be seen in Table 4.1, DMH-K and TMIO-Na treated fabrics had the same initial chlorine loading which was almost half of the TTDD-K treated swatches. Because TTDD-K has two nitrogen sites as a binding point for the oxidative halogen, the oxidative halogen loading capacity was twice that of DMH-K and TMIO-Na.

In general, all three treatments provided remarkable washing stabilities compared to some of the previously studied N-halamine coatings.[22] Even after 50 times of laundering, all of them retained enough oxidative halogen for an effective biocidal activity. Therefore,

bleaching may not be necessary after the washings. Even though they have different functional groups as the active site, there were minor differences observed between the stabilities of these three treatments. Stability of the oxidative halogen can be evaluated from Table 4.2 using the formula below;

$$\text{Halogen Stability (\%)} = \left(\frac{\text{X column} + (\text{Initial Loading} - \text{Y column})}{\text{Initial Loading}} \right) * 100 \quad (2)$$

As expected, due to presence of the amine functionality, the TTDD-K and TMIO-Na treated fabrics exhibited superior halogen stabilities as compared to the DMH-K treatment. On the other hand, the TMIO-Na treated fabrics provided the least durable coating (Y and Z columns) the among others. A possible reason for this unexpected durability result might be dissolution or degradation of the copolymer P from the fabric surface during the treatment procedure.

Table 4. 1. Stability toward washing of coatings on the cotton (Cl^+% remaining)[a].

Number of Machine Cycles	DMH Treated			TTDD Treated			TMIO Treated		
	X	Y	Z	X	Y	Z	X	Y	Z
0	0.22			0.38			0.21		
5	0.17	0.22	0.20	0.35	0.36	0.35	0.15	0.19	0.20
10	0.16	0.21	0.20	0.33	0.34	0.35	0.14	0.18	0.20
25	0.15	0.20	0.19	0.31	0.32	0.34	0.13	0.16	0.18
50	0.14	0.20	0.19	0.28	0.31	0.33	0.13	0.15	0.17

X: Chlorinated before washing, Y: Chlorinated before washing and rechlorinated after washing, Z: Unchlorinated before washing, but chlorinated after washing, [a] The error in the measured Cl^+ weight percentage values was ±0.01.

4.3.3. UVA Light Stabilities

The chlorinated and unchlorinated cotton swatches (3 % copolymer coated and 0.5 M N-halamine treated) were exposed to UVA light for times up to 96 h, and the results are summarized in Table 4.2. The oxidative halogen was lost gradually upon exposure to UVA light in all of the treatments. However, this loss was slower for DMH treatment which involves an amide functionality. Rechlorinations performed subsequent to 24 h exposures revealed that the halogen loss was not only because of N-Cl bond dissociation, but also because of a slight photodecomposition taking place in the coatings. The magnitude of this decomposition at the end of 96 h exposure was in increasing order of DMH-treated < TTDD-treated < TMIO-treated fabrics. On the other hand, no decomposition was observed for the unchlorinated samples in any of the treatments.

Table 4. 2. Effect of UVA irradiation on the coatings (Cl^+% remaining)[a].

Exposure Time (h)	DMH Treated		TTDD Treated		TMIO Treated	
	C	U	C	U	C	U
0	0.26		0.41		0.24	
1	0.24		0.15		0.21	
3	0.20		0.08		0.12	
6	0.18		0.06		0.09	
12	0.14		0.03		0.04	
24	0.11		0.01		0.02	
24-Re	0.22	0.24	0.41	0.40	0.20	0.24
48	0.06		0.02		0.01	
48-Re	0.18	0.26	0.36	0.39	0.14	0.25
72-Re	0.13	0.25	0.26	0.38	0.07	0.25
96-Re	0.09	0.24	0.11	0.40	0.04	0.24

C: Chlorinated, U: Unchlorinated, Re: Rechlorinated [a] The error in the measured Cl^+ weight percentage values was ±0.01.

Figure 4.5 shows UV/vis spectra of the chlorinated and unchlorinated DMH and TMIO compounds (0.02 mol/L in methanol). TMIO exhibited a wider absorption band with maximal absorption at 255 nm as compared to DMH. Upon chlorination, the absorption band and molar absorptivity of both compounds increased significantly causing dissociation of the N-Cl bonds.[23] In the UVA region, the unchlorinated DMH and TMIO (0.02 mol/L in methanol) showed almost no absorption which explains the stability of the unchlorinated swatches against UVA light shown in Table 4.2. On the other hand, the chlorinated TMIO exhibited a more intense and broader absorption band in the range of 315 to 400 nm (UVA region) as opposed to the chlorinated DMH compound. This is the reason for faster oxidative halogen loss induced by UVA light exposure in the TMIO treated swatches as compared to the DMH treated fabrics. Moreover, this broader absorption might also have an effect on increased magnitude of the photolytic decomposition shown in Table 4.2. The exact mechanism of this decomposition is under study.

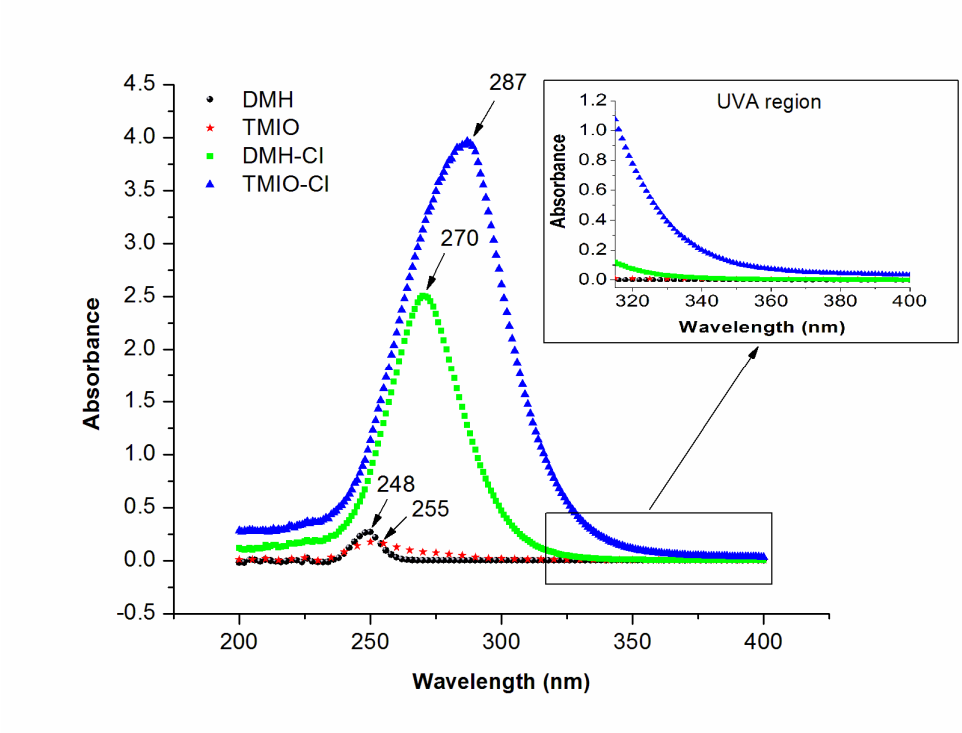

Figure 4. 5. UV/vis spectra of DMH (5,5-dimethylhyndatoin), TMIO (2,2,5,5-tetramethylimidazolidinone), DMH-Cl (1,3-dichloro-5,5-dimethylhyndatoin), TMIO-Cl (1,3-dichloro-2,2,5,5-tetramethylimidazolidinone).

4.3.4. Bicodial Efficacies

The cotton swatches were challenged with about 6 log of *S. aureus* and *E. coli* O157:H7 for antimicrobial assessment. The cotton fabric coated with 3 wt % copolymer P was treated with 0.5 M of DMH-K, TMIO-Na and TTDD-K salt solution according to the procedure explained in the experimental section. Antimicrobial efficacy is very dependent on oxidative halogen loading on surfaces.[21] Therefore, a fourth set of experiments was performed by treating 1.5 % copolymer P coated cotton fabric with 0.5 M TTDD-K solution so as to have similar chlorine loading as for the other two N-halamine treatments. As can be seen in Table 4.3, the control samples which were not chlorinated did not provide significant bacteria reduction even for the longest contact time. The limited reductions that they

exhibited are due to adhesion of bacteria rather than the inactivation. On the other hand, the chlorinated swatches effectively inactivated all of the Gram-negative and Gram-positive bacteria within brief contact times. The rate of bacteria inactivation depended on chemical composition of the N-halamine structures. N-halamines having amide functionality are known to show a faster biocidal activity that are N-halamines containing amine groups because of their weaker N-Cl bond stregnth.[11] Therefore, the TMIO and TTDD treated fabrics exhibited a lower inactivation as compared to the DMH treatment due to the presence of a hindered amine group in their chemical structures. Similarly, in spite of having around the same chlorine loadings, the TTDD treatment provided a more rapid complete inactivation of *E. coli* as compared to the TMIO treatment, since TTDD has dual (amide and hindered amine) functional groups. As expected, increasing chlorine loading of the TTDD treated fabrics resulted in a more rapid complete inactivation of the Gram-negative bacteria. In general, all three treatments exhibited remarkable biocidal efficacies as compared to other types of biocides.

Table 4. 3. Bicodial efficacies of the treated cotton fabrics.

Sample (Cl^+ %)	Contact time (min)	Log Reduction[a]	
		S. aureus	***E.Coli O157:H7***
DMH treatment	10	0.24	0.03
TMIO treatment	10	0.02	0.03
TDDD-L[b] treatment	10	0.33	0.12
TTDD-H[c] treatment	10	0.40	0.12
DMH treatment Cl^+ % 0.24	2	6.05	2.71
	5	6.05	6.03
	10	6.05	6.03
TMIO treatment Cl^+ % 0.26	2	1.78	1.12
	5	6.05	4.20
	10	6.05	6.03
TTDD-L treatment Cl^+ % 0.24	2	2.58	0.52
	5	6.05	6.03
	10	6.05	6.03
TTDD-H treatment Cl^+ % 0.42	2	6.05	6.03
	5	6.05	6.03
	10	6.05	6.03

[a]The inoculum concentrations were 6.05, and 6.03 logs for *S. aureus* and *E. coli O157:H7*, respectively. [b]1.5 wt % copolymer P coated fabric treated with TTDD-K was used. [c]3 wt % copolymer P coated fabric treated with TTDD-K was used.

4.4. Conclusions

Heterocyclic N-halamine structures containing amide or amine functional groups were anchored to cotton fabric through epoxide bonding to address the stabilities and durabilities of the structures. The coatings exhibited potent antimicrobial activities against *S. aureus* and *E. coli O157:H7* with around 6 log inactivation within 2 to 10 min contact time. It was observed that the amide-containing N-halamine treatment provided more rapid inactivation of Gram-negative and Gram-positive bacteria as compared to the amine N-halamine treatment. Even though, the oxidative halogen was more stable toward hydrolysis in the amine-treated swatches, the amide-treated swatches provided a better wash fastness.

In general, all of the treatments exhibited superior durability against repeated laundering such that bleaching was not necessary after each washing cycle. On the other hand, a photolytic decomposition induced by UVA light exposure was observed for all of the chlorinated fabrics. The amide-containing N-halamine was least prone to this decomposition among the treatments.

4.5. References

(1) Gagliotti, C.; Balode, A.; Baquero, F.; Degener, J.; Grundmann, H.; Gür, D.; Jarlier, V.; Kahlmeter, G.; Monen, J.; Monnet, D. L. *Euro Surveill* **2011**, *16*, 1-5.

(2) Colak, S.; Tew, G. N. *Macromolecules* **2008**, *41*, 8436-8440.

(3) Klibanov, A. M. *Journal of Materials Chemistry* **2007**, *17*, 2479-2482.

(4) Sauvet, G.; Dupond, S.; Kazmierski, K.; Chojnowski, J. *Journal of Applied Polymer Science* **2000**, *75*, 1005-1012.

(5) El-Shishtawy, R. M.; Asiri, A. M.; Abdelwahed, N. A. M.; Al-Otaibi, M. M. *Cellulose* **2011**, *18*, 1-8.

(6) Kenawy, E. R.; Worley, S. D.; Broughton, R. *Biomacromolecules* **2007**, *8*, 1359-1384.

(7) Sun, Y.; Sun, G. *Macromolecules* **2002**, *35*, 8909-8912.

(8) Goddard, J. M.; Hotchkiss, J. H. *Journal of Food Protection* **2008**, *71*, 2042-2047.

(9) Akdag, A.; Okur, S.; McKee, M. L.; Worley, S. D. *Journal of Chemical Theory and Computation* **2006**, *2*, 879-884.

(10) Denyer, S. P.; Stewart, G. *International biodeterioration & biodegradation* **1998**, *41*, 261-268.

(11) Qian, L.; Sun, G. *Journal of Applied Polymer Science* **2004**, *91*, 2588-2593.

(12) Kocer, H. B.; Worley, S. D.; Broughton, R. M.; Huang, T. S. *Reactive and Functional Polymers* **2011**, *71*, 561-568.

(13) Ren, X.; Kocer, H. B.; Kou, L.; Worley, S. D.; Broughton, R. M.; Tzou, Y. M.; Huang, T. S. *Journal of Applied Polymer Science* **2008**, *109*, 2756-2761.

(14) Lin, J.; Winkelmann, C.; Worley, S. D.; Broughton, R. M.; Williams, J. F. *Journal of Applied Polymer Science* **2001**, *81*, 943-947.

(15) Worley, S. D.; Li, F.; Wu, R.; Kim, J.; Wei, C. I.; Williams, J. F.; Owens, J. R.; Wander, J. D.; Bargmeyer, A. M.; Shirtliff, M. E. *Surface Coatings International Part B: Coatings Transactions* **2003**, *86*, 273-277.

(16) Ren, X.; Akdag, A.; Zhu, C.; Kou, L.; Worley, S. D.; Huang, T. S. *Journal of Biomedical Materials Research Part A* **2009**, *91*, 385-390.

(17) Cerkez, I.; Kocer, H. B.; Worley, S. D.; Broughton, R. M.; Huang, T. S. *Langmuir* **2011**, *27*, 4091-4097.

(18) Sun, Y.; Sun, G. *Journal of Applied Polymer Science* **2003**, *88*, 1032-1039.

(19) Ren, X.; Kou, L.; Liang, J.; Worley, S. D.; Tzou, Y. M.; Huang, T. S. *Cellulose* **2008**, *15*, 593-598.

(20) Liang, J.; Chen, Y.; Ren, X.; Barnes, K.; Worley, S. D.; Broughton, R. M.; Cho, U.; Kocer, H.; Huang, T. S. *Industrial & Engineering Chemistry Research* **2007**, *46*, 6425-6429.

(21) Kocer, H. B.; Cerkez, I.; Worley, S. D.; Broughton, R. M.; Huang, T. S. *ACS Applied Materials & Interfaces* **2011**, *3*, 3189-3194.

(22) Kocer, H. B.; Akdag, A.; Ren, X.; Broughton, R. M.; Worley, S. D.; Huang, T. S. *Industrial & Engineering Chemistry Research* **2008**, *47*, 7558-7563.

(23) Chen, Z.; Sun, Y. *Industrial & Engineering Chemistry Research* **2006**, *45*, 2634-2640.

4.6. Supporting Information

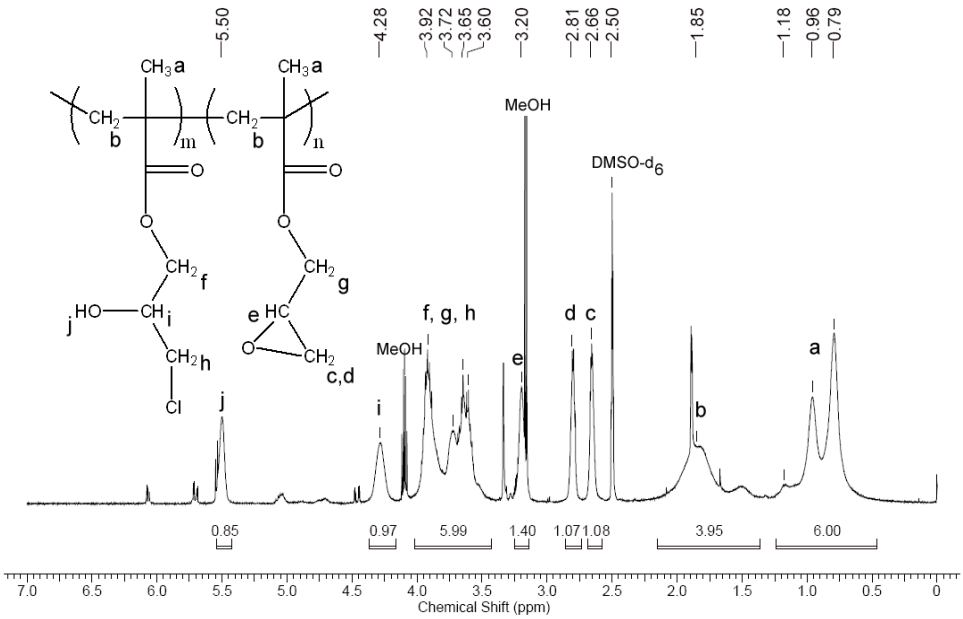

Figure SP.4. 1. ^{1}H NMR spectra of the synthesized copolymer P (solvent: DMSO-d_6).

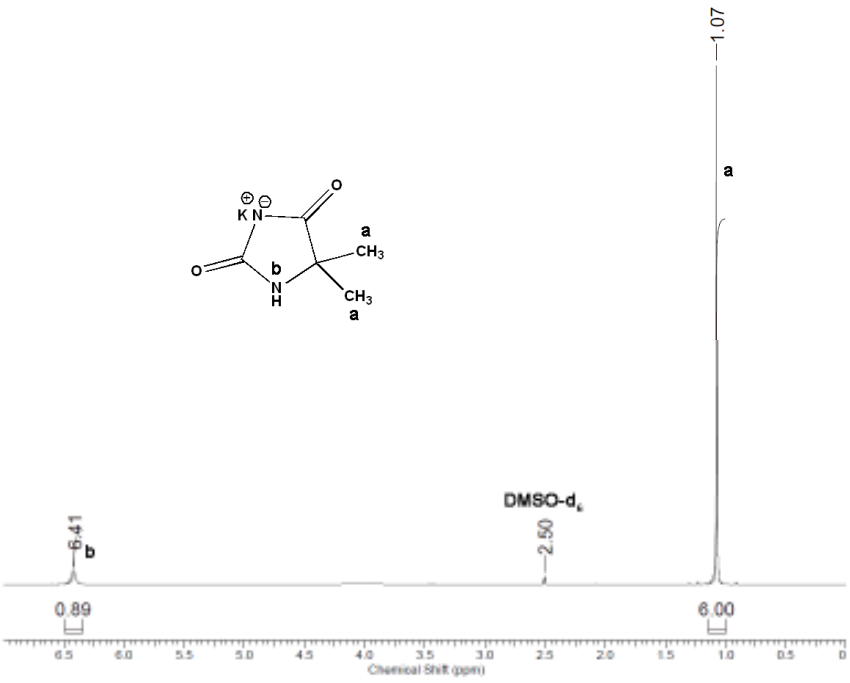

Figure SP.4. 2. ^{1}H NMR Spectra of DMH-K (DMSO-d_6).

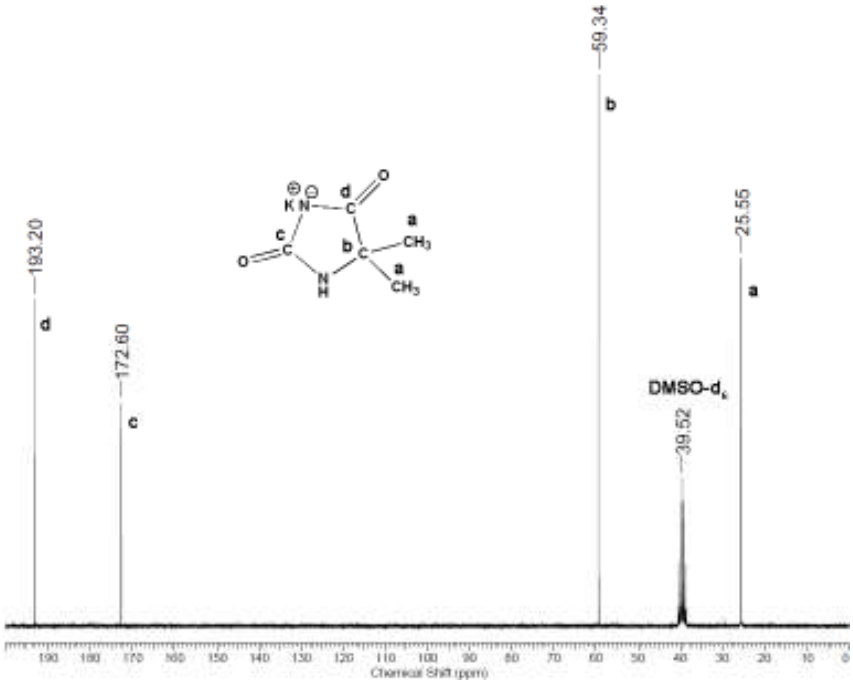

Figure SP.4. 3. ^{13}C NMR Spectra of DMH-K (DMSO-d_6).

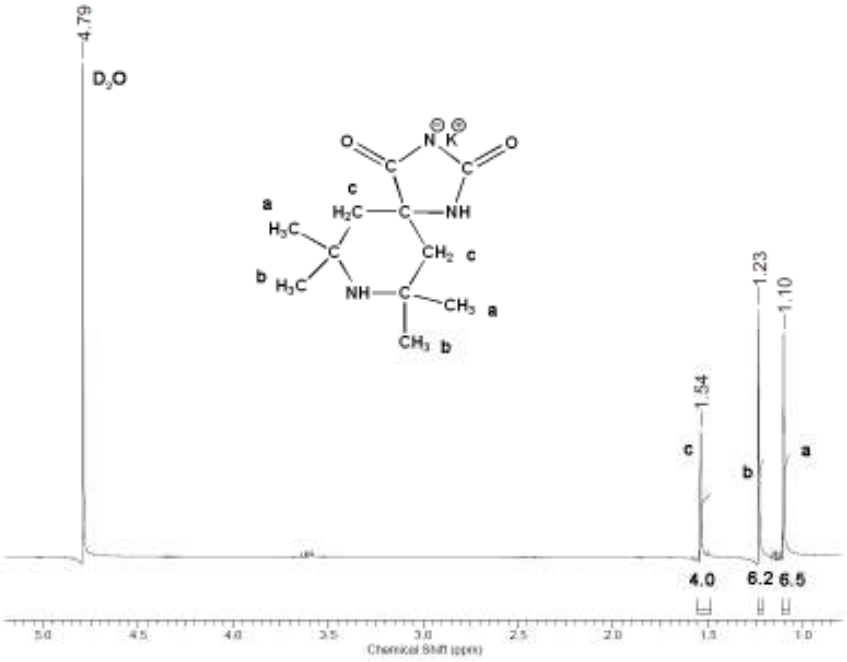

Figure SP.4. 4. ^{1}H NMR Spectra of TTDD-K (solvent: D_2O).

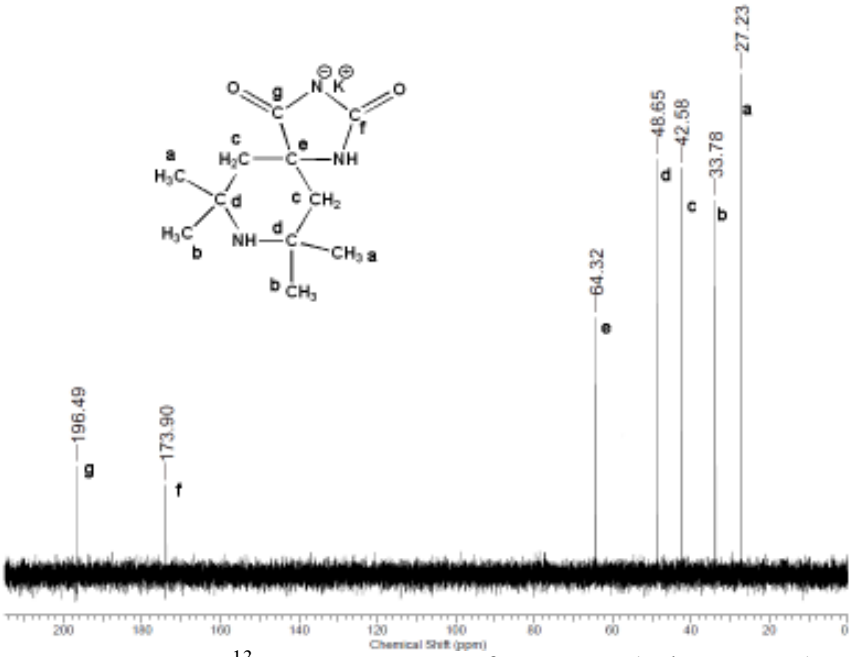

Figure SP.4. 5. ^{13}C NMR Spectra of TTDD-K (solvent: D_2O).

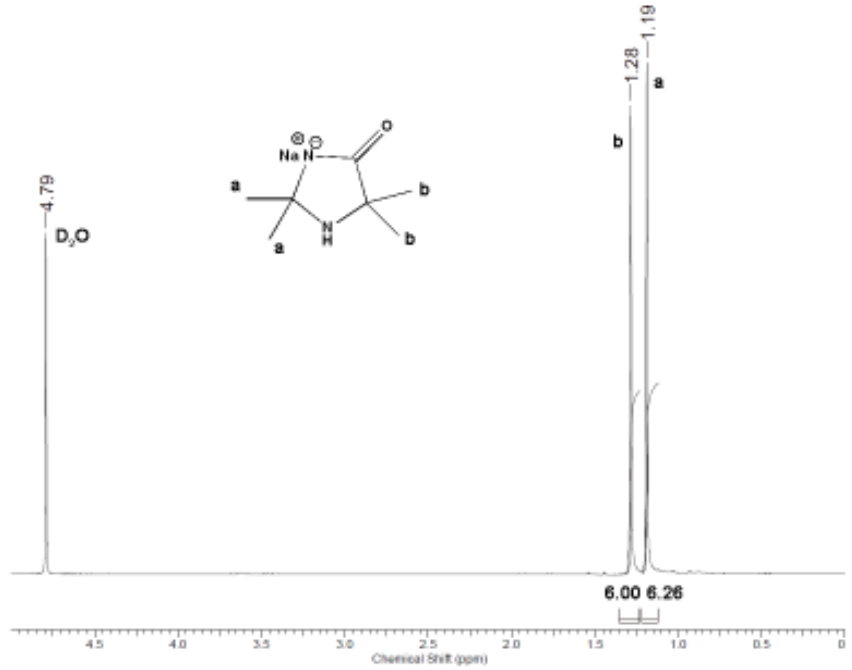

Figure SP.4. 6. ^{1}H NMR Spectra of TMIO-Na (D_2O).

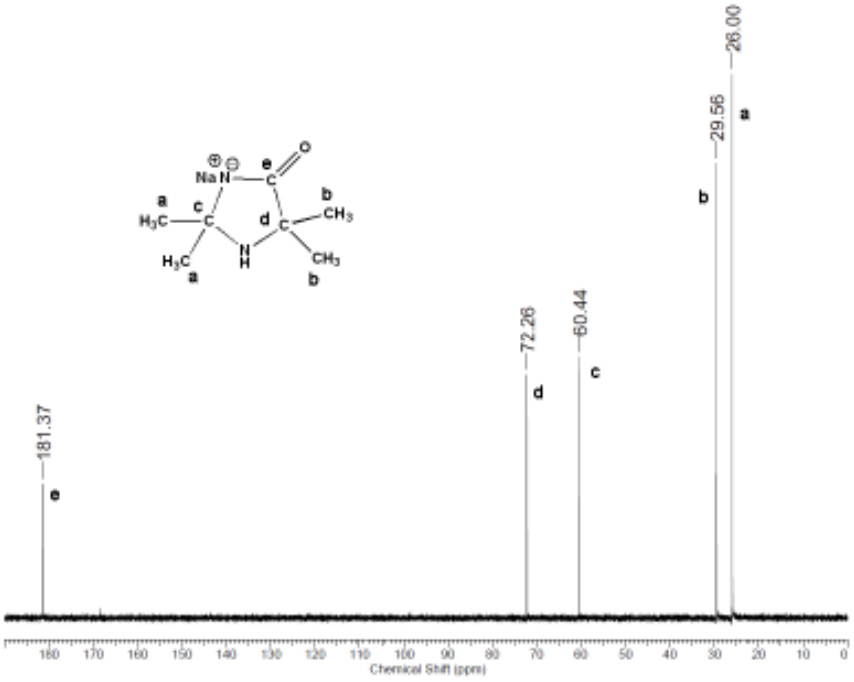

Figure SP.4. 7. ^{13}C NMR Spectra of TMIO-Na (D_2O).

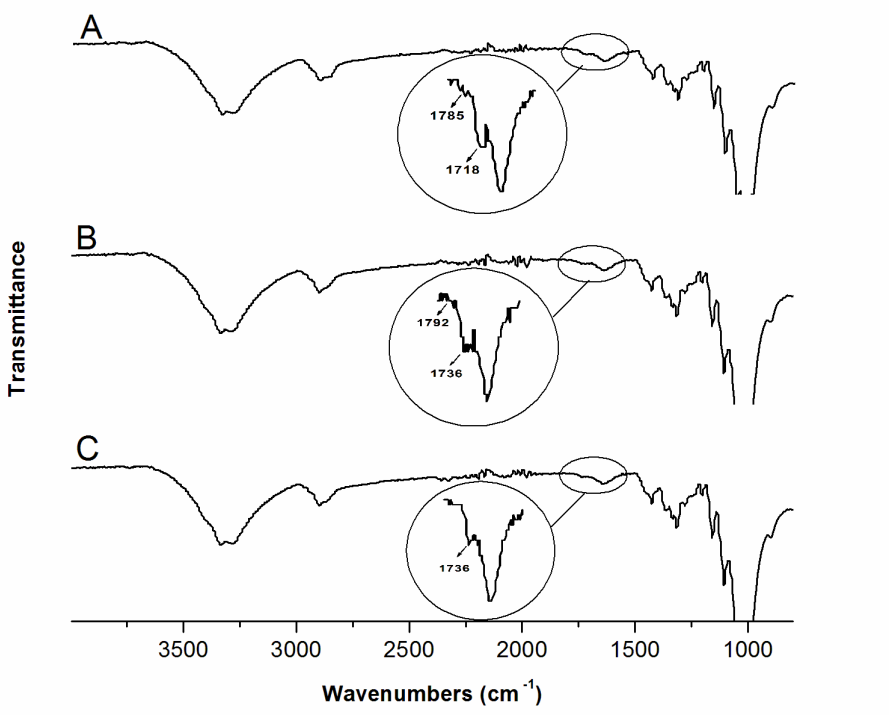

Figure SP.4. 8. ATR-IR characterization of cyclic N-halamine treated fabrics after chlorination. A: DMH-K treated cotton fabric. B: TTDD-K treated cotton fabric. C: TMIO-Na treated cotton fabric.

CHAPTER 5

N-HALAMINE COPOLYMERS FOR BIOCIDAL COATINGS

5.1. Introduction

Hospital-acquired infections are one of the main causes of mortality and morbidity around the world, and they are expected to be even more significant due to increasing world's population and urbanization, emergence of new types of microorganisms, and increasing bacterial resistance to antibiotics.[1] Textile materials, particularly natural fibers, are prone to microbial growth. Use of contaminated medical textiles is an important contributor to cross-infection. Therefore, antimicrobial treatment of medical textiles is crucial to prevent health-acquired infections.[2] In that sense, quaternary ammonium salts,[3-5] N-halamines,[6-9] metal ions[10] and biguanides[11] have been immobilized onto surfaces to reduce the risk of spreading pathogenic microorganisms.

As one of the most effective biocides, N-halamine biocidal coatings for surfaces have created a great deal of interest in recent years due to their long-term stabilities, non-toxicities to humans, and antimicrobial activities against a broad spectrum of microorganisms including Gram-negative and Gram-positive bacteria, viruses, fungi, and yeasts.[12] N-halamines inactivate microorganisms through direct transfer of the oxidative halogen to the cell membrane leading to cell death.[13] Once all of the oxidative halogen on the surface is consumed, it can be recharged by exposure to dilute household bleach. Antimicrobial activity rates increase from amine- to amide- to imide-containing N-

halamines, whereas the halogen stability decreases in that order.[14] Thus, the biocidal activity rate of N-halamines can be tuned by the use of different functional groups as the active site.

Work in these laboratories has produced numerous N-halamine biocidal coatings on various surfaces such as cotton,[15] nylon,[16] polyester,[17] and silica gel.[18] These coatings exhibited potent antimicrobial activity against Gram-negative and Gram-positive bacteria within brief contact times. Even though the aforementioned coatings provided sufficient washing stabilities, ultraviolet light (UV) stabilities generally need to be improved, since an irreversible decomposition can take place upon exposure to UV light. In a recent study, the mechanism of the photolytic decomposition for a siloxane group-containing N-halamine coating was explained by a halogen radical migration to the alkyl side chain connected to the siloxane tethering group resulting in alpha/beta scission, leading to loss of N-halamine from the surface.[19] In this study, a vinyl N-halamine monomer, hydantoin acrylamide (HA), was copolymerized with silane-, epoxide-, and hydroxyl group-containing monomers, and the resultant copolymers were coated onto cotton fabric for the purpose of addressing the UV light stabilities, biocidal efficacies, and washing stabilities of N-halamines immobilized by different tethering groups.

5.2. Experimental

5.2.1. Materials and Instrumentation

All starting chemicals were purchased from Aldrich Chemical Company (Milwaukee, WI), TCI America (Boston, MA), or Alfa Aesar (Heysham, UK), and used as is unless otherwise noted. Desized, scoured, and bleached (100%) cotton (Style 400 Cotton Print Cloth) was obtained from Testfabrics. Inc. (West Pittson, PA). Clorox® brand (Clorox,

Inc., Oakland, CA) household bleach was used for chlorination. Bacteria cultures of *Staphylococcus aureus* ATCC 6538 and *Escherichia coli* O157:H7 ATCC 43895 were purchased from American Type Culture Collection (Rockville, MD), and Trypticase soy agar was obtained from Difco Laboratories (Detroit, MI). ATR-IR data recorded with 64 scans at 4 cm^{-1} resolution were obtained with a Nicolet 6700 FT-IR spectrometer with an ATR (Attenuated Total Reflectance) accessory using a diamond crystal.

5.2.2. Synthesis of the copolymers

HA monomer was synthesized by a procedure outlined previously.[20] The copolymer, poly (hydantoinyl acrylamide-co-3-(trimethoxysilyl)propyl methacrylate) (HASL), was synthesized by dissolving an eqiomolar (6 mmol) mixture of HA and 3-(trimethoxysilyl)propyl methacrylate (SL) in 5 mL of methanol together with 0.03 g of initiator, azobis(isobutyronitrile) (AIBN). The mixture was deoxygenated by flushing nitrogen though the solution for 10 min. The polymerization reaction was performed by stirring the solution at 65 °C for 2 h under nitrogen protection (Figure 5.1). The copolymer was obtained as a white solid by evaporation of the solvent and unreacted monomers.

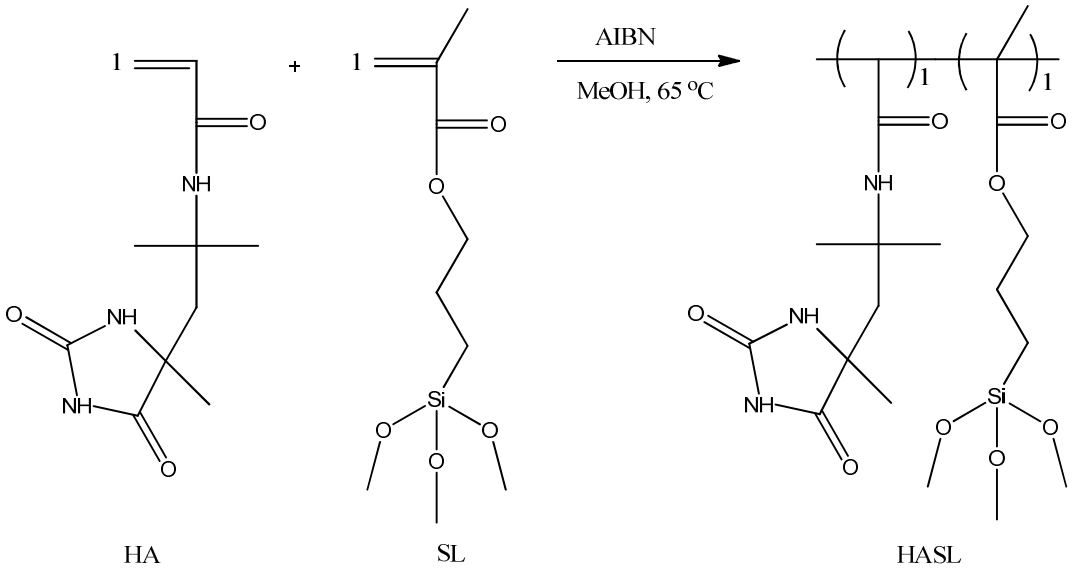

Figure 5. 1. Synthesis of HASL copolymer.

The copolymer HASL structure was characterized by FTIR spectroscopy. As can be seen in Figure 5.2, the band for the imide carbonyl stretching mode of the hydantoin ring was obtained at 1768 cm^{-1}. The vibrational band for the amide carbonyl stretching mode could not be distinguished due to its overlapping with the carbonyl stretching modes of the ester groups present in the SL structure. The vibrational bands at 1651 cm^{-1} and 1077 cm^{-1} in spectrum C correspond to aliphatic amide carbonyl stretching and the Si–O–C asymmetric stretching mode, respectively. The stretching vibration of the vinyl bonds of the monomers disappeared in the copolymer spectra suggesting a completion of polymerization.

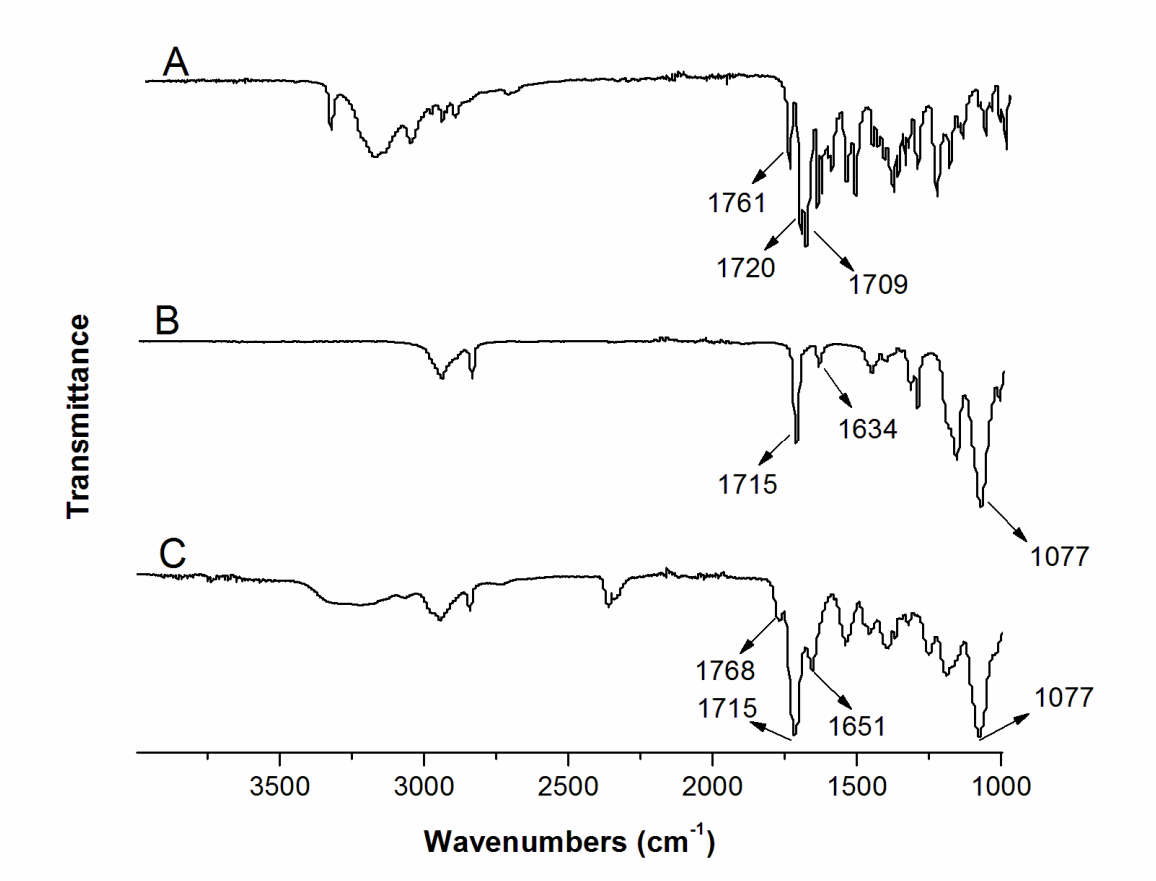

Figure 5. 2. FTIR Spectra of A: Hydantoin acrylamide, B: 3-(trimethoxysilyl)propyl methacrylate, C: HASL copolymer.

The copolymer poly(hydantoinyl acrylamide-co-glycidyl methacrylate) (HAGM) was prepared by free radical polymerization of HA and glycidyl methacrylate (GM). Briefly, 1.91 g (8 mmol) of HA, 1.17 g (8 mmol) of glycidyl methacrylate (GM), 0.031 g of AIBN, and 7 mL of methanol were mixed in a 50 mL round-bottom flask. Nitrogen was bubbled through the solution for 15 min to eliminate any dissolved oxygen. The polymerization was performed by stirring the mixture at 65 °C for 75 min under nitrogen atmosphere (Figure 5.3). When the solution was cooled to room temperature, the copolymer was precipitated

from the solution. The copolymer HAGM was recovered by filtration and then further purified by rinsing with methanol.

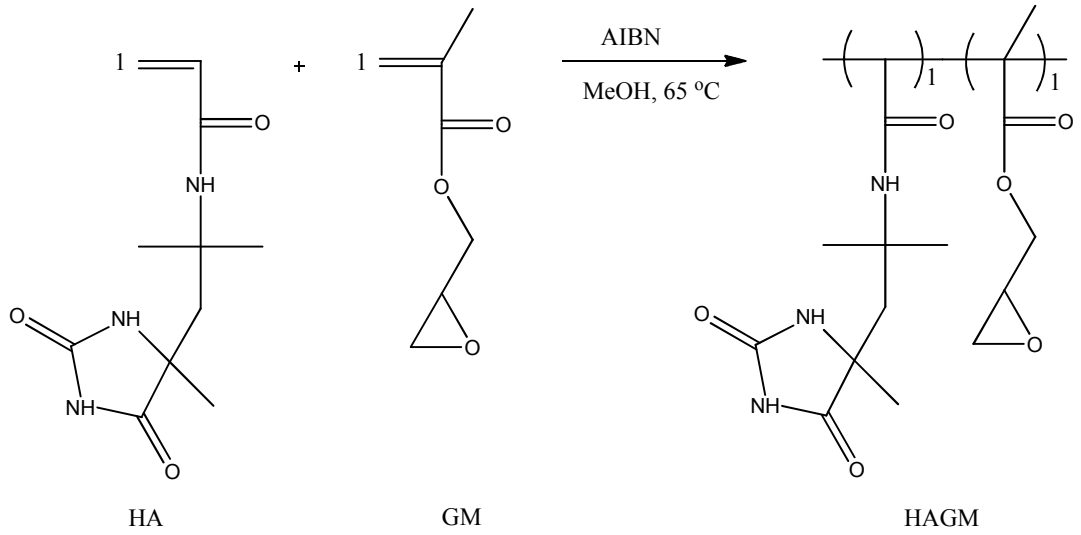

Figure 5. 3. Synthesis of HAGM copolymer.

FTIR characterization of the copolymer HAGM is shown in Figure 5.4. The double bond stretching modes of the monomers disappeared in the copolymer spectrum (C). The aliphatic amide and the imide carbonyl stretching modes were obtained at 1768 and 1655 cm^{-1}, respectively. On the other hand, the amide carbonyl stretching bands of the hydantoin ring could not be identified in spectrum C, since the ester carbonyl stretching bands of SL overlapped with it. In addition, the N-H bending (amide) modes of HA and the epoxy group stretching modes of GM could clearly be identified in the copolymer spectra by bands at 1539 cm^{-1} and 903 cm^{-1}, respectively.[21]

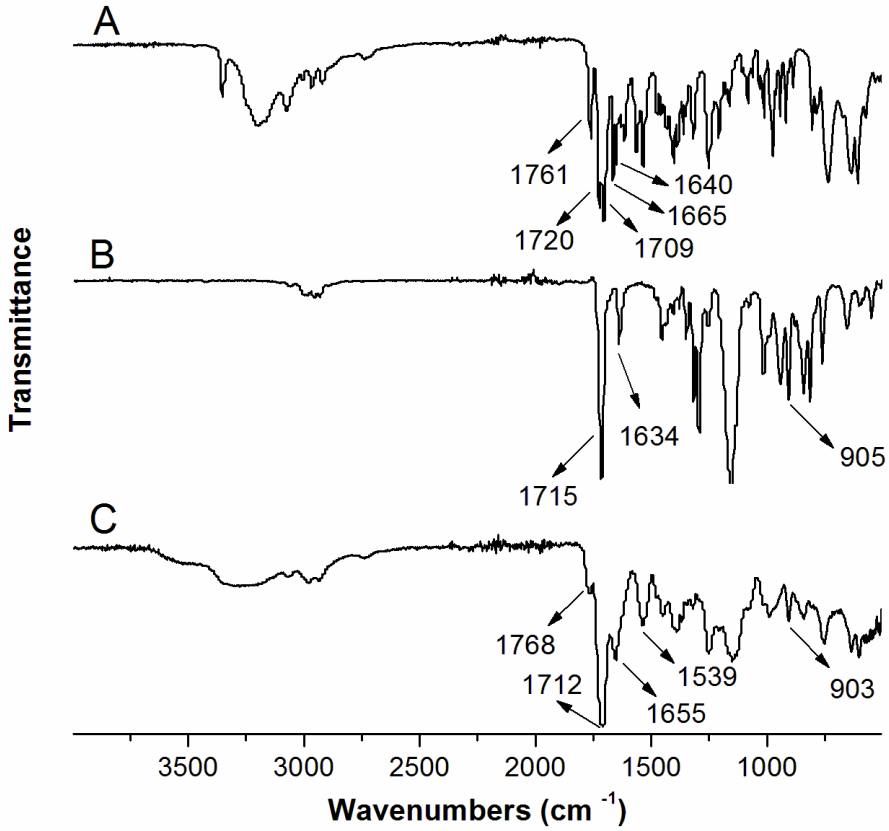

Figure 5. 4. FTIR Spectra of A: Hydantoin acrylamide, B: Glycidyl methacrylamide, C: HAGM copolymer.

The copolymer poly(hydantoinyl acrylamide-co-2-hydroxyethylmethacrylate) (HAOH) was prepared by addition polymerization of HA and 2-hydroxyethylmethacrylate (OH). In general in a 50 mL round-bottom flask, 1.44 g (6 mmol) of HA, 0.82 g (6 mmol) of 2-hydroxyethylmethacrylate (OH), 0.023 g of AIBN, and 5 mL of methanol were mixed. After a 15 min nitrogen purge through the solution, the mixture was stirred at 65 °C for 3 h (Figure 5.5). The solvent and unreacted OH were removed by evaporation, and the copolymer was obtained as white pellets.

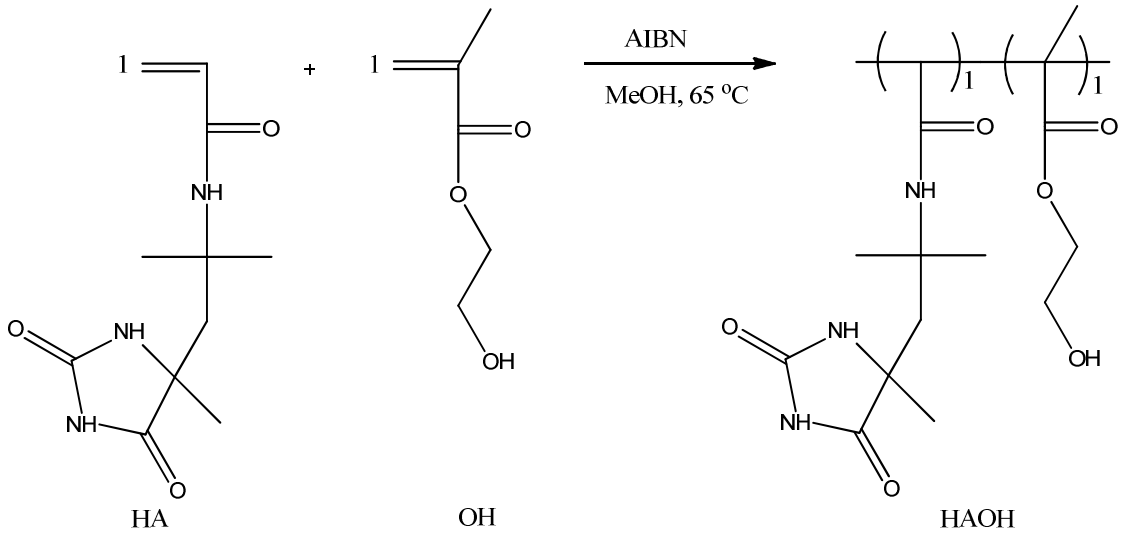

Figure 5. 5. Synthesis of HAOH copolymer.

Figure 5.6 shows the FTIR characterization of the copolymer HAOH. The N-H bending modes of the aliphatic and cyclic amide groups of HA could be identified by a broad absorption band at 1540 cm^{-1} in the copolymer spectrum. The hydroxyl group stretching modes of the monomer HA was observed at 3492 cm^{-1} in the spectrum C. In addition, absence of the vinyl bond stretching in the copolymer spectra indicated a complete polymerization process.

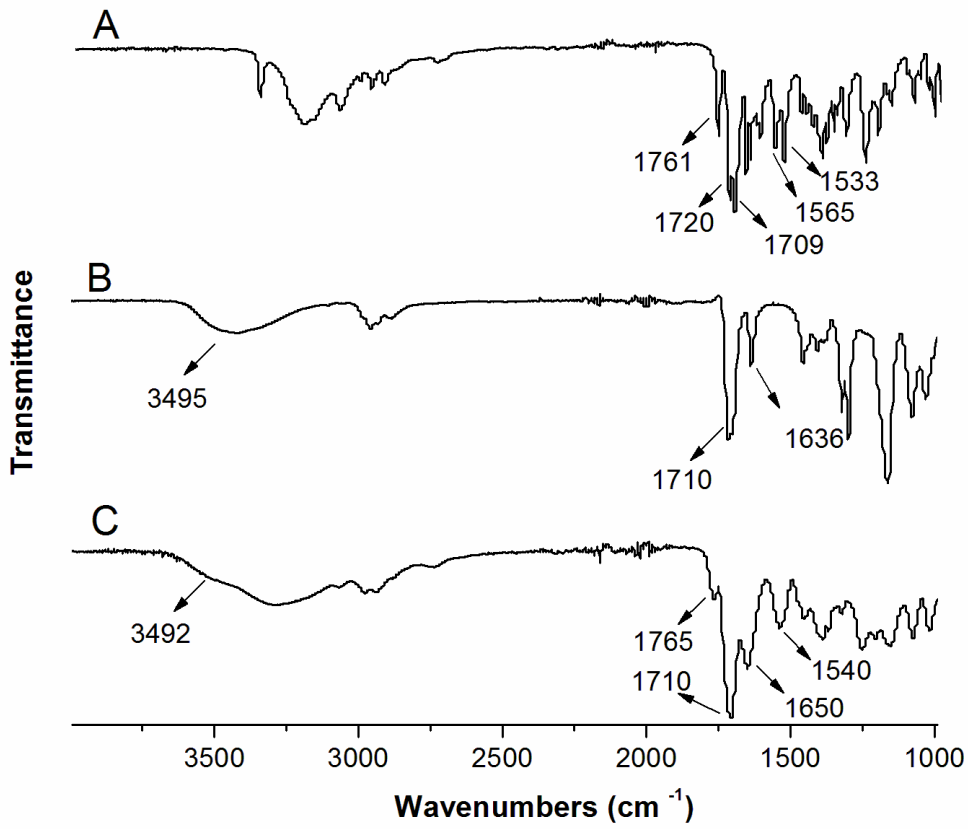

Figure 5. 6. FTIR Spectra of A: Hydantoin acrylamide, B: 2-hydroxyethylmethacrylate, C: HAOH copolymer.

5.2.3. Coating and Chlorination Procedure

The synthesized copolymers were dissolved in proper solvents at specified concentrations so as to have about the same oxidative halogen loading on the surface. The copolymer HASL was dissolved in an ethanol/water mixture (3:2 by weight) at a concentration of 3 wt %. Similarly, 4 wt % of the copolymer HAGM was dissolved in an acetone/water mixture (3:2 by weight). Since the copolymer HAOH do not contain any tethering groups for covalent bonding with cellulose, 1,2,3,4-butanetetracarbocylic acid (BTCA) was used as a crosslinking agent. Thus, 3 wt % of the copolymer HAOH was dissolved in an ethanol/water mixture (3:2 by weight), and then to that solution was added

5.7 wt % BTCA (twice the molar amount of the copolymer HAOH). All of the solutions were stirred for 15 min to create a uniform solution, and then the cotton fabric was immersed in the coating solutions for 15 min. A uniform coating on the surface was obtained by padding the samples through a laboratory wringer (Birch Brothers Southern, Waxhaw, NC). The HASL and HAGM coated fabrics were cured at 165 °C for 1 h; whereas the HAOH coated fabric was first dried at 130 °C for 10 min, followed by curing at 175 °C for 5 min. Finally, all of the swatches were washed with a 0.5 wt % detergent water solution for 15 min.

Household bleach, Clorox®, was used to halogenate the coated fabrics. The swatches were immersed in 10 wt % bleach solution at pH 7 for 1h, followed by rinsing with distilled water. Then the fabrics were dried at 45 °C for 1 h to remove occluded chlorine from the surfaces. An iodometric/thiosulfate titration was used to determine oxidative Cl^+% content on the swatches. The weight percentage of chlorine was calculated according to equation 1.

$$Cl^{+}\% = \left(\frac{35.45 * N * V}{2 * W} \right) * 100 \quad (1)$$

In this equation Cl^+% is the weight percent of oxidative chlorine on the samples, N and V are the normality (equiv/L) and volume (L) of the $Na_2S_2O_3$ (titrant), respectively, and W is the weight of the cotton sample in g.

5.2.4. Stability Testing

The stabilities of the coated cotton fabrics were evaluated against repeated launderings and UVA light exposure. A standard washing test according to AATCC Test Method 61 was employed to address the stability and rechargeability of chlorine on the cotton samples toward washings. Briefly, cotton swatches (2.54 x 5.08 cm^2) were placed in

150 mL of 0.15 wt % AATCC detergent water solution and agitated with 50 stainless steel balls in a rotating canister at 49 °C. An equivalent of 5, 10, 25, and 50 washes were conducted using a laboratory Launder-Omoter. After the washing test, the chlorine stability was evaluated by measuring the remaining chlorine on the surface with the analytic titration method mentioned above. As a second experiment, the chlorinated and unchlorinated swatches were bleached after the washing test to address the durability of the coatings.

UVA light stability of the coatings were evaluated using an Accelerated Weathering Tester (The Q-panel Company, Cleveland, OH, USA). The chlorinated and unchlorinated swatches were placed in the UV chamber (Type A, 315-400 nm) for a specified exposure time. The chlorine loadings remaining on the surface after the exposure were determined by the titration method described above. In a second experiment, the chlorinated and unchlorinated swatches were chlorinated at one day exposure intervals to address the rechargeability of the coatings.

5.2.5. Antimicrobial Efficacy Testing

Antimicrobial efficacies of the coatings were evaluated using a "sandwich test" in which the swathes were challenged with *Staphylococcus aureus* (ATCC 6538) and *Escherichia coli* O157:H7 (ATCC 43895). The bacteria were suspended in 100 μM phosphate buffer at pH 7, and 25 μL of this suspension was placed between two identical 1 cm^2 swatches. Sufficient contact with the microorganisms was obtained by placing a sterile weight on top of the swatches for specified contact times. Then the fabrics were vortexed for 2 min in 5.0 mL of 0.02 N sodium thiosulfate solution to neutralize the oxidative halogen. Serial dilutions of this solution were prepared and plated on Trypticase soy agar plates. After

incubation for 24 h at 37 °C, the viable bacteria were enumerated for biocidal efficacy evaluation.

5.3. Results and Discussions

5.3.1. Characterization of the Coatings

The FTIR characterization of the coatings on cotton fabric is shown in Figure 5.7. The bands corresponding to the amide carbonyl stretching modes of the hydantoin ring and the carbonyl stretching modes of the ester groups present in the copolymer structures overlapped at 1718, 1711 and 1719 cm^{-1} for HASL, HAGM, and HAOH, respectively. The bands for the imide carbonyl stretching modes of the hydantoin ring were observed at 1768 and 1771 cm^{-1} for HASL and HAGM, respectively; whereas they could not be identified for the HAOH copolymer due to a broad absorption band corresponding to ester carbonyl stretching.

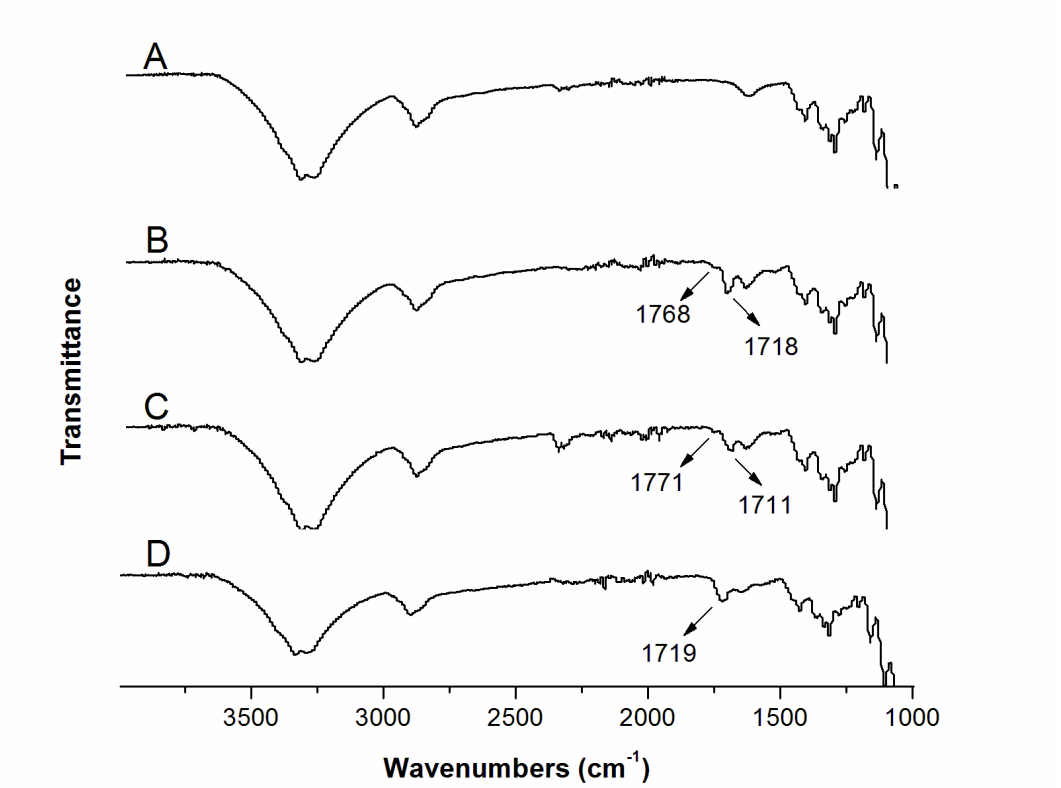

Figure 5. 7. FTIR Spectra of the coatings before chlorination A: Cotton fabric, B: HASL coated cotton fabric, C: HAGM coated cotton fabric, D: HAOH coated cotton fabric.

When the copolymer coated cotton fabrics were chlorinated, the imide and the amide carbonyl vibrational stretching modes shifted to higher wavenumbers due to reduced hydrogen bonding. In addition, upon chlorination, a new band at 1568 cm^{-1} formed for the HAOH coated cotton fabric (Figure 5.8-C). This new band corresponds to the carbonyl stretching modes of the carboxylate anion which was formed by the hydrolysis of the some ester linkages between the cotton and BTCA caused by NaOH present in the bleach solution.[22]

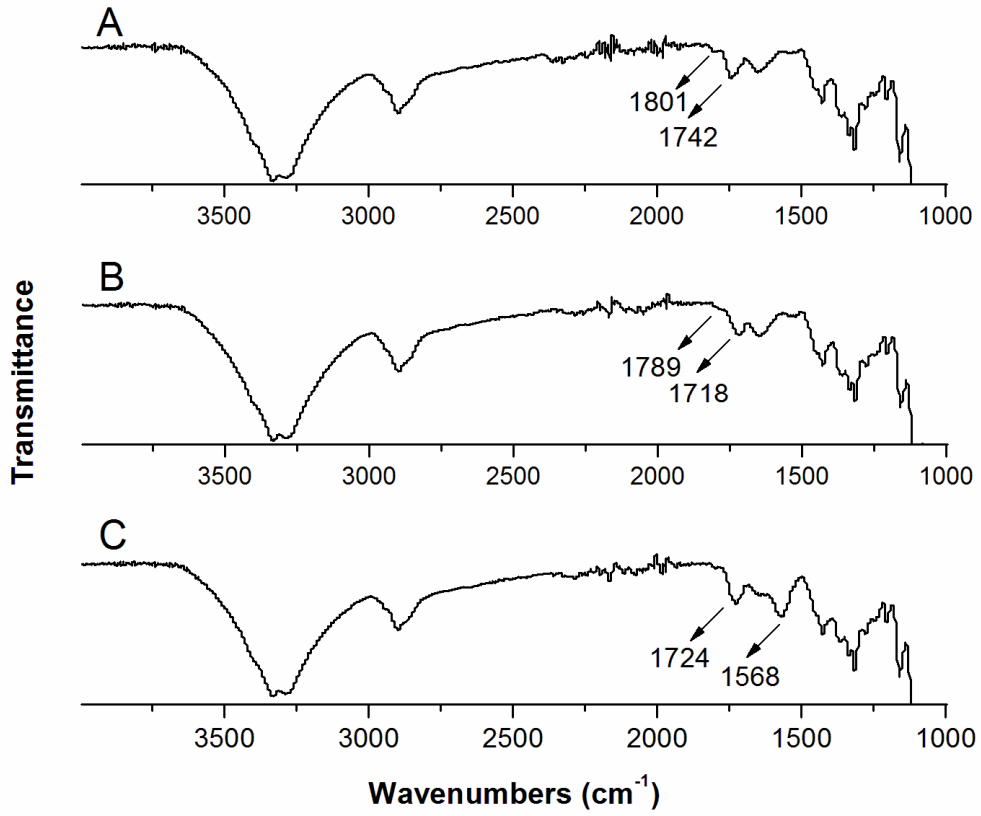

Figure 5. 8. FTIR Spectra of the coatings after chlorination A: HASL coated cotton fabric, B: HAGM coated cotton fabric, C: HAOH coated cotton fabric.

5.3.2. Washing Stabilities

Stabilities of the copolymer coated cotton fabrics against repeated laundering are summarized in Table 5.1. As expected, a progressive decline in the chlorine loadings of the coated fabrics was obtained when the number of washing cycles increased (X columns). However, the rate of the oxidative halogen loss depended on the copolymer types. It was reported in an earlier study that 0.05 wt % chlorine loading on cotton fabric was sufficient for an effective biocidal activity.[23] Therefore, HAGM and HAOH coated fabrics were still biocidal after the equivalent of 25 and 50 times of laundering, whereas the HASL coated fabric lost its antimicrobial functionality after 25 washing cycles. On the other hand, most of

the oxidative halogen could be restored upon rechlorination revealing that nitrogen-halogen bond breakage was responsible for most of the chlorine loss in the X columns. Moreover, the coatings were exceptionally durable on the surface for all of the copolymer coatings. There were minor differences between the durabilities of the different tetherings. The polymeric nature of the coatings, which allows multiple covalent bonding between the cellulose surface and the copolymer backbones could explain these remarkable washing durabilities.[24]

Table 5. 1. Stability toward washing of coatings on the cotton (Cl^+% remaining)[a].

	HASL			HAGM			HAOH		
MW	**X**	**Y**	**Z**	**X**	**Y**	**Z**	**C**	**Y**	**Z**
0	0.28			0.36			0.35		
5	0.08	0.28	0.27	0.18	0.34	0.33	0.15	0.32	0.32
10	0.06	0.28	0.26	0.14	0.32	0.32	0.14	0.32	0.31
25	0.03	0.26	0.24	0.11	0.31	0.30	0.11	0.31	0.30
50	0.00	0.24	0.23	0.10	0.29	0.29	0.06	0.31	0.29

X: Chlorinated before washing, Y: Chlorinated before washing and rechlorinated after washing, Z: Unchlorinated before washing, but chlorinated after washing, MW: Number of machine washing cycles [a] The error in the measured Cl^+ weight percentage values was ±0.01.

5.3.3. UVA Light Stabilities

UVA light stabilities of the coated cotton fabrics (chlorinated and unchlorinated) are summarized in Table 5.2. As can be seen, all of the chlorinated swatches lost most of their chlorine loading progressively upon one day of exposure to UVA light. However, the remaining chlorine on the fabrics would still provide an effective biocidal activity at the end of a one day exposure. Chlorinated swatches were rechlorinated at 24 h UVA light exposure intervals to analyze if the lost halogen can be regenerated repetitively. After the third rechlorination (72 h exposed), 32, 25, and 59 % of the initial chlorine could not be restored

for HASL, HAGM, and HAOH, respectively. On the other hand, when the unchlorinated swatches were halogenated after the UVA exposure, they exhibited chlorine loading close to the initial loading, revealing that when there is halogen on the surface, an irreversible decomposition takes place induced by UVA light exposure. HAGM copolymer was the least, and HAOH copolymer was the most prone of the structures to this degradation. The mechanism for the photolytic decomposition of N-halamines containing a siloxane moiety was reported in an earlier study, ie. that a halogen radical migration takes place which results in an alpha and/or beta scission causing partial loss of N-halamine moiety from the surface.[19] The same type of halogen transfer might be responsible for the decomposition obtained in these three polymeric coatings. However, further studies are needed to explain the exact mechanism responsible for the degradation observed in this study.

Table 5. 2. Stability toward UVA light exposure of coatings on the cotton (Cl^+% remaining)[a].

	HASL		**HAGM**		**HAOH**	
	C	**U**	**C**	**U**	**C**	**U**
Initial	0.28		0.32		0.32	
1	0.21		0.24		0.27	
2	0.19		0.21		0.24	
3	0.20		0.19		0.17	
6	0.14		0.16		0.16	
12	0.07		0.14		0.13	
24	0.05		0.11		0.10	
24-Re	**0.26**	**0.27**	**0.28**	**0.31**	**0.31**	**0.32**
48	0.06		0.08		0.08	
48-Re	**0.21**	**0.29**	**0.25**	**0.33**	**0.24**	**0.31**
72	0.03		0.09		0.06	
72-Re	**0.19**	**0.28**	**0.24**	**0.31**	**0.13**	**0.29**

[a] The error in the measured Cl^+ weight percentage values was ±0.01. Re: Rechlorination C: Chlorinated swatches U: Unchlorinated swatches

5.3.4. Biocidal Efficacies

The chlorinated and unchlorinated cotton swatches were challenged with about 6 log of *S. aureus* and *E. coli* O157:H7, and the test results are summarized in Table 5.3. As expected, the control samples which were not chlorinated did not provide significant bacteria reduction. It is well known that the limited reduction that the control samples exhibited was due to adhesion of the bacteria to the surface, rather than its inactivation.[15-18] On the other hand, all of the polymeric coatings exhibited complete inactivation of the Gram-positive bacteria within 2 min of contact time in the first experiment. Moreover, the HASL and HAOH coated swatches inactivated all of the Gram-negative bacteria within 2 min, whereas 5 min were needed for the complete inactivation for the HAGM coated fabric. The biocidal test was repeated with shorter contact times ranging from 1 to 5 min. In the repeated experiment, the HAGM coated fabrics inactivated about the same concentration of Gram-negative and Gram-positive bacteria within 1 min of contact time. This inconsistency is due to the difference in chlorine loadings of the HAGM coated fabrics used in two experiments. Even though the concentration of the HAGM copolymer applied onto the cotton fabric was the same, the actual copolymer on the surface was higher in the first experiment as evidenced by its higher weight gain and higher chlorine loadings. It was reported in an earlier study that increasing chlorine loading increases the hydrophobicity of the coatings which can result in poor contact with the microorganisms.[25] The lower amount of chlorine loadings on HAGM treated fabrics in the second experiment resulted in a more rapid biocidal activity against *S. aureus* and *E. coli* O157:H7. Similarly, the HAOH coated swatches exhibited complete inactivation of Gram-negative and Gram-positive bacteria (about 6 log) within 1 min of contact time. On the other hand, 2 min was necessary for the

same biocidal efficacies for the HASL coated fabrics. In general, all of the polymeric coatings studied in this work exhibited remarkable antimicrobial activity compared to other types of biocides.

Table 5. 3. Biocidal efficacies of the coated cotton fabrics.

Experiment 1[a]				Experiment 2[b]			
Sample	**Time (min)**	**Log Reduction**		**Sample**	**Time (min)**	**Log Reduction**	
		E.Coli O157:H7	***S. aureus***			***E.Coli O157:H7***	***S. aureus***
HASL	10	0.26	0.18	**HASL**	5	0.03	0.20
HAGM	10	0.09	0.27	**HAGM**	5	0.12	0.23
HAOH	10	0.12	0.17	**HAOH**	5	0.02	0.29
HASL	2	6.55	6.56	**HASL**	1	1.21	4.41
Cl^+ %	5	6.55	6.56	**Cl^+ %**	2	6.52	6.24
0.25	10	6.55	6.56	**0.25**	5	6.52	6.24
HAGM	2	3.61	6.56	**HAGM**	1	6.52	6.24
Cl^+ %	5	6.55	6.56	**Cl^+ %**	2	6.52	6.24
0.36	10	6.55	6.56	**0.26**	5	6.52	6.24
HAOH	2	6.55	6.56	**HAOH**	1	6.52	6.24
Cl^+ %	5	6.55	6.56	**Cl^+ %**	2	6.52	6.24
0.35	10	6.55	6.56	**0.28**	5	6.52	6.24

[a]:The inoculum concentrations were 6.55, and 6.56 logs for *E. coli,* and *S. aureus*, respectively. [b]:The inoculum concentrations were 6.52, and 6.24 logs for *E. coli,* and *S. aureus*, respectively.

5.4. Conclusions

Random copolymers of hydantoin acrylamide and a silane-, an epoxide-, and a hydroxyl group-containing monomer were synthesized, characterized, and coated onto cotton fabric through hydrolysis of alkoxy groups and formation of silyl ether bonding, opening of the epoxide ring and subsequent reaction with hydroxyl groups on cellulose, and crosslinking between the hydroxyl groups on the copolymer and on cellulose, respectively.

All of the coatings exhibited potent antimicrobial activity with inactivation of about 6 log of *S. aureus* and *E.* coli *O157:H7* within min contact time. In addition, the copolymeric coatings were remarkably stable against repeated launderings such that recharging after each wash should not be necessary. On the other hand, a photolytic decomposition induced by UVA light exposure was observed for all of the chlorinated coatings. However, the magnitude of this decomposition was lower compared to some of the previously studied N-halamine coatings. The epoxide group containing copolymer was least prone to this decomposition among the three copolymers studied in this work.

5.5. References

(1) Ducel, G.; Fabry, J.; Nicolle, L. *Prevention of hospital acquired infections: a practical guide*; 2 ed. Geneva, 2002.

(2) Borkow, G.; Gabbay, J. *Medical Hypotheses* **2008**, *70*, 990-994.

(3) Colak, S.; Tew, G. N. *Macromolecules* **2008**, *41*, 8436-8440.

(4) Nurdin, N.; Helary, G.; Sauvet, G. *Journal of Applied Polymer Science* **1993**, *50*, 663-670.

(5) Lin, J.; Qiu, S.; Lewis, K.; Klibanov, A. M. *Biotechnology and Bioengineering* **2003**, *83*, 168-172.

(6) Worley, S. D.; Williams, D. E. *CRC Critical Reviews in Environmental Control* **1988**, *18*, 133-175.

(7) Sun, G.; Xu, X. *Text Chem Color* **1998**, *30*, 26-30.

(8) Sun, Y.; Sun, G. *Journal of Polymer Science Part A: Polymer Chemistry* **2001**, *39*, 3348-3355.

(9) Liu, S.; Zhao, N.; Rudenja, S. *Macromolecular Chemistry and Physics* **2010**, *211*, 286-296.

(10) El-Shishtawy, R. M.; Asiri, A. M.; Abdelwahed, N. A. M.; Al-Otaibi, M. M. *Cellulose* **2011**, *18*, 75-82.

(11) Ikeda, T.; Yamaguchi, H.; Tazuke, S. *Antimicrobial Agents and Chemotherapy* **1984**, *26*, 139-144.

(12) Sun, G.; Wheatley, W. B.; Worley, S. D. *Industrial & Engineering Chemistry Research* **1994**, *33*, 168-170.

(13) Denyer, S. P. *International Biodeterioration & Biodegradation* **1995**, *36*, 227-245.

(14) Qian, L.; Sun, G. *Journal of Applied Polymer Science* **2004**, *91*, 2588-2593.

(15) Cerkez, I.; Kocer, H. B.; Worley, S. D.; Broughton, R. M.; Huang, T. S. *Langmuir* **2011**, *27*, 4091-4097.

(16) Lin, J.; Winkelman, C.; Worley, S. D.; Broughton, R. M.; Williams, J. F. *Journal of Applied Polymer Science* **2001**, *81*, 943-947.

(17) Ren, X.; Kocer, H. B.; Kou, L.; Worley, S. D.; Broughton, R. M.; Tzou, Y. M.; Huang, T. S. *Journal of Applied Polymer Science* **2008**, *109*, 2756-2761.

(18) Liang, J.; Owens, J. R.; Huang, T. S.; Worley, S. D. *Journal of Applied Polymer Science* **2006**, *101*, 3448-3454.

(19) Kocer, H. B.; Akdag, A.; Worley, S. D.; Acevedo, O.; Broughton, R. M.; Wu, Y. *ACS Applied Materials & Interfaces* **2010**, *2*, 2456-2464.

(20) Kocer, H. B.; Worley, S. D.; Broughton, R. M.; Huang, T. S. *Reactive and Functional Polymers* **2011**, *71*, 561-568.

(21) Mao, Y.; Gleason, K. K. *Langmuir* **2004**, *20*, 2484-2488.

(22) Sricharussin, W.; Ryo-Aree, W.; Intasen, W.; Poungraksakirt, S. *Textile Research Journal* **2004**, *74*, 475-480.

(23) Liang, J.; Wu, R.; Wang, J. W.; Barnes, K.; Worley, S. D.; Cho, U.; Lee, J.; Broughton, R. M.; Huang, T. S. *Journal of Industrial Microbiology and Biotechnology* **2007**, *34*, 157-163.

(24) Kocer, H. B.; Cerkez, I.; Worley, S. D.; Broughton, R. M.; Huang, T. S. *ACS Applied Materials & Interfaces* **2011**, *3*, 2845-2850.

(25) Ren, X.; Akdag, A.; Kocer, H. B.; Worley, S. D.; Broughton, R. M.; Huang, T. S. *Carbohydrate Polymers* **2009**, *78*, 220-226.

CHAPTER 6

N-HALAMINE BIOCIDAL COATINGS VIA A LAYER-BY-LAYER ASSEMBLY TECHNIQUE

6.1. Introduction

Antimicrobial coatings of medical textiles and devices have been studied extensively as a means to prevent healthcare related infections. N-halamines have been widely used as biocides due to their superior biocidal functions against a broad spectrum of microorganisms, such as Gram-negative and Gram-positive bacteria, fungi, yeasts and viruses.[1,2] Since they are contact biocides and contain oxidative halogen which can be directly transferred to the microbial cell membrane, inactivation of a microorganism takes place in a very short time without the release of free halogen into the system.[2] Moreover, they can be regenerated simply by aqueous chlorine exposure (see Figure 6.2 and 6.4). Work in these laboratories focused on novel biocidal N-halamine derivatives for water disinfection in the 1980's.[3] Later, polymeric N-halamines were reported for aqueous media disinfection as well as for antimicrobial treatment of textiles.[4,5] To date, several polymers and fibers including cellulose, nylon,[6] PET,[7,8] polyurethane,[9] polyacrylonitrile,[10, 11] and Kraton rubber™[12] were rendered biocidal upon N-halamine incorporation. Among them, cellulose has been studied extensively, and several N-Halamine moieties have been attached by grafting,[13 – 15] blending,[16] or coating.[17-19]

The layer-by-layer assembly (LbL) technique is a simple and powerful method used for functional thin film fabrications.[20] Multilayer thin films are created by consecutive

alternate deposition of positively and negatively charged (typically polymeric) species. The process involves alternatively soaking charged or polar substrates in dilute aqueous solution of ionic species, followed by rinsing, and drying steps at intervals, as shown in Figure 6.1.Each cationic and anionic layer pair is called a bilayer (BL); it has a thickness value that varies between 1-100 nm dependent upon pH, ionic strength, molecular weight, counterion, temperature, and chemistry.[21,22] In addition to electrostatic attractions, hydrogen bonding,[23] covalent bonding,[24] and charge transfer[25] have been utilized for thin layer deposition. Several functional thin films such as conductive,[21,23,26,27] antireflective,[28] low-oxygen permeable,[22] antimicrobial,[29-31] and flame retardant[32] have been created by using the LbL assembly technique.

Of particular relevance to the current work are the antimicrobial coatings created previously by the LbL surface deposition technique. Kotov and coworkers[31] showed that silver nanoparticles could be incorporated into a film by the LbL technique creating a surface active against *E. coli* bacteria with significant inhibition noted after 18 h of contact. Also, Grunlan, et. al.,[29,30] have created antimicrobial coatings by the LbL technique which contained biocidal quaternary ammonium functionalities which provided measureable zones of inhibition against *E. coli* and *S. aureus*. We have decided to explore the potential of the LbL deposition technique using N-halamine biocidal moieties, since these moieties have proven superior to other surface biocides for the reasons stated above.

To date, numerous N-halamines have been successfully coated onto cotton through covalent bonding; nevertheless, limitations of durability and stability of these coatings suggest that different techniques may be appropriate. Thus, in this study, N-halamine polyelectrolytes have been deposited onto cotton fabric via LbL assembly. Since bleached

cotton is inherently negatively charged as indicated by a negative zeta potential,[18] oppositely charged N-halamine copolymers were deposited without need of surface modification. To the best of our knowledge, this paper is the first study reporting antimicrobial functionally of N-halamine biocidal coatings utilizing the layer-by-layer assembly technique.

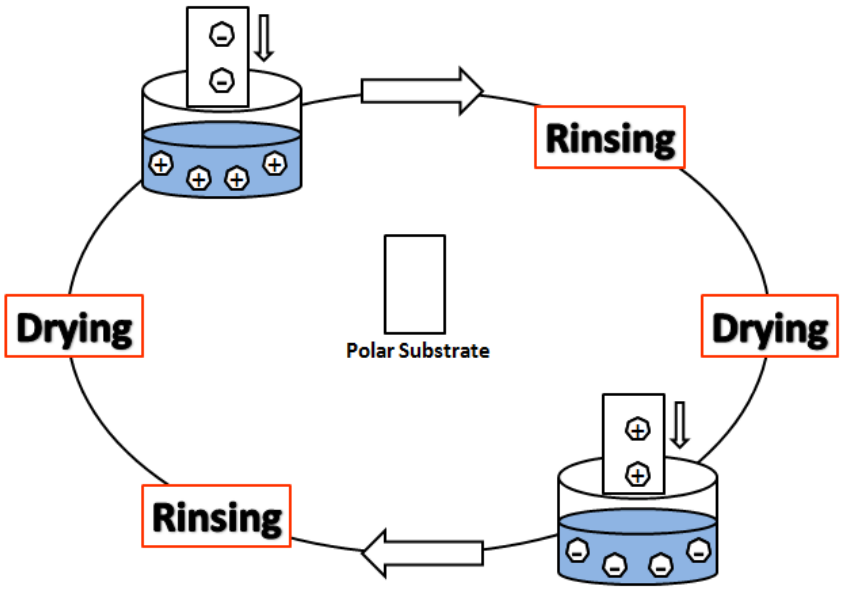

Figure 6. 1. LbL assembly process steps.

6.2. Experimental

6.2.1. Materials and Instrumentation

All starting chemicals and solvents were purchased from Aldrich Chemical Company (Milwaukee, WI) or TCI America (Boston, MA), and used as is unless otherwise noted. Desized, scoured, and bleached (100%) cotton (Style 400 Cotton Print Cloth) was obtained from Testfabrics. Inc. (West Pittson, PA). Chlorox® brand (Chlorox, Inc., Oakland, CA) household bleach was used for chlorination. Bacteria cultures of *Staphylococcus aureus* ATCC 6538 and *Escherichia coli* O157:H7 ATCC 43895 were purchased from American Type Culture Collection (Rockville, MD), and Trypticase soy

agar was obtained from Difco Laboratories (Detroit, MI). FTIR data were collected by a Nicolet 6700 spectrometer at 4 cm^{-1} resolution with 32 scans. ^{1}H NMR data were obtained with a Bruker 400 spectrometer. A Leica Ultracut T Ultramicrotome (Leica Microsystems, Inc., U.S.A.) and Zeiss EM10C Transmission Electron Microscope (Carl Zeiss SMT, Germany) were used for cross sectional imaging of polyelectrolytes deposited onto cotton fibers.

6.2.2. Synthesis of Poly(2, 2, 6, 6–tetramethyl–4-piperidyl-methacrylate–co-trimethyl-2-methacryloxyethylammonium chloride (PMPQ)

An equimolar (10 mmol) mixture of 2,2,6,6–tetramethyl–4-piperidyl methacrylate and trimethyl-2-methacryloxyethylammonium chloride was dissolved in 10 mL of ethanol (EtOH), and then 1 % by wt azobisisobutyronitrile (AIBN) was added into the solution, which was stirred until all of the ingredients were completely dissolved. N_2 was bubbled into the solution for 15 min. The polymerization reaction was carried out under nitrogen atmosphere at 90 °C for 2 h. EtOH was removed by evaporation, and then the structure of the copolymer was confirmed by FTIR and NMR characterization. As can be seen in Figure 6.3, the band for the double bond vibrational mode (1634 cm^{-1}) disappears in the copolymer spectra, indicating completed polymerization. NMR spectra are included in the supporting information.

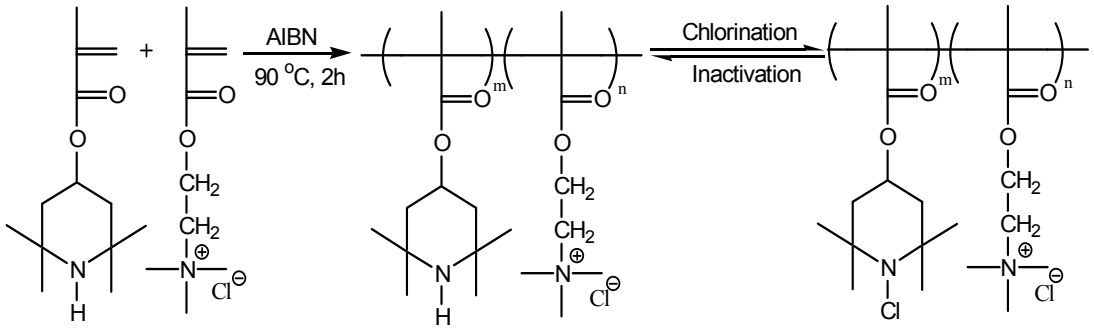

Figure 6. 2. Preparation of poly PMPQ.

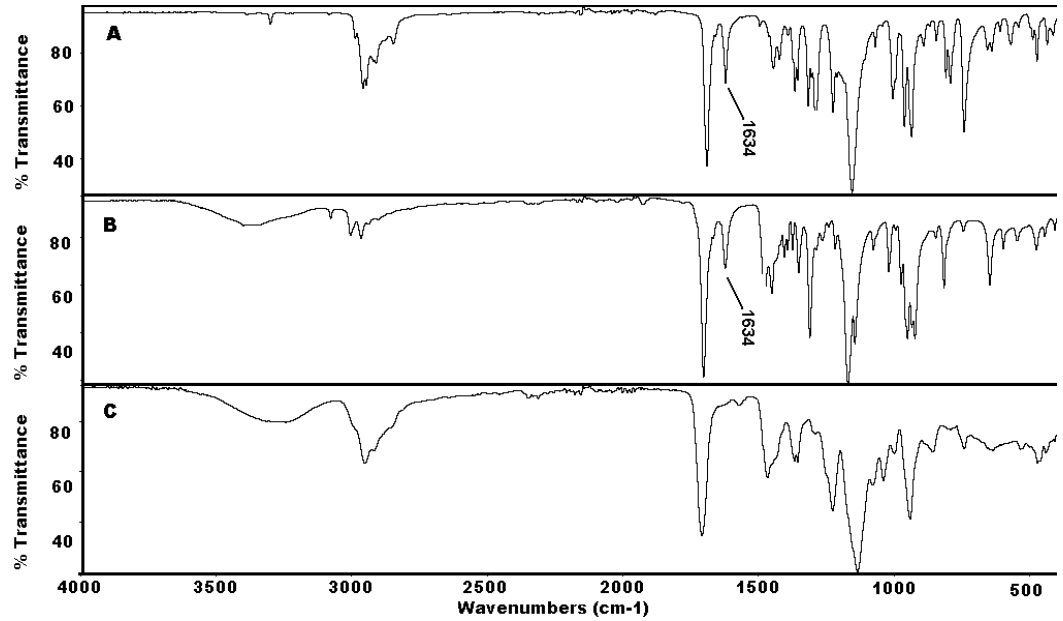

Figure 6. 3. FTIR spectra of (A) 2,2,6,6–tetramethyl–4-piperidyl methacrylate, (B) Trimethyl-2-methacryloxyethylammonium chloride, (C) PMPQ.

6.2.3. Synthesis of Poly(2, 2, 6, 6–tetramethyl-4-piperidyl methacrylate–co-acrylic acid potassium salt) (PMPA)

An equimolar mixture (10 mmol) of 2,2,6,6–tetramethyl–4-piperidyl methacrylate and acrylic acid was polymerized as described above. Once the polymerization was completed, 10 mmol KOH were added into the copolymer solution, and the mixture was refluxed for 10 min in order to produce the potassium salt of the copolymer. Subsequently,

the reaction vessel was cooled to room temperature, and EtOH was removed by evaporation. The copolymer structure was confirmed by FTIR and NMR. As it can be seen in Figure 6.5, the vinyl bond stretching band (1634 cm^{-1}) disappears in the copolymer spectra, and a new band around 1560 cm^{-1} appears as an indication the salt formation. NMR spectra are included in the supporting information.

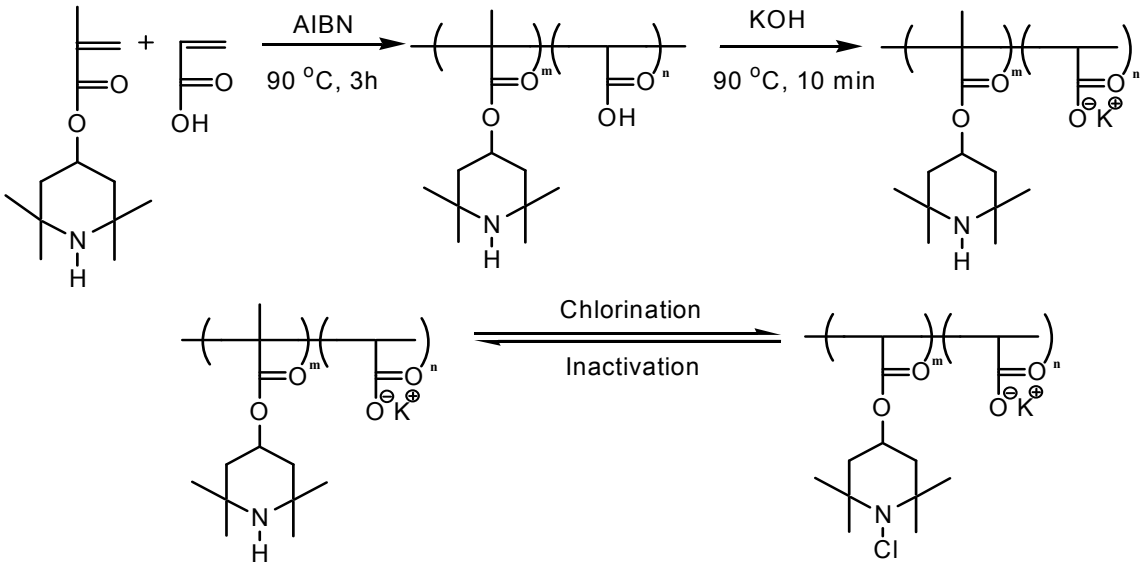

Figure 6. 4. Preparation of poly PMPA.

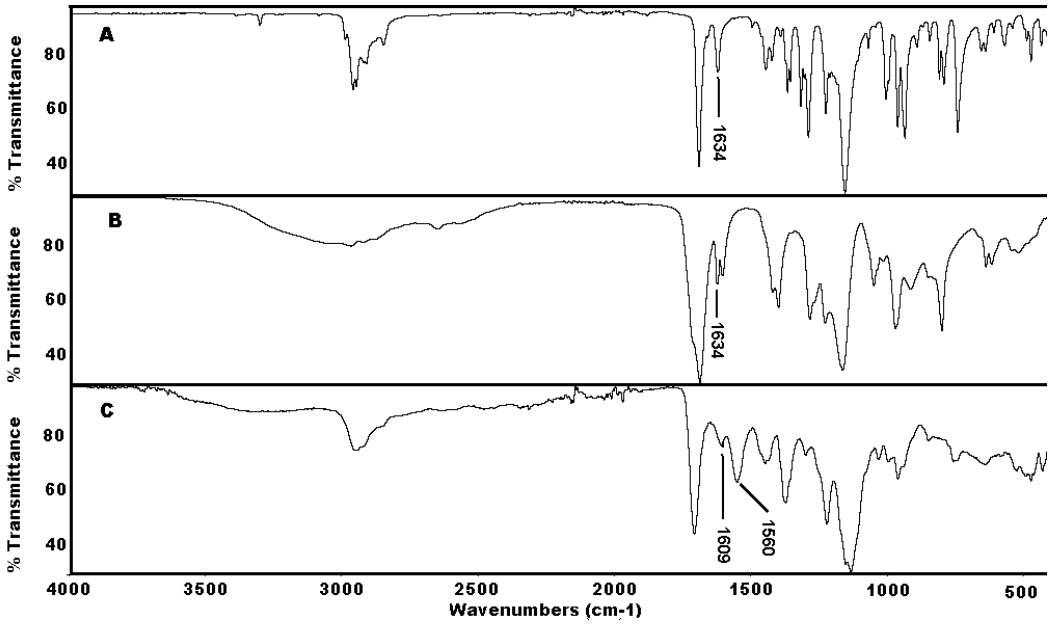

Figure 6. 5. FTIR spectra of (A) 2, 2, 6, 6–tetramethyl–4-piperidyl methacrylate, (B) Acrylic acid, (C) PMPA.

6.2.4. Layer-by-Layer Deposition onto Cotton

Cationic and anionic dilute copolymer solutions were prepared by dissolving 0.2 % by wt PMPQ and PMPA in water in separate glass containers, and for a second set of experiments, in ethanol. Bleached cotton swatches were alternatively dipped into these solutions starting with the cationic solution, since the cotton surface is negatively charged. The first dip lasted for 5 min to ensure reasonable attraction with the substrate, and subsequent dips lasted for 1 min. After each dipping, the samples were dried at 100 °C for 5 and 2 min to remove the solvent water or ethanol, respectively. Between the dipping and drying steps, the swatches were rinsed with deionized water for 30 sec in order to remove loosely attached polyelectrolytes. After the desired number of bilayers was reached, the samples were stored at 100 °C for 12 h, and then washed vigorously with 0.5 % by wt detergent water for 15 min followed by rinsing with distilled water before chlorination.

6.2.5. Chlorination and Analytical Titration

Coated samples were chlorinated with a 10 % aqueous solution of household bleach (0.6 % by wt Cl^+) at pH 7 (also pH 8.2 and pH 11 were employed in other experiments with no significant differences) for 1 h and then rinsed with distilled water. The cotton swatches were dried at 45 °C for 1 h to remove any free chlorine from the surfaces. In order to determine the oxidative Cl^+% content on the cotton, a modified iodometric/thiosulfate titration was conducted.[17] In this procedure a mixture of 90 mL of ethanol and 10 mL of 0.1 N acetic acid was used as a solvent. The weight percentage of chlorine was calculated according to Equation 1.

$$Cl^+\% = [(N \times V \times 35.45) / (2 \times W)] \times 100 \quad (1)$$

In this equation Cl^+% is the weight percent of oxidative chlorine on the samples, N and V are the normality (equiv/L) and volume (L) of the $Na_2S_2O_3$ (titration solvent), respectively, and W is the weight of the cotton sample in g.

6.2.6. Transmission Electron Microscopy (TEM)

Individual fibers were removed from the coated fabric and embedded into epoxy resin. The resin was incubated at 70 °C for 24 h. Ultrathin cross sections were cut with a diamond knife and then subjected to image analysis.

6.2.7. UVA Light Stability Test

An Accelerated Weathering Tester (The Q-panel Company, USA) was used to evaluate UVA light stability of the coatings. Chlorinated and unchlorinated cotton swatches containing 50 BL's were exposed to UVA light (Type A, 315 – 400 nm) for times in the

range of 1-24 h. After a certain time of irradiation, one set of chlorinated samples was titrated to assess chlorine loss by UVA exposure, and the other set was rechlorinated and then titrated in order to address any decomposition in the structure. Additionally, unchlorinated samples exposed to UVA were chlorinated, and then titrated in order to assess the photolytic stability of the unchlorinated coatings.

6.2.8. Washing Stability Test

Durabilities of the coatings and stabilities of the chlorine toward repeated washing cycles were evaluated by using the standard test method AATCC 61-1996. In this method, 2.54 X 5.08 cm cotton swatches containing 15 BL's were subjected to repeated laundry washings inside stainless steel canisters containing 50 stainless steel balls with 150 mL of 0.15 % AATCC detergent water solution. Rotation of 45 min of a Lauder-Ometer at 42 rpm and 49 °C is considered to 5 machine washings, and each swatch was washed the equivalent of 5, 15, 25, and 50 machine washing cycles. After washing, samples were rinsed with distilled water three times and allowed to dry at ambient temperature for 24 h. In order to evaluate the stability of chlorine toward washing, one set of the samples was chlorinated before washing. To address the durability of unchlorinated and chlorinated coatings as a function of washing cycles, a second set of the samples was chlorinated both before and after the washings, and a third set was chlorinated only after the washings.

6.2.9. Biocidal Efficacy Test

A modified AATCC "sandwich test", where chlorinated and unchlorinated (control sample) swatches containing 15 BL's were challenged with *Staphylococcus aureus* (ATCC

6538) and *Escherichia coli* O157:H7 (ATCC 43895), was conducted. Bacteria were suspended in pH 7, 100 μM phosphate buffer to produce a suspension of known population (colony forming units, CFU). Then, 25 μL of this suspension were placed in the center of a 2.54 cm square swatch and covered by a second identical swatch which was held in place by a sterile weight to ensure good contact with the bacteria. After a certain time of contact, samples were quenched with 5.0 mL of sterile 0.02 N sodium thiosulfate solution to neutralize the chlorine, and vortexed for 2 min in order to remove bacteria from the surfaces. Serial dilutions were made using pH 7, 100 μM phosphate buffer and plated on Trypticase soy agar plates. The plates were incubated at 37 °C for 24 h and then counted for viable CFU of bacteria for the biocidal efficacy analysis.

6.3. Results and Discussion

6.3.1. Characterization of the Coating on Cotton

FTIR spectroscopy was used to confirm the presence of the coating on the cotton fabric. Figure 6.6. shows the spectra for coated and uncoated cotton at different numbers of bilayers (BL's). Note that the coated cotton has an additional band at 1722 cm^{-1} corresponding to the ester carbonyl stretching mode of the copolymers. Moreover, this new band intensifies as the number of bilayers increases (B to D), verifying that the thin layer deposition was occurring on the cotton.

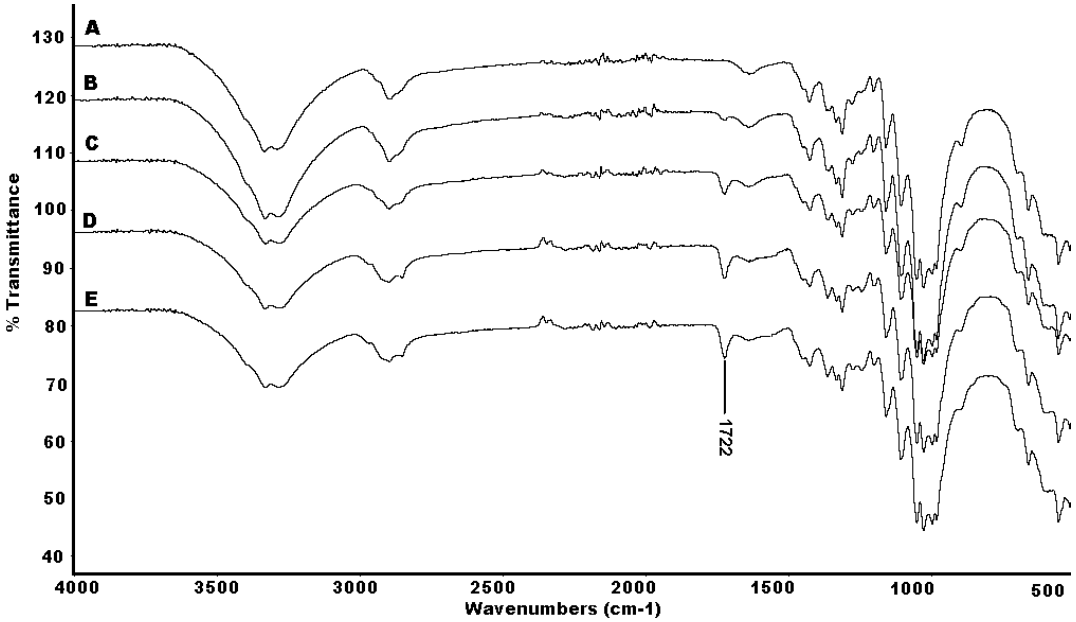

Figure 6. 6. FTIR spectra of (A) cotton, (B) 10 BL coated cotton, (C) 30 BL coated cotton, (D) 50 BL coated cotton, (E) 50 BL coated cotton and chlorinated.

Additionally, chlorine loadings with respect to number of BL's were measured (Figure 6.7). Chlorine loadings increased linearly with increasing numbers of BL's deposited. The solvent used to dissolve the ionic copolymers had an effect on the magnitude of this increment. Even though the concentration of the copolymers was the same, the increase in chlorine loading (polymer deposited) was greater in solvent water as compared to EtOH. The amount of copolymers on the cotton was determined by measuring the weight gain at standard lab conditions (65 % RH and 25 ^{o}C). After a 30 BL coating, 2.5 % and 3.5 % weight gains were observed for deposition from EtOH and water, respectively. It has been previously reported in a LbL study that when the solvent was an EtOH/water mixture, that the thickness of the polyelectrolyte thin film was less than that for pure water.[33] Therefore, it is believed that the thicker layers obtained by using water as a solvent are related to solvent polarity, or perhaps surface tension. Since fewer BL's were required to reach an equivalent

Cl^+ content, water was used as a solvent to coat samples for biocidal efficacy and UVA light and washing stability tests.

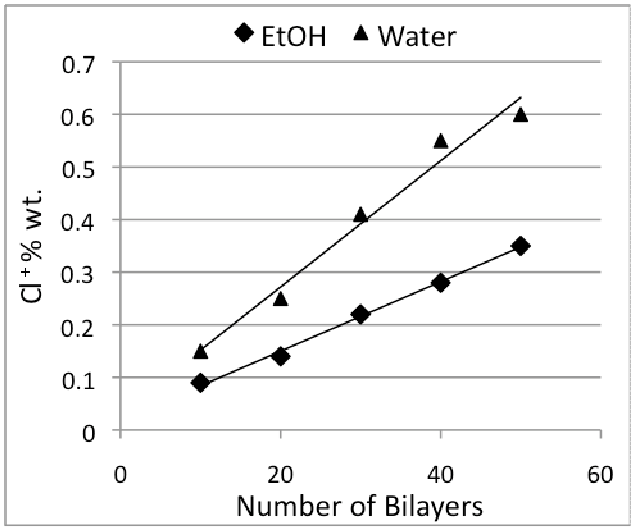

Figure 6. 7. Effect of number of bilayer on chlorine loading.

Figure 6.8 shows a TEM image of coated cotton yarns. Coating can be seen around the fiber as a white uniform line at the edges. The line is lighter than cotton since it has less electron density than the fiber. The thickness of the coating is approximately 150 nm for 50 BL's, corresponding to about 3 nm for each BL.

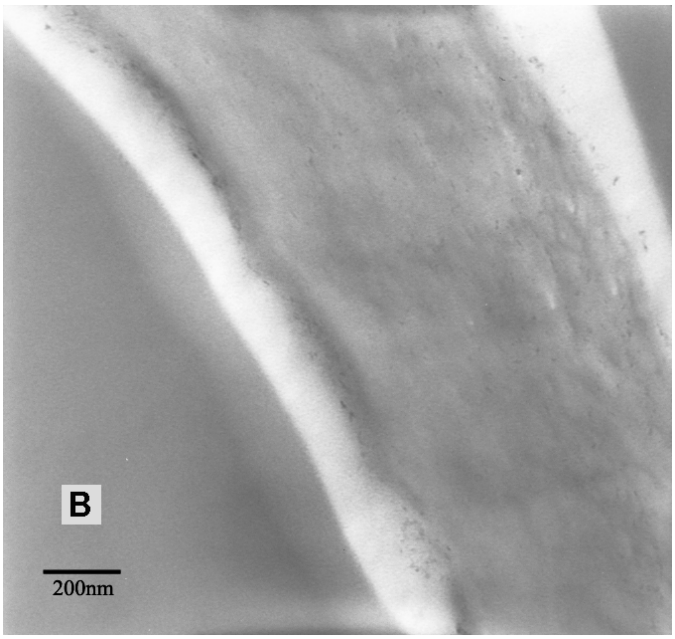

Figure 6. 8. TEM micrographs of 50 BL coated cotton.

6.3.2. Stability of the Coating toward Ultraviolet Light Irradiation

Table 6.1 shows the UVA light stability of the coatings on cotton fabric. After 3 h of accelerated UVA exposure, around half of the oxidative chlorine was lost, and most of it had disappeared after 12 h, indicating a progressive dissociation of the N-Cl bond upon UVA exposure. However, there was 0.04 Cl^{+}% remaining at the end of the 24 h exposure signifying that the coating would still provide an antimicrobial property.[17]

Table 6. 1. Stability of coatings toward UVA exposure (Remaining Cl^+ % by wt)[a].

Exposure Time (h)	Chlorinated	Unchlorinated[b]
0	0.60	
0.5	0.50	0.59
1	0.44	
2	0.31	
3	0.28	0.58
6	0.10	
12	0.08	
24	0.04	0.59
Rechlorination	0.48	

[a] Errors are estimated to be ± 0.01
[b] Chlorinated after UV exposure

When a 24 h UVA-exposed sample was treated with aqueous bleach solution, 80 % of the initial chlorine loading could be restored. These results suggest that the oxidative chlorine loss was due not only to N-Cl bond dissociation, but also to some decomposition of the coating. On the other hand, unchlorinated samples showed almost no decomposition because 98 % of the expected chlorine loading could be obtained after 24 h of UVA irradiation. This observation led to the conclusion that the presence of chlorine bonded to nitrogen increased the decomposition that occurred upon UVA exposure, as observed in a previous study.[34] The mechanism for this decomposition is under study.

6.3.3. Stability and Durability of the Coating toward Washing

Durability of the coating and stability of oxidative chlorine were evaluated using the standard washing test previously described. The results are summarized in Table 6.2. In this table the X column represents the pre-chlorinated samples for stability assessment of oxidative chlorine; the Y column shows pre- and post-chlorinated samples for durability

evaluation of the coating, and the Z column represents post-chlorinated samples after a specified number of washing cycles in order to address the pre-chlorination effect on durability of the coatings. Hydrolysis of the N-Cl bond with increased number of washing cycles resulted in a loss of oxidative chlorine. However, even after an equivalent of 50 machine washings, this loss was only 27 % (X column) which is much less than for previously reported studies involving *N*-halamine biocides coated onto cotton through covalent binding.[2,18,19,35] Moreover, upon rechlorination, 86 % (Y column) of the chlorine was restored after the 10 washing cycles (equivalent to 50 machine washes) showing an excellent durability. Durability of the coating was better for the chlorinated samples than for the unchlorinated ones (Z) presumably because pre-chlorination makes the surface more hydrophobic, thus reducing the coating loss during laundering.[7,8] All of the samples would still be antimicrobial after 50 machine washings since they all still had more than 0.05 Cl^+ % remaining.[35,36] Therefore, depending on exposure to microbial and chemical challenges, bleach might not be necessarily required in each washing cycle.

Table 6. 2. Stability of coatings toward washing (Remaining Cl^+ % by wt)[a].

Number of Washing cycles [b]	X	Y	Z
0	0.22		
1	0.21	0.22	0.19
3	0.20	0.22	0.19
5	0.19	0.20	0.18
10	0.16	0.19	0.18

[a] Errors are estimated to be ± 0.01.
[b] A washing cycle is equivalent to five machine washings in AATCC Test Method 61.
X: Chlorinated before washing. Y: Chlorinated before washing and rechlorinated after washing. Z: Unchlorinated before washing, but chlorinated after washing.

6.3.4. Biocidal Efficacy Test

Chlorinated and unchlorinated cotton swatches treated with N-halamine polyelectrolytes were challenged with *S. aureus* and *E. coli* O157:H7 at a concentration of 9.33×10^6 and 1.40×10^7 CFU, respectively. The results are summarized in Table 6.3. It was observed that chlorinated swatches provided complete inactivation of *S. aureus* within 15 min of contact time. However, the unchlorinated control sample showed only a 0.73 log reduction even after 60 min contact time. Adhesion of the bacteria to the fiber surface was responsible for this small degree of reduction experienced by the control sample. A similar result was obtained for *E. coli* O157:H7. Control samples exhibited a limited degree of bacterial reduction, whereas the chlorinated swatches provided 4.2 log (99.99 %) and 7.1 log (100 %) reduction within 5 and 15 min contact times, respectively. These results suggest that oxidative chlorine could diffuse from inner BL's to the surface BL where it contacts the bacterial cells. Furthermore, 0.21 Cl^+% obtained by treatment from water solvent, corresponding to 15 BL's, was shown to have effective biocidal activity. Extensive prior work in these laboratories has indicated that comparable biocidal efficacies for N-chloramine coatings in general occur for Cl^+ loadings on cotton near 0.2 % by wt. Since an equivalent Cl^+ content could be obtained with EtOH by 30 BL deposition, we expect that LbL treatment to be equally effective.

Table 6. 3. Biocidal test results of N-halamine coated cotton via LbL assembly.

Samples	Contact Time (min)	Bacterial Reduction (Log)	
		S. aureus [a]	*E. coli* [b]
Control	60	0.73	0.04
Coated cotton 0.21 wt% Cl^+	5	3.94	4.21
	15	6.97	7.15
	30	6.97	7.15
	60	6.97	7.15

[a] Inoculum population was 9.33×10^6 CFU.
[b] Inoculum population was 1.40×10^7 CFU.

6.4. Conclusions

Ionic N-halamine precursor copolymers were synthesized and successfully coated onto cotton via the layer-by-layer assembly technique. The coatings were rendered biocidal upon exposure to dilute household bleach. A linear increase in chlorine loading was obtained with increasing number of bilayers. Chlorinated samples exhibited effective biocidal activity against S. *aureus* and E. *coli* O157:H7 in relatively short contact times. Within 15 min, all Gram positive and Gram negative bacteria were inactivated by the chlorinated samples; whereas, unchlorinated control samples did not demonstrate significant bacterial reductions. Only 15 BL's was sufficient for effective biocidal activity. Results from washing testing revealed excellent stability and durability of the coatings during laundering. Even after an equivalent of 50 machine washings, only 27 % oxidative chlorine loss was observed, and 86 % of the lost chlorine could be restored upon rechlorination. Moreover, even though slight decomposition took place during UVA exposure, the

magnitude of decomposition was not as substantial as for previously reported N-halamine coatings. Further studies will be needed to explain the mechanism of this decomposition.

This study revealed that highly effective N-halamine biocidal coatings can be prepared via the layer-by-layer assembly technique. In this study ionic copolymers of 2, 2, 6, 6–tetramethyl–4-piperidyl methacrylate were used as N-halamine precursors, but the work could be extended to other N-halamine precursors. Since the charged copolymers are very soluble in water, coating via the LbL technique may have industrial potential for antimicrobial functional or multifunctional coating of textiles.

6.5. References

(1) Sun, G.; Wheatley, W. B.; Worley, S. D. *Ind. Eng. Chem. Res.* **1994***, 33,* 168-170.

(2) Barnes, K.; Liang, J.; Wu, R.; Worley, S. D.; Lee, J.; Broughton, R. M.; Huang, T. S. *Biomaterials* **2006**, *27*, 4825-4830.

(3) Worley, S. D.; Williams, D. E. *CRC Crit. Rev. Environ. Ctrl.* **1988**, *18*, 133-175 and references therein.

(4) Eknoian, M. W.; Putman, J. H.; Worley S. D. *Ind. Eng. Chem. Res.* **1998**, *37*, 2873-2877.

(5) Worley, S. D.; Sun, G. *Trends Polym. Sci.* **1996***, 4*, 364-370 and references therein.

(6) Lin, J.; Winkelmann, C.; Worley S. D.; Broughton, R. M.; Williams, J. F. *J. Appl. Polym. Sci.* **2001**, *81*, 943–947.

(7) Lin. J.; Winkelmann, C.; Worley, S. D.; Kim, J.; Wei, C. I.; Cho, U.; Broughton, R. M.; Santiago, J. I.; Williams, J. F. *J. Appl. Polym. Sci.* **2002**, *85*, 177–182.

(8) Ren, X.; Kocer, H. B.; Kou, L.; Worley, S. D.; Broughton, R. M.; Tzou, Y. M.; Huang, T. S. *J. Appl. Polym. Sci.* **2008**, *109*, 2756–2761.

(9) Worley, S. D.; Li, F.; Wu, R.; Kim, J.; Wei, C. I.; Williams, J. F.; Owens, J. R.;Wander, J. D.; Bargmeyer, A. M.; Shirtliff, M. E. *Surf. Coat. Int. Part B: Coat. Trans.* **2003**, *86*, 273-277.

(10) Lee, J. Broughton, R. M.; Liang, J.; Worley, S. D.; Huang, T. S. *Res. J. Text. Apparel* **2006**, *10*, 61–65.

(11) Ren, X.; Akdag, A.; Zhu, C.; Kou, L.; Worley, S. D.; Huang, T. S. J. *Bio. Mat.*

Res. Part A, **2009**, *91*, 385-90.

(12) Elrod, D. B.; Figlar, J. G.; Worley, S. D.; Broughton, R. M.; Bickert, J. R.; Santiago, J. I.; Williams, J. F. *Rub. Chem. Tech.* **2001***, 74*, 331–337.

(13) Sun, Y.; Sun, G. *J. Appl. Polym. Sci*. **2003**, *88*, 1032–1039.

(14) Luo, J.; Sun., Y. *J. Polym. Sci.: Part A: Polym. Chem.* **2006**, *44*, 3588-3600.

(15) Liu, S.; Sun, G. *Carbohydrate Polym.* **2008**, *71*, 614-625

(16) Lee, J.; Broughton, R. M.; Worley, S. D.; Huang, T. S. *J. Eng. Fib. Fab.* **2007**,*2*, 25-32.

(17) Liang, J.; Chen, Y.; Ren, X.; Wu, R.; Barnes, K.; Worley, S. D.; Broughton, R. M.; Cho, U.; Kocer H.; Huang, T. S. *Ind. Eng. Chem. Res.* **2007**, *46*, 6425- 6429.

(18) Ren X.; Kou, L.; Kocer, H, B.; Zhu, C.; Worley, S. D.; Broughton, R. M.; Huang, T. S.; *Coll. Surf. A: Physicochem. Eng. Asp.* **2008**, *317* , 711–716.

(19) Kou, L.; Liang, J.; Ren, X.; Kocer, H. B.; Worley, S. D.; Tzou, Y. M.; Huang, T. S. *Ind. Eng. Chem. Res.* **2009**, *48*, 6521-6526.

(20) Decher, G., Hong, D. J.; Schmitt, J. *Thin Solid Films* **1992**, *210/211(2)*, 831 835.

(21) Dawidczyk, T. J.; Walton M. D.; Jang, W. S; Grunlan, J. C. *Langmuir* **2008**, *24*, 8314-8318.

(22) Jang, W. S.; Rawson, I.; Grunlan, J. C. *Thin Solid Films* **2008**, *516*, 4819-4825.

(23) Stockton, W. B.; Rubner, M, F. *Macromol.* **1997**, *30*, 2717–2725.

(24) Seo, J.; Schattling, P.; Lang, T.; Jochum, F.; Nilles, K.; Theato, P.; Char, K. *Langmuir* **2010**, *26*, 1830–1836.

(25) Shimazaki, Y.; Mitsuishi, M.; Ito, S.; Yamamoto, M. *Langmuir* **1997**, *13*, 1385-1387.

(26) Etika, K. C.;Liu, L.; Hess, L. A.; Grunlan, J. C. *Carbon.* **2009**, *47,* 3128-3136.

(27) Lee, S. W.; Kim, B.; Chen, S.; Horn, Y. S.; Hammond, P. T. *J. Am. Chem. Soc*. **2009**, *131*, 671–679.

(28) Hiller. J.A; Mendelsohn, J. D.; Rubner, M. F. *Nature Mater.* **2002**, *1*, 59–63.

(29) Grunlan, J. C.; Choi, J. K.; Lin A. *Biomacromol.* **2005**, *6*, 1149-1153.

(30) Dvoracek, C. M.; Sukhonosova, G.; Benedik, M. J.; Grunlan, J. C. *Langmuir* **2009**, *25*, 10322-10328.

(31) Podsiadlo, P.; Paternel, S.; Rouillard, J. M.; Zhang, Z. F.; Lee, J.; Lee, J. W.; Gulari, E.; Kotov, N. A. *Langmuir* **2005,** *21,* 11915-11921

(32) Li, Y. C.; Schulz, J.; Grunlan, J. C. ACS *Appd. Mat. and Interf.* **2009**, *1*, 2338-2347.

(33) Seo, J.; Lutkenhaus, L. J.; Kim, J.; Hammond, T. P.; Char, K. *Macromolecules* **2007**, *40*, 4028-4036.

(34) Kocer, H. B.; Akdag, A.; Worley, S. D.; Acevedo, O.; Broughton, R. M.; Wu, Y. *Appl. Mat. & Interf.* **2010**, *2*, 2456–2464.

(35) Liang, J.; Wu, R.; Wang, J. W.; Barnes, K.; Worley, S. D.; Cho, U.; Lee, J.; Broughton, R. M.; Huang, T. S. *J. Ind. Microbiol. Biotechnol.* **2007**, *34*, 157–163.

(36) Kocer, H., B.; Akdag, A.; Ren, X.; Broughton, R. M.; Worley, S. D.; Huang, T. S. *Ind. Eng. Chem. Res.* **2008**, *47*, 7558-7563.

6.6. Supporting Information

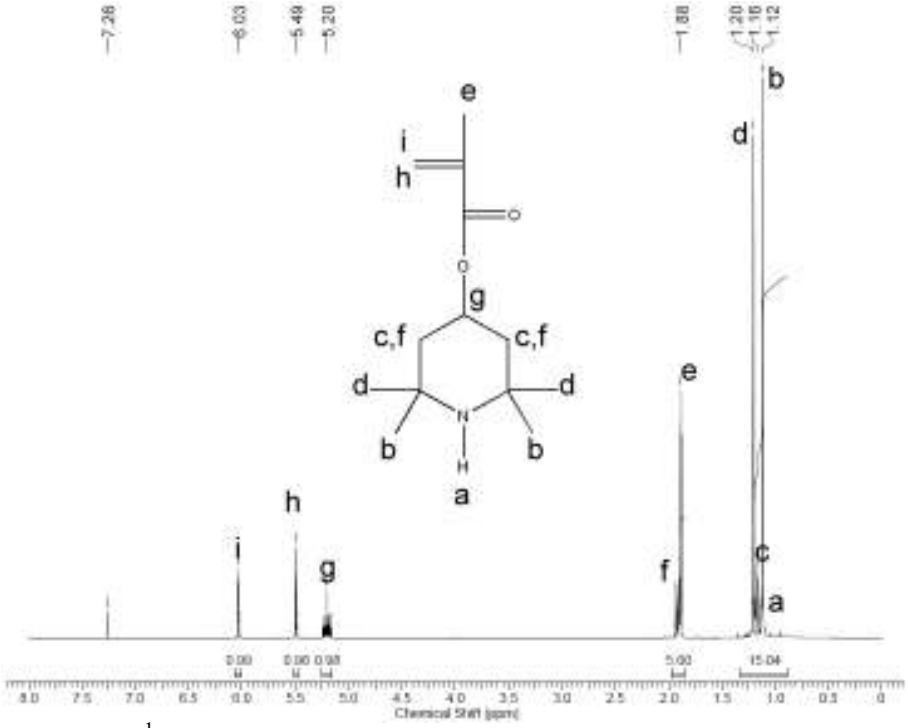

Figure Sp.6. 1. ^{1}H NMR spectra of 2,2,6,6-tetramethyl-4-piperidyl methacrylate (solvent:$CDCl_3$).

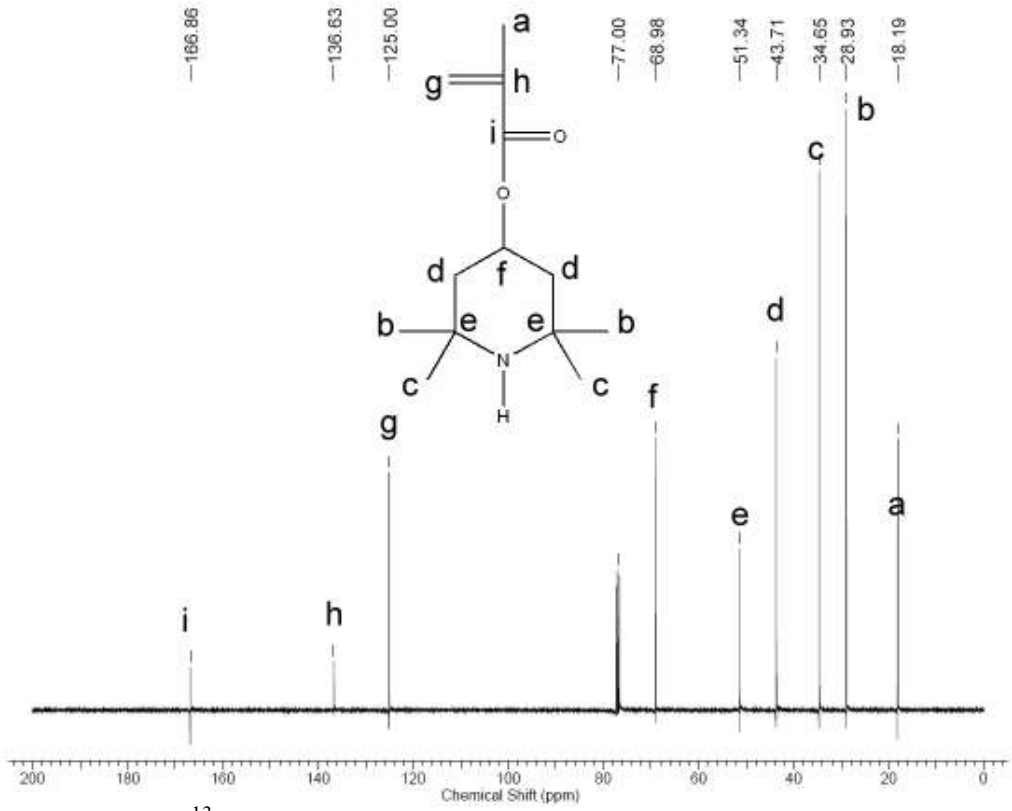

Figure Sp.6. 2. ^{13}C NMR spectra of 2,2,6,6-tetramethyl-4-piperidyl methacrylate (solvent:$CDCl_3$).

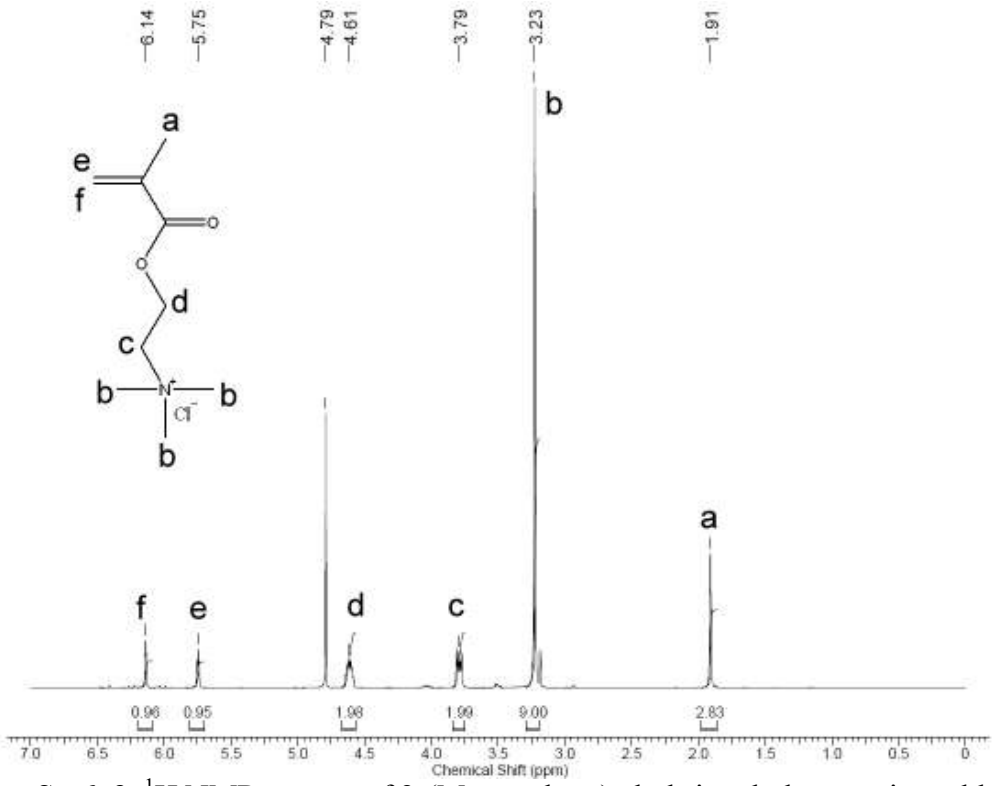

Figure Sp.6. 3. ^{1}H NMR spectra of 2-(Metacryloxy)ethyltrimethylammonium chloride (solvent: D_2O).

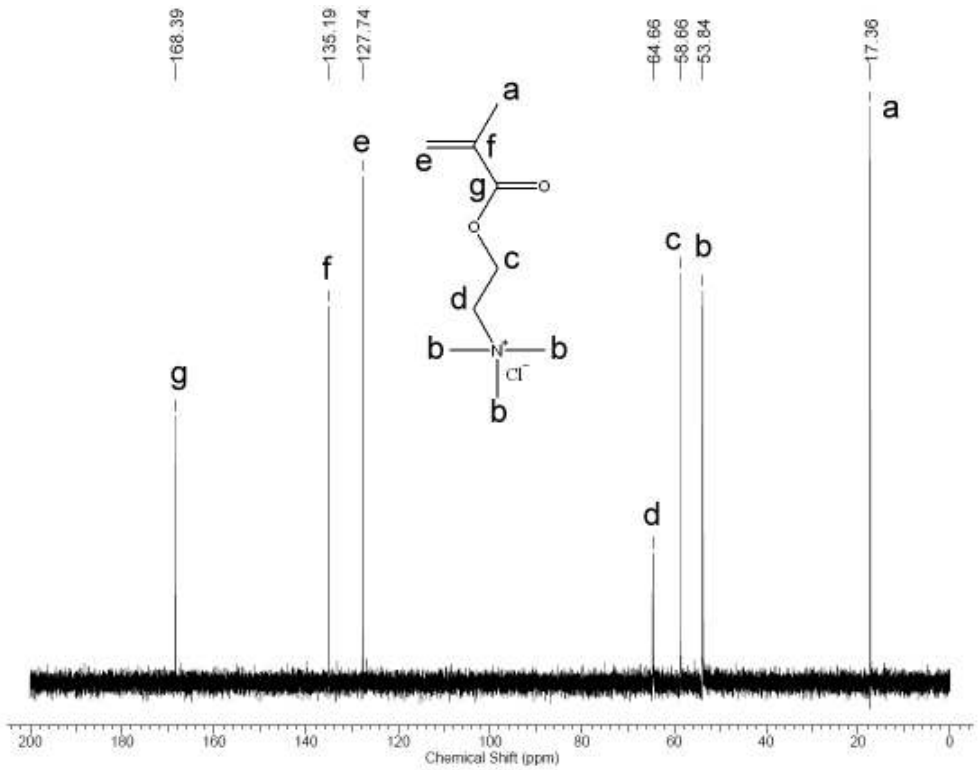

Figure Sp.6. 4. ^{13}C NMR spectra of 2-(Metacryloxy)ethyltrimethylammonium chloride (solvent: D_2O).

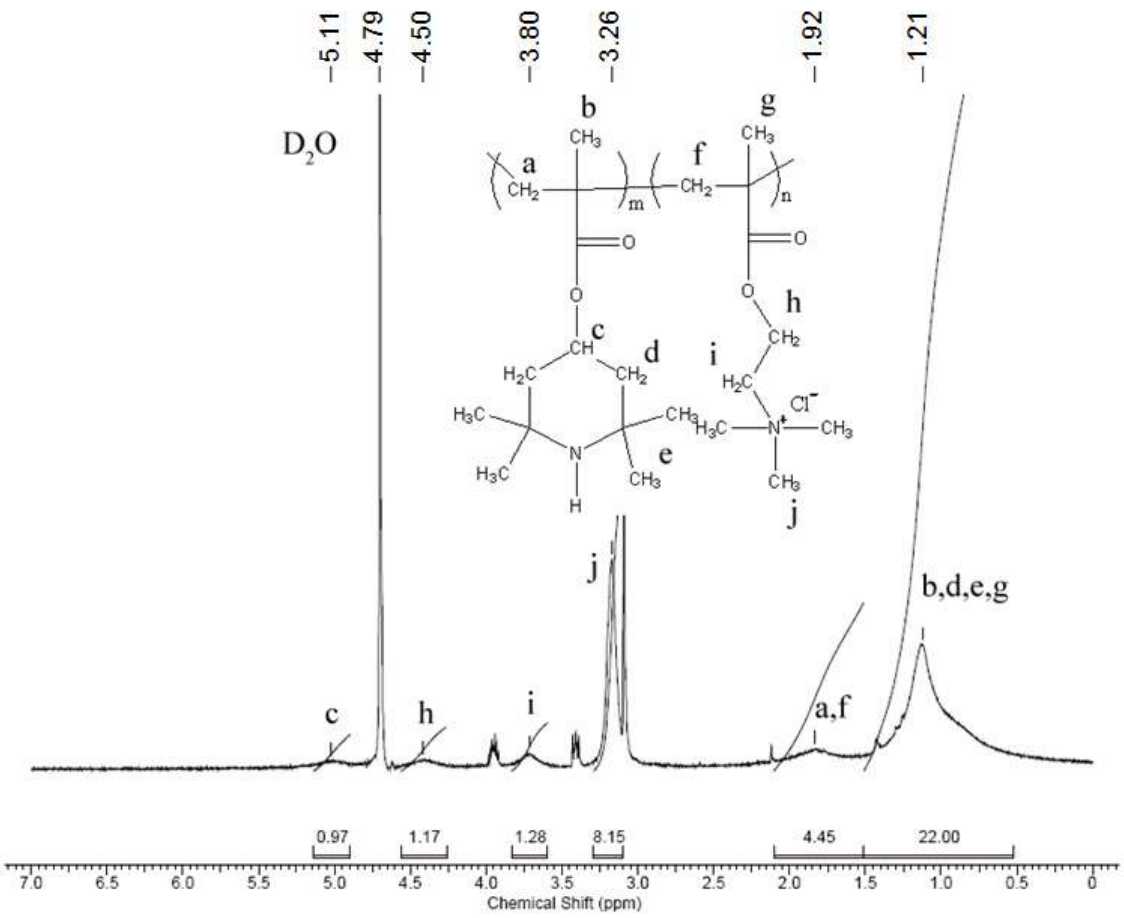

Figure Sp.6. 5. ^{13}C NMR spectra of PMPQ (solvent: D_2O).

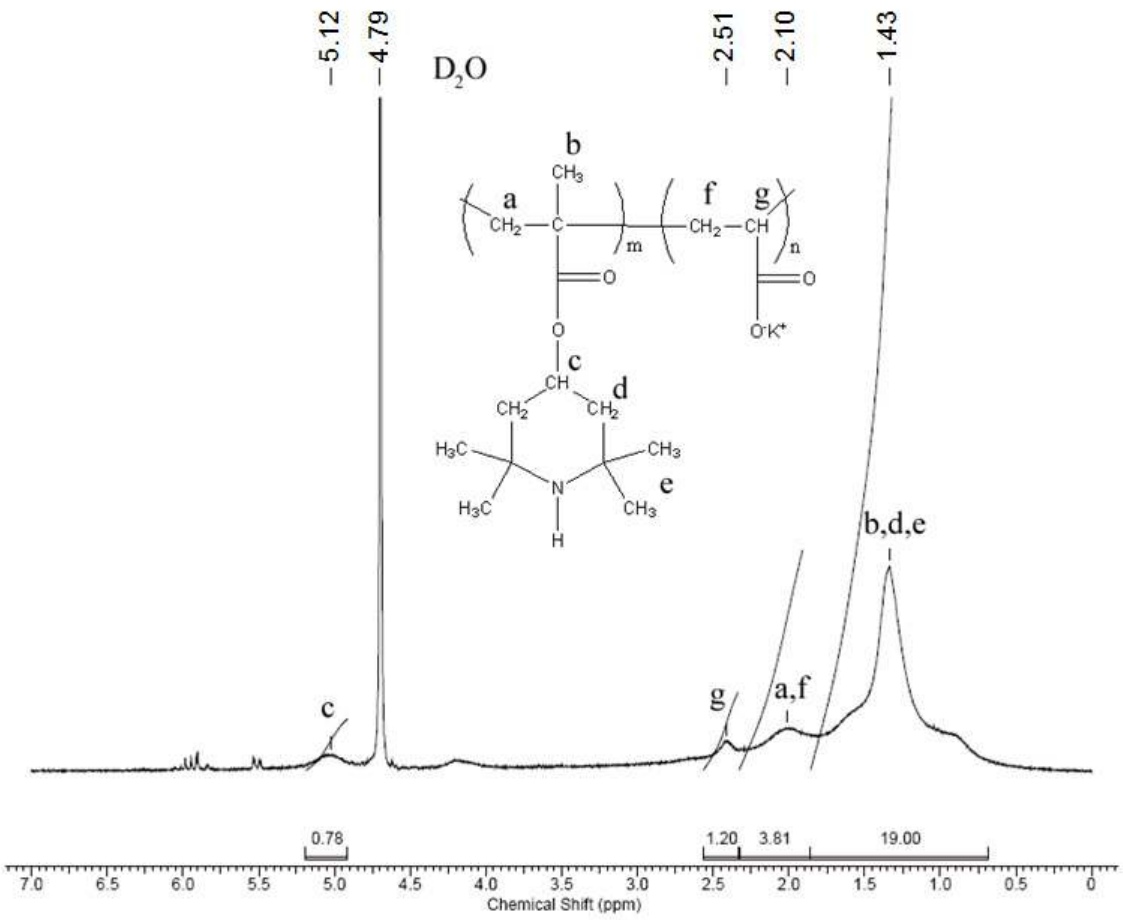

Figure Sp.6. 6. ^{13}C NMR spectra of PMPA (solvent: D_2O).

CHAPTER 7

CONCLUSIONS

In summary, five different approaches were utilized to improve the washing and UVA light stabilities of N-halamine biocidal coatings. Increasing crosslinking improved the washing and UVA light stabilities substantially, since the crosslinking agent shielded the N-halamine precursor from the mechanical effects of washings and UV photons. Therefore, crosslinking can be used as a tool to enhance the stabilities of N-halamine coatings.

It was experimentally proven that polymeric N-halamines have better wash fastness, since their polymeric nature allows multiple covalent bonding between the cellulose surface and the copolymer backbones.

Amide-containing N-halamines exhibited better UV light stability compared to hindered amine-containing N-halamines due to their less intense and narrower UV light absorption bands in the range of 315 to 400 nm.

N-halamines exhibited better stabilities when they were covalently attached to cellulose by epoxide tetherings compared to silane and poly carboxylic acid tetherings.

N-halamines could also be attached to polar surfaces through electrostatic attractions using a layer-by-layer assembly technique. This technique has industrial potential, since this does not require the use of any organic solvents.